



New processes and materials in conducting polymers/

| | |
|---------------|---|
| Item Type | dissertation |
| Authors | Machado, Joseph M. |
| DOI | 10.7275/727b-hk18 |
| Download date | 2025-05-11 12:33:27 |
| Link to Item | https://hdl.handle.net/20.500.14394/16877 |

UMASS/AMHERST



312066007447408

NEW PROCESSES AND MATERIALS IN CONDUCTING POLYMERS

A Dissertation Presented

By

JOSEPH M. MACHADO

Submitted to the Graduate School of the
University of Massachusetts in partial fulfillment
of the requirements for the degree of

DOCTOR OF PHILOSOPHY

September 1988

Department of Polymer Science and Engineering

© Copyright by Joseph M. Machado 1988

All Rights Reserved

NEW PROCESSES AND MATERIALS IN CONDUCTING POLYMERS

A Dissertation Presented

By

JOSEPH M. MACHADO

Approved as to style and content by:

Frank E. Karasz

Frank E. Karasz, Chairperson of Committee

Robert W. Lenz

Robert W. Lenz, Member

Paul M. Lahti

Paul M. Lahti, Member

William J. MacKnight

Professor William J. MacKnight, Head

Department of Polymer Science and Engineering

To my wife, Carolyn, and my son, Benjamin

ACKNOWLEDGMENTS

The field of conducting polymers is an interdisciplinary one. The significant advances made in this area have come chiefly from the combined efforts of chemists, physicists, and polymer scientists. The success of this dissertation was, likewise, the result of collaboration with a number of colleagues having various areas of expertise. I, first, express my appreciation to Professor Frank E. Karasz. His high expectations and standards and the confidence he showed in me gave me the confidence and motivation to successfully approach this undertaking. The freedom and responsibility he gave me allowed me to grow with this project and for that I am indebted.

The large scale preparation and molecular weight analysis of the precursor polymer used in this study was performed in collaboration with Dr. Lothar Franke, whose technical excellence and general good humor made this aspect of the work a pleasure. The design and fabrication of processing equipment was performed in collaboration with Foster-Miller Engineering. Particularly at FMI, Dr. Robert Kovar, Mr. Jim Burnett, and Dr. Mark Druy made invaluable contributions to this work. The spirit of cooperation, enthusiasm and commitment to excellence shown by the FMI team made this work enjoyable and rewarding. The work involving PPV blends was performed in collaboration with Dr. Joseph Schlenoff whose expertise in electrochemistry was of paramount significance to the project. I am happy to acknowledge the contributions of Mr. Paul Glatkowski, a laboratory technician, who assisted me in nearly every aspect of the project. Paul's enthusiasm, motivation,

observational skills, and technical ability were an invaluable asset. I would also like to formally thank Mr. Michael Massee for his collaboration in mechanical testing and x-ray diffraction studies, and less formally for helpful discussions, ideas, advice, commiseration and friendship. I am pleased to acknowledge the help and guidance of Dr. David Gagnon who introduced me to many experimental methods and who generated many useful ideas during the early stages of this work. The influence he has had on this project and on my professional development are considerable. I would also like to thank the other members of my dissertation committee, Professors Robert W. Lenz and Paul M. Lahti for their advice and guidance throughout this work. I also thank Ms. Lorraine Cox for enormous assistance in preparing this manuscript. Various other members of the Polymer Science and Engineering community are thanked: graduate students, post-docs, and staff for their help and friendship during my sojourn here.

I am grateful also to the influential people in my life, in particular, my father whose patience, encouragement and wisdom have been a continuing source of guidance. My most heartfelt thanks are extended to my wife, Carolyn, whose loving devotion, emotional support, kindness, friendship, and infinite patience have given this work true meaning. I also thank my son, Benjamin, who unknowingly provided enormous incentive and inspiration for concluding this work.

ABSTRACT

NEW PROCESSES AND MATERIALS IN CONDUCTING POLYMERS

September 1988

JOSEPH M. MACHADO, B.S., UNIVERSITY OF LOWELL

Ph.D., UNIVERSITY OF MASSACHUSETTS

Directed by: Professor Frank E. Karasz

Electrically conducting polymers possessing fully conjugated backbones have been the subject of considerable scientific and technological interest. However, the complete characterization and utilization of these materials have been limited by their generally poor processibility. In this dissertation the poly(sulfonium salt) precursor route to poly(phenylene vinylene) has been used to expand the range of processing methods available to conducting polymers. The available range of conducting polymer materials was also expanded by introducing techniques to blend PPV with other polymers.

A continuous process was developed to produce highly oriented PPV film. The process allows excellent control over drawing conditions and has been used to prepare high quality PPV film of uniform draw ratio between one and twelve. The processing behavior of the PPV precursor

infrared dichroism. Chemical doping with AsF_5 and SbF_5 vapors showed that electrical conductivity as high as 10^4 S/cm in the machine direction could be obtained. The electrical conductivity in both the machine and transverse directions, as a function of draw ratio and orientation, was determined. The mechanical properties of oriented PPV film were investigated. For highly oriented materials, a Young's modulus of 37 GPa in the machine direction was measured.

Techniques were developed to prepare biaxially oriented PPV film. Biaxial stretching strongly influenced the state of molecular orientation, the attainable electrical conductivity, and the conductivity anisotropy.

By combining the soluble precursor polymer and an additional polymer in solution, PPV was blended with a series of insulating water soluble polymers. Thermal analysis indicated that these blends were phase separated mixtures. For certain of these blends a very strong synergistic effect for the rates of chemical and electrochemical doping and for the final conductivity was observed. Accelerated doping was a result of improved dopant transport into the blend materials, aided by the added constituents.

A systematic study of the poly(phenylene vinylene)/poly(ethylene oxide) blend system was undertaken relating composition and morphology to the rates of chemical and electrochemical doping and to attainable conductivity.

TABLE OF CONTENTS

| | Page |
|---|------|
| ACKNOWLEDGMENTS..... | v |
| ABSTRACT..... | vii |
| LIST OF TABLES..... | xii |
| LIST OF FIGURES..... | xiv |
| Chapter | |
| I. INTRODUCTION..... | 1 |
| Overview..... | 1 |
| Objectives..... | 2 |
| Organization..... | 4 |
| II. LITERATURE REVIEW..... | 6 |
| Materials and Applications..... | 6 |
| Problems and Solutions..... | 8 |
| Polymeric Precursor Routes..... | 12 |
| The Poly(phenylene vinylene) Precursor Route..... | 18 |
| Conducting Polymer Blends..... | 24 |
| III. EXPERIMENTAL PROCEDURES..... | 28 |
| Preparation and Processing..... | 28 |
| Bis-Sulfonium Monomer Synthesis..... | 29 |
| Precursor Polymer Synthesis..... | 29 |
| Film Casting..... | 32 |

| | |
|---|-----|
| Uniaxial Stretching..... | 34 |
| Biaxial Stretching..... | 37 |
| Characterization Techniques..... | 41 |
| Infrared Dichroism..... | 41 |
| Tensile Properties..... | 42 |
| Chemical Doping Procedures..... | 43 |
| Blend Studies..... | 47 |
| Blend Preparation..... | 47 |
| Differential Scanning Calorimetry..... | 49 |
| Optical Microscopy..... | 50 |
| Extraction Studies..... | 51 |
| Electrochemical Doping..... | 51 |
| IV. PROCESSING AND CHARACTERIZATION OF UNIAXIALLY ORIENTED PPV. | 52 |
| Polymer Synthesis and Film Casting..... | 52 |
| Processing Behavior..... | 56 |
| Deformation Analysis..... | 59 |
| Molecular Orientation..... | 69 |
| Doping Studies..... | 81 |
| V. MECHANICAL PROPERTIES OF ORIENTED PPV..... | 86 |
| Background..... | 86 |
| "As Stretched" Films..... | 87 |
| Oriented and Annealed PPV..... | 91 |
| VI. BIAXIALLY ORIENTED PPV..... | 102 |
| Processing..... | 103 |

| | |
|---|-----|
| Structural Characterization..... | 106 |
| Electrical Conductivity..... | 109 |
| | |
| VII. POLY(PHENYLENE VINYLENE) BLENDS..... | 114 |
| Blend Characterization..... | 115 |
| Chemical Doping Studies..... | 119 |
| Electrochemical Doping | 121 |
| | |
| VIII. POLY(PHENYLENE VINYLENE)/POLY(ETHYLENE OXIDE) BLENDS..... | 127 |
| Optimization of Elimination..... | 127 |
| Chemical Microstructure..... | 130 |
| Thermal Properties..... | 133 |
| Morphology..... | 135 |
| Chemical Doping..... | 149 |
| Electrochemical Doping..... | 163 |
| | |
| IX. CONCLUSIONS..... | 169 |
| Processing | 169 |
| Blends | 172 |
| Future Directions..... | 173 |
| | |
| REFERENCE SECTION..... | 176 |
| | |
| BIBLIOGRAPHY..... | 188 |

LIST OF TABLES

| <u>Table</u> | <u>Page</u> |
|--|-------------|
| 1 Processing conditions for oriented PPV film used in this study..... | 71 |
| 2 Calculated values of theta for PPV IR absorbances..... | 73 |
| 3 Electrical conductivity and molar dopant uptake for chemically doped PPV film..... | 84 |
| 4 Tensile properties of "as stretched" PPV film measured in the machine direction..... | 90 |
| 5 Tensile properties of annealed PPV film measured in the transverse direction..... | 99 |
| 6 Mechanical anisotropy and electrical anisotropy of oriented PPV film..... | 101 |
| 7 Electrical conductivity and electrical anisotropy of SbF ₅ doped, uniaxially oriented PPV film..... | 112 |
| 8 Electrical conductivity and electrical anisotropy of SbF ₅ doped biaxially oriented PPV of machine draw ratio, λ_1 , and transverse draw ratio, λ_2 | 113 |
| 9 Elemental analysis results for a series of PPV blends and the pure constituents..... | 117 |
| 10 Electrical conductivity and dopant weight uptake for AsF ₅ doped PPV blends and pure constituents..... | 122 |
| 11 Initial current density for the first and second charging cycles upon electrochemical doping of PPV blends..... | 125 |
| 12 Elemental analysis results for a series of PPV/PEO blends.. | 132 |

| | | |
|----|--|-----|
| 13 | Conductivity and dopant uptake of chemically doped PPV/PEO blends..... | 162 |
| 14 | Charging rate, conductivity, and conductivity ratio (doping homogeneity) upon electrochemical doping of PPV/PEO blends. | 168 |

LIST OF FIGURES

| <u>Figure</u> | | <u>Page</u> |
|---------------|--|-------------|
| 1 | Examples of acceptor doping of conjugated polymers: a) chemical, b) electrochemical..... | 3 |
| 2 | Schematic diagram of the conducting polymer precursor method..... | 13 |
| 3 | Examples of conducting polymer precursor routes..... | 14 |
| 4 | Synthesis of the Durham precursor to polyacetylene..... | 16 |
| 5 | Biotechnological pathway to the poly(p-phenylene) precursor..... | 19 |
| 6 | Synthesis of the poly(phenylene vinylene) precursor used in this work..... | 20 |
| 7 | Examples of in situ conducting polymer blend preparation techniques..... | 25 |
| 8 | Apparatus for the synthesis of the poly(sulfonium salt) precursor polymer..... | 31 |
| 9 | a) Diagram of uniaxial web stretching device used for PPV processing..... b) Simplified schematic diagram of above apparatus emphasizing roll geometry and film path..... | 35 |
| 10 | Diagram of transverse stretching apparatus used for two-stage biaxial stretching of PPV film..... | 39 |
| 11 | Diagram of bubble expansion process for equibiaxial stretching of PPV precursor..... | 40 |
| 12 | Four-probe apparatus for simultaneous chemical doping and conductivity measurement..... | 44 |
| 13 | Vacuum line assembly for chemical doping reactions..... | 46 |
| 14 | Schematic diagram of blend preparation method..... | 48 |
| 15 | a) Photograph of film casting apparatus..... b) Photograph of uniaxial web stretching apparatus in operation (draw ratio = 10.0)..... | 55 |
| 16 | Processing behavior for PPV precursor as a function of heated roll temperature and draw ratio..... | 58 |

| | | |
|----|--|----|
| 17 | Optical micrographs of oriented PPV film prepared under various processing conditions..... | 61 |
| 18 | Normalized macroscopic dimensional changes sustained by the film during stretching..... | 64 |
| 19 | Photograph of deformation zone for material stretched at a draw ratio of 10.0 | 66 |
| 20 | Dichroic ratios of several PPV infrared absorption bands as a function of draw ratio..... | 72 |
| 21 | First order orientation function of PPV molecular axis with respect to the machine direction, calculated from the 558 cm^{-1} dichroic ratio, plotted as a function of (\square) draw ratio and (\bullet) extensional deformation corrected for volume shrinkage(see text)..... | 75 |
| 22 | The 2948 cm^{-1} PPV "impurity" infrared band for sample PPV-4 with incoming radiation polarized (—) in the machine direction and (---) in the transverse direction..... | 79 |
| 23 | Electrical conductivity of oriented PPV, after SbF_5 doping, measured (\circ) in the machine direction and (\blacklozenge) in the transverse direction plotted as a function of draw ratio..... | 82 |
| 24 | Chemical structure of partially converted PPV precursor directly after stretching process..... | 88 |
| 25 | Stress-strain curves for "as-stretched" (unannealed) PPV precursor stretched to a series of draw ratios. Measurements were made in the machine direction..... | 89 |
| 26 | Stress-strain curves for fully annealed PPV stretched to a series of draw ratios. Measurements were made in the machine direction..... | 92 |
| 27 | Young's modulus measured in the machine direction for annealed PPV plotted as a function of draw ratio..... | 94 |
| 28 | Tensile strength (\square) and ultimate elongation (\circ) measured in the machine direction for annealed PPV plotted as a function of draw ratio..... | 96 |
| 29 | Stress-strain curves for fully annealed PPV stretched to a series of draw ratios. Measurements were made in the transverse direction..... | 98 |

| | | |
|----|--|-----|
| 30 | Attainable deformation window using two-stage biaxial stretching..... | 104 |
| 31 | X-ray diffraction patterns of biaxially stretched PPV..... | 108 |
| 32 | Normalized DSC thermograms of pure components and blends.... | 118 |
| 33 | Conductivity as a function of time for PPV and nominal 50/50 blends upon exposure to 50 torr AsF ₅ vapor..... | 120 |
| 34 | Doping level as a function of time for PPV and nominal 50/50 blends doped electrochemically at +4.1 V versus Li in 1M LiClO ₄ /propylene carbonate electrolyte..... | 124 |
| 35 | Conductivity of electrochemically doped 50/50 wt % PPV/PEO blends as a function of elimination temperature for a series of annealing times..... | 129 |
| 36 | Regions of the infrared spectra of 50/50 wt % PPV/PEO blends annealed under various conditions..... | 131 |
| 37 | Melting point (□) and degree of crystallinity (●) of the PEO component as a function of the blend composition in PPV/PEO blends | 134 |
| 38 | Optical micrographs of spherulites in "as cast" PXD/PEO blends showing decreasing birefringence with increasing PXD contents..... | 137 |
| 39 | Optical micrographs of PPV/PEO blends showing separate PPV and PEO domains upon melting..... | 141 |
| 40 | Optical micrographs of a 10/90 PXD/PEO blend at various temperatures..... | 144 |
| 41 | Optical micrograph of 30/70 wt % PXD/PEO blend cast under vacuum at 900°C and quenched to R.T. showing grainy morphology..... | 147 |
| 42 | The weight fraction of PEO which could be extracted with chloroform for PPV/PEO blends as a function of blend composition..... | 148 |
| 43 | Electrical conductivity as a function of time of exposure of 65 torr AsF ₅ (dopant) to a variety of PPV/PEO blends.... | 152 |
| 44 | Weight uptake of dopant (AsF ₅) normalized to sample surface area as a function of (time) ^{1/2} upon exposing PPV to dopant vapor..... | 154 |
| 45 | Weight uptake of dopant (AsF ₅ ; 65 torr) as a function of (time) ^{1/2} of exposure to dopant for O: pure PEO; ◆ : 50/50 wt % PPV/PEO..... | 155 |

| | | |
|----|---|-----|
| 46 | Final conductivity (after AsF ₅ doping) as a function of composition for PPV/PEO blends prepared under various conditions..... | 157 |
| 47 | Doping level (measured coulometrically) as a function of time at constant potential (+ 4.1 V vs Li) during electrochemical doping of PPV/PEO blends of various compositions | 167 |

CHAPTER I

INTRODUCTION

Overview

In the context of this work the term conducting polymer will be used to denote the class of organic polymers possessing a fully conjugated backbone. This class of materials whose prototype is polyacetylene has been shown to attain metallic or semi-conducting electrical properties upon appropriate treatment.¹ Other materials which have been, or could be, considered conducting polymers are: (1) non-conjugated macromolecules possessing pendant moieties which form charge-transfer complexes and achieve moderate levels of conductivity ($\sim 10^{-3}$ S/cm). An example of this class is poly(2-vinyl pyridine/iodine).² (2) metal or graphite filled polymer composites where high levels of conductivity are achieved by virtue of the inorganic filler;³ (3) ion conducting polymeric solid electrolytes. A number of macromolecules which can attain a crown ether-like conformation (e.g. polyethylene oxide, polyepichlorohydrin) are capable of complexing with and dissolving inorganic salts and transporting metallic cations at reasonable rates.⁴

To achieve high conductivity in fully conjugated polymers, the chains must be oxidized or reduced so that electrons are transferred to or from the π -conjugated system. This process is commonly referred to as "doping" in a poor analogy to the familiar inorganic semiconductor process. The doping of conducting polymers may be performed by either

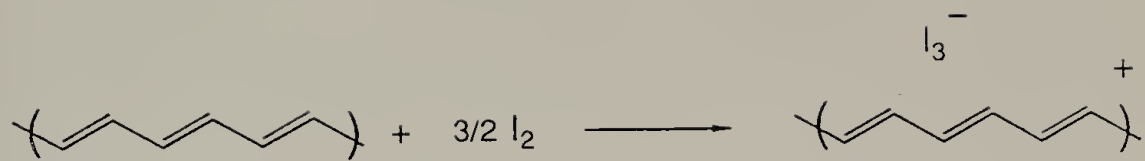
chemical or electrochemical means.⁴ The acceptor doping (p-doping) processes are illustrated in Fig. 1 (page 3). The polymer may be chemically doped merely by exposure to an oxidizing agent, commonly I₂ or AsF₅, which accepts an electron from the π-system. The chemical dopant generates a stable anion, often by disproportionation, and a macromolecular charge transfer complex results. Electrochemically, this process is performed by applying a sufficiently positive bias to the polymer which is kept in contact with an electrolyte solution. Electrons flow out of the polymeric electrode and charge neutrality is preserved by the diffusion of electrolytic anions into the polymeric electrode. In either case the same type of macromolecular charge transfer complex is formed. Donor doping (n-doping) is analogous. Chemically it is performed by exposure to reducing agents such as sodium napthalide and electrochemically it is performed by applying a sufficiently negative bias to the polymer in an electrochemical cell.

It has been shown that the charged sites residing on the polymer chain as a result of doping are the carriers responsible for charge transport in these materials. Electrical conductivities in the range of 1-10⁵ S/cm have been observed.

Objectives

One of the recognized deficiencies associated with conducting polymers is their lack of processibility. An approach to this problem which has proven to be useful in the case of the conducting polymer poly(phenylene vinylene) (PPV) is to prepare a soluble non-conjugated

a



b

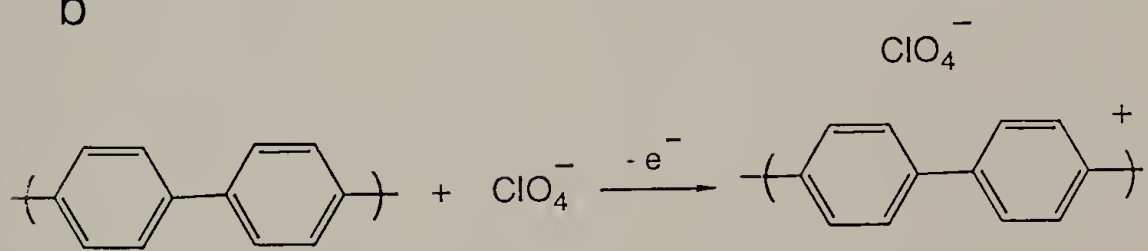


Figure 1. Examples of acceptor doping of conjugated polymers:
a) chemical, b) electrochemical

polymer which can be fabricated into the desired shape and then converted to the conjugated form in a subsequent operation⁵. This process will be explained fully in subsequent chapters, however, within the context of this approach the objectives of this dissertation are:

- 1) to develop routine procedures for the large scale synthesis of the precursor polymer;
- 2) to develop a continuous and controllable technique for the preparation of highly oriented PPV film;
- 3) to develop novel processing techniques using the PPV precursor;
- 4) to exploit advantages associated with solubility and/or deformability of the precursor polymer towards the development of improved conducting materials.

Organization

The remainder of this dissertation will describe how these objectives have been achieved. Chapter II is a literature review which emphasizes techniques by which improved processibility has been attained in various conducting polymer systems. Chapter III comprises a description of the experimental methods used including synthetic techniques, processing apparaata, and characterization methods. Chapter IV is a discussion of the continuous uniaxial stretching behavior of the PPV precursor and also includes orientation characterization and electrical conductivity results. Chapter V is an analysis of the anisotropic

mechanical properties of oriented PPV. Chapter VI introduces two novel processing techniques for preparing biaxially oriented PPV and includes chemical doping results. Chapter VII presents a survey study of a series of PPV blends with respect to chemical and electrochemical doping behavior. Chapter VIII includes a detailed study of the morphology and electrical properties of poly(phenylene vinylene)/poly(ethylene oxide) blends prepared over a wide range of conditions. Both chemical and electrochemical doping results are presented. Chapter IX presents a summary of the major results and conclusions and closes with suggestions for future directions and continuations of this work.

Chapter II

LITERATURE REVIEW

Materials and Applications

Reviews of electrically conducting polymers often begin with the statement that: in 1977 polyacetylene after being exposed to iodine achieved a metal-like conductivity.⁶ This event sparked major interest in the unusual properties of this and related materials. Although polyacetylene continues to be the most well-studied conducting polymer, a considerable diversity of conjugated polymers have been prepared and shown to exhibit conducting or semi-conducting behavior. The list includes: substituted polyacetylenes⁷ and poly(diacetylenes)⁸, poly(p-phenylene)⁹, a family of poly(arylene vinylenes)¹⁰, polypyrroles¹¹, polythiophenes¹², other poly(heterocycles)¹³, poly(aniline)¹⁴, cross-conjugated polymers¹⁵, and various fused ring systems such as poly(azulene).^{16,17} In addition, many copolymers among these have been prepared.^{7,18} Indeed, the universality of conjugated polymers exhibiting conducting behavior has been amply demonstrated.

To complement the diversity of conducting polymer structures which have been synthesized, a range of potential applications has been proposed. Certainly the most thoroughly investigated of these applications is secondary battery electrodes. As a result of their conductivity and ability to undergo reversible electrochemical oxidation and reduction, conjugated polymers are useful materials for the storage of electrical

energy¹⁹. Organic conducting polymers possess certain advantages over conventional battery electrode materials (e.g. lead, nickel) arising chiefly from: their high energy density (on a weight basis) (>100 Ah/kg), the ability to molecularly tailor the oxidation or reduction potential, and their amenability to thin film fabrication.

Rechargeable batteries have been prepared using polyacetylene as both cathode and anode and poly(ethylene oxide) as solid electrolyte (the all plastic battery).²⁰ In addition batteries possessing lithium anodes have been prepared using poly(p-phenylene)²¹, poly(pyrrole)^{22,23}, and poly(aniline)²⁴ as cathode materials. The usefulness of conducting polymers in battery applications has been extensively reviewed and largely accepted.^{21,25} Many authors have pointed out, however, that although battery electrodes provide a viable initial application for conducting polymers, it does not represent a high volume market.²⁶ Beyond batteries, more sophisticated solid state electronic devices have been fabricated using conducting polymers in traditional semiconductor applications. Schottky diodes and heterojunctions have been prepared between conducting polymers and inorganic substrates.^{27,28,29} A polyacetylene solar cell has also been demonstrated.³⁰ Field effect transistors using polythiophene³¹ and poly(N-methyl pyrrole)³² as channel materials have been fabricated. Very recently, an all-polymer field effect transistor was reported using microphotolithographic techniques to selectively undope (reduce) portions of an electro-deposited layer of poly(3-methyl thiophene). Thus poly(3-methyl thiophene) acts as source, channel and drain material. Submicron spatial resolution was reported.³³

A variety of optical display applications have been proposed for conducting polymers which exploit the electrochromic effect accompanying oxidation or reduction. Advantages over conventional liquid crystal display devices include a wider viewing angle, lower power consumption, and solid state construction. Displays containing polypyrrole³⁴ and polyaniline²⁴ have been made. Additional applications such as chemical sensor elements and non-linear optical materials have also been considered. A full discussion of proposed applications for conducting polymers is available elsewhere.³² Of course, the replacement of conventional metals for current transmission (wires) has been envisioned,³⁵ although it is universally agreed that more specialized applications should be initially pursued. It has been pointed out that the most significant advantage of organic conducting polymers (and perhaps all organic materials) lies in the ability to specifically control properties through subtle manipulation of chemical structure and morphology.³⁶

Problems and Solutions

In spite of the fact that materials are available and applications have been identified, the anticipated commercial development of conducting polymers is not a reality. The explanation lies chiefly in two deficiencies of these materials which have greatly hindered their development.

The first of these is the poor atmospheric stability which the "doped" materials generally exhibit. It has long been recognized that

doping is an electron transfer process which leaves the polymer chain in an ionized state.³⁷ The charged species thus formed (polarons, bipolarons, charged solitons) are the carriers responsible for conduction.³⁸ However, these species also retain much of the chemical reactivity of a conventional carbenium ion or carbanion, although they are partially stabilized by delocalization. Indeed, Wnek has used n-doped polyacetylene as an intermediate in preparing alkylated polyacetylenes, invoking classical carbanion chemistry.³⁹ Therefore, exposure of doped materials to atmospheric oxygen and moisture generally leads to the destruction of charge carriers in conducting polymers.

Successful strategies to reduce or eliminate such degradation have been developed. The simple use of protective barrier coatings has been demonstrated.⁴⁰ Perhaps a more elegant approach is to control π -electron density on the conjugated chain in order to enhance charge carrier stability. This approach has been particularly successful with acceptor doping of materials possessing electron-rich π systems, so that upon oxidation, the carbenium ions generated are inherently more stable. For this reason poly(pyrrole), poly(thiophene), and poly(aniline) exhibit remarkable atmospheric stability in the oxidized, conducting form.⁴¹ In principle this strategy could also be used to stabilize n-doped polymers by preparing electron-poor π systems, however, this approach has been less successful. One restriction of this technique is that moieties introduced to influence π electron density must themselves be inert towards reaction with the dopant. Nevertheless, within the framework of this approach, the preparation of long term environmentally stable conducting polymers can be anticipated.

The second major deficiency which has largely impeded the development of conducting polymers is poor processibility. Early on, it was recognized that the combination of inexpensive and versatile fabrication, characteristic of polymeric materials, combined with the electrical properties of metals and semiconductors would provide enormous incentive for the development of "conducting plastics". However, the effective π -electron backbone conjugation, which provides the pathways for conduction in these materials, generally imparts sufficient rigidity to the chains to prevent solubility, melting, or thermal softening. Therefore, conducting polymers are not at all amenable to the various processing techniques which have been developed for conventional polymeric materials.

Approaches to alleviate this intractibility have been varied. Initially, substituted acetylenes were prepared which attained solubility as a result of steric restrictions to effective conjugation. However, low conductivities were also obtained.^{7,42}. Random copolymers have been prepared with monomers which act to break up conjugation and provide flexible links along the chain. Soluble copolymers have been prepared between acetylene and carbon monoxide⁴³, methyl acetylene⁷, and phenyl acetylene⁴². In these cases, the attainment of solubility has required excessive compromises in conductivity.

Alternatively, block and graft copolymers have been prepared in an attempt to preserve the long conjugation lengths necessary for conduction and still impart a sufficient entropic driving force (provided by flexible blocks) to induce solubility. Diblock copolymers have been

synthesized comprising polyacetylene segments with segments of polystyrene or polyisoprene. These are prepared by the transformation of living anionic chain ends (polystyryl or polyisoprenyl lithium) to coordination catalyst chain ends followed by acetylene polymerization.⁴⁴ Using this approach, a copolymer with an isoprene block of about 10,000 daltons and acetylene block of about 2000 daltons exhibited solubility in organic solvents and could be doped with I₂ to conductivities of 1-10 S/cm.⁴⁵ However, it appears that the structural window for obtaining combined solubility and high conductivity in these materials is rather narrow.⁴⁶ Soluble graft copolymers, in which polyacetylene has been grafted onto polyisoprene, polybutadiene, and polystyrene carrier chains, have been synthesized, although no conductivity data were reported.^{47,48}

A very promising class of completely soluble conducting polymers are 3-alkyl substituted polythiophenes.⁴⁹⁻⁵² These materials may be polymerized either chemically or electrochemically to molecular weights in the range of 10³- 10⁴ daltons. It appears that any alkyl group larger than ethyl is sufficient to impart good solubility in organic solvents. Conductivities in the range of 1-100 S/cm have been reported. 3-alkyl thiophenes may also be copolymerized amongst themselves to control properties.⁵⁰ The ability to melt process these materials has been reported although no details have been given. Very recently, a subclass of these materials, ω -sulfonate 3-alkyl poly(thiophenes), has been prepared.⁵³ These materials are water soluble and self-doping (the dopant counterion is covalently attached to the chain). It is expected

that this class of conducting polymers will receive increasing attention.

Polymeric Precursor Routes

An alternative approach for providing processibility to conducting polymers has been developed which entirely circumvents the intractability of the fully conjugated polymer by performing fabrication or shaping operations on a non-conjugated precursor polymer. The precursor is processible by conventional means and can be converted to the conjugated form in a subsequent post-shaping operation. The conversion from precursor to conjugated polymer is most conveniently performed by means of a thermally activated elimination reaction (although a photo-induced elimination would find obvious lithographic applications). The process is shown schematically in Fig. 2 (page 13). Such a precursor system, although conceptually simple, is in practice highly constrained because the thermal conversion to the conjugated form (elimination) must proceed uncatalyzed to very high conversion and in the absence of side reactions in order to yield materials of appreciable conductivity. For example, the dehydrochlorination of polyvinyl chloride or pyrolysis of poly(vinyl acetate) does not produce conducting polyacetylene.^{54,55} To date, only three precursor systems have been successful in producing highly conducting materials. These are shown in Fig. 3 (page 14).

The "Durham" route to polyacetylene introduced by Feast is perhaps the most well known precursor system.⁵⁶ This precursor is prepared by ring opening metathesis polymerization of a tricyclic monomer shown in

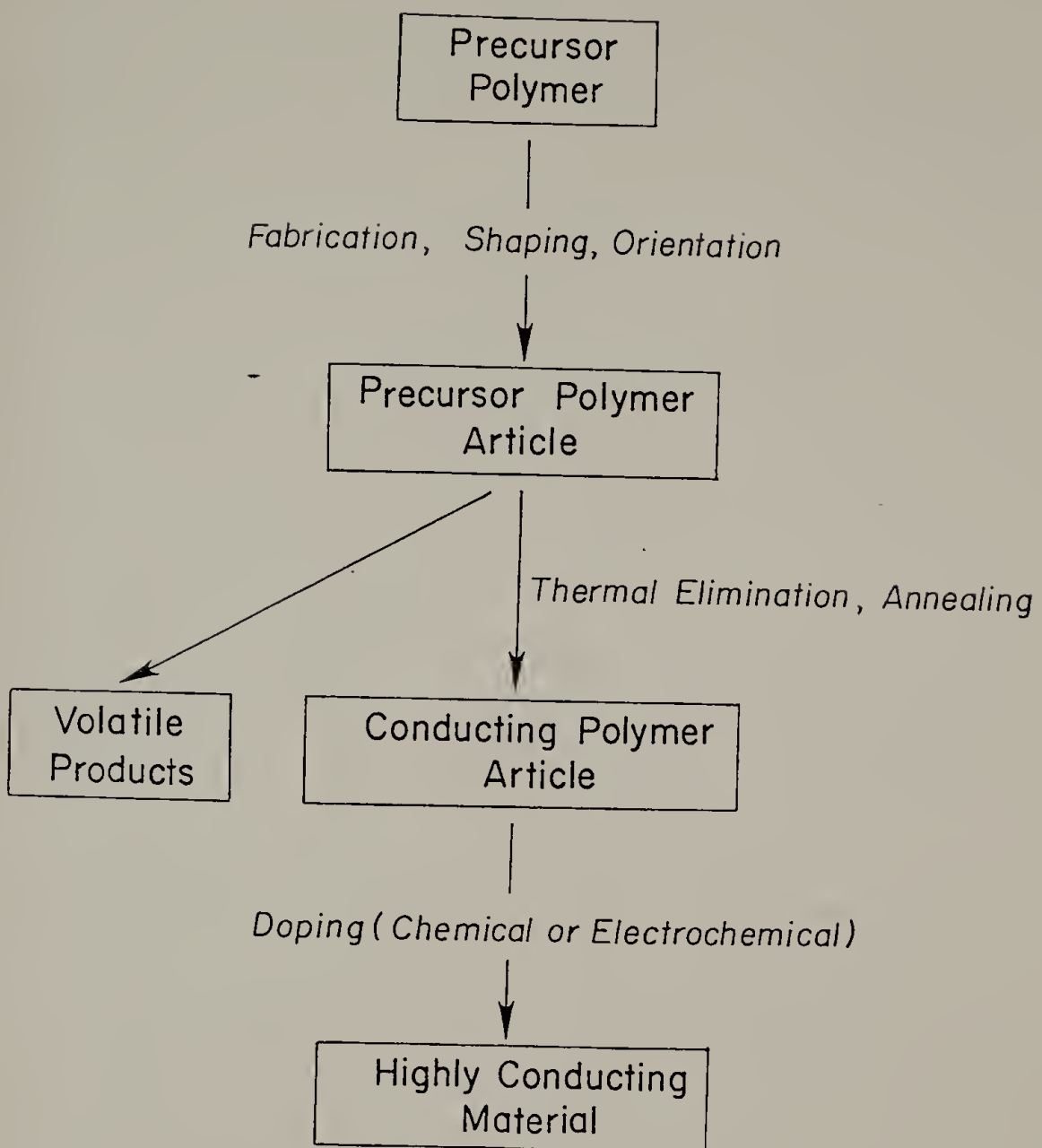


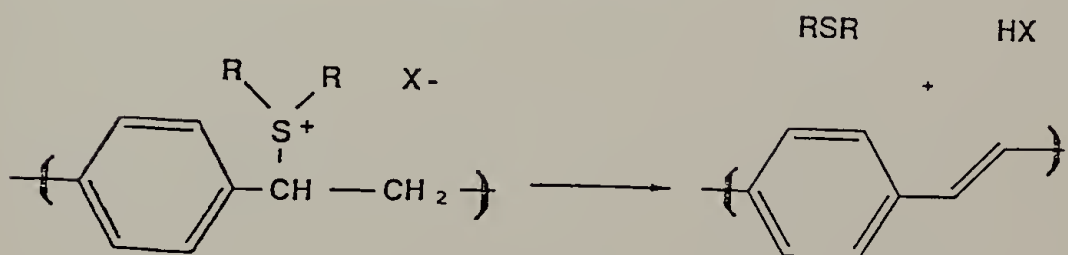
Figure 2. Schematic diagram of the conducting polymer precursor method



Edwards and Feast , 1980



Ballard et. al. , 1983

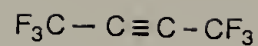


Wessling and Zimmerman , 1968

Figure 3. Examples of conducting polymer precursor routes

Fig. 4 (page 16). The resultant polymer is of high molecular weight ($M_w \sim 3 \times 10^5$)⁵⁷ and exhibits solubility in a range of organic solvents. The precursor polymer can be cast from solution forming coherent, strong, flexible films. At room temperature and above these films undergo retro-Diels Alder elimination producing predominantly cis-polyacetylene and α,α' hexafluoro-o-xylene (related precursor polymers which release different aromatic elimination products have also been prepared).⁵⁸ It has been shown that upon warming these films to about 60°C the rapid evolution of the elimination product results in a softening of the material. During this time the material may sustain considerable deformation (>2000%) which may be used to fabricate the polymer into a desired shape or to orient the polymer chains in a flow field.^{59,60,61} The extensional deformation (stretching) of Durham precursor films, to draw ratios up to twenty, followed by subsequent annealing at higher temperatures to complete the elimination and effect cis-trans isomerization of the polyacetylene, has been shown to produce polyacetylene of essentially perfect uniaxial orientation and enhanced crystallinity relative to the unstretched material.⁶²

It has been suggested that the measured properties of oriented Durham polyacetylene should most closely approach the ultimate "intrinsic" properties of the polyacetylene chain because these materials are comprised of perfectly oriented, highly crystalline arrays of polyacetylene chains free from complex morphological factors such as interfibrillar contacts or grain boundaries which are thought to limit the attainable properties of the conventional Shirakawa material.



+

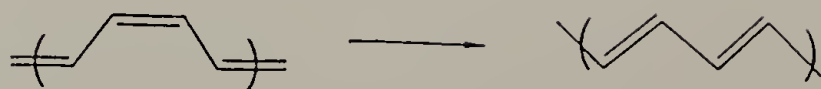
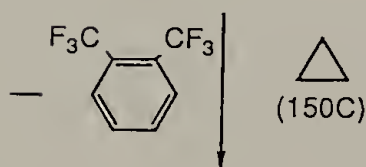
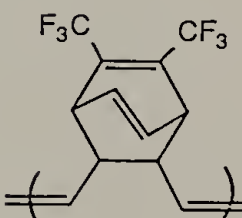
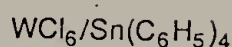
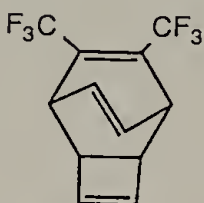


Figure 4. Synthesis of the Durham precursor to polyacetylene

Chemical doping experiments have not supported these expectations. The highest reported conductivities of oriented Durham polyacetylene are 2200 S/cm for I₂ doped material and 1250 S/cm for AsF₅ doped material.^{63,64} These values result from measurements parallel to the direction of chain orientation. By comparison, partially stretch-aligned Shirikawa polyacetylene (draw ratio ~ 3) has been doped to conductivities in excess of 1000 S/cm.⁶⁵ Indeed, the report by Naarmann that chemically pure polyacetylene prepared by a modified Shirakawa technique may attain a conductivity in excess of 10⁵ S/cm⁶⁶, has caused theoretical workers to re-examine the ultimate properties of the polyacetylene chain.⁶⁷ Townsend has used resonance Raman spectroscopy to show that Durham polyacetylene possesses a shorter conjugation length than the Shirakawa material.⁶⁴ Thus the Durham material must be considered non-ideal in terms of chemical microstructure, and serves to illustrate the difficulty of inducing pure intramolecular elimination in the solid state.

Nevertheless, the Durham precursor is promising from a technological perspective because it provides two opportunities for shaping operations. Conventional solution casting and spinning techniques are possible during the soluble stage as well as very large strain solid deformation processing during the "plasticized" stage.

It may also be noted that recent advances in olefin metathesis catalysis⁶⁷ have allowed the introduction of "living" methasis polymerizations which have been used to prepare controlled microstructure block copolymers containing the Durham precursor as well as the direct preparation of polyacetylene blocks from cyclooctatetraene.⁶⁸

A precursor route to poly(p-phenylene) is also available⁶⁹ (see Fig. 5 [page 19]). The monomer, 5,6 diacetoxy 1, 3 cyclohexadiene is prepared by esterification of the corresponding alcohol, which is an isolatable intermediate in the microbial oxidation of benzene. The esterified monomer polymerizes by simple 1, 4 addition using a free radical initiator. The resulting polymer shown in Fig. 2b can be prepared in high molecular weights (up to 1.5×10^5 daltons) and is soluble in organic solvents. Solution cast films undergo elimination upon heating ($\sim 200^\circ\text{C}$) releasing acetic acid and yielding poly(p-phenylene). No chemical doping results have been published.

The Poly(phenylene vinylene) Precursor Route

The material of interest in the present study is poly(p-phenylene vinylene) (PPV). Its preparation through Wittig condensation⁷⁰ or dehydrohalogenation⁷¹ producing intractible powders has been detailed elsewhere. In this work PPV is prepared from its water soluble precursor, poly(xylolidene dialkyl sulfonium halide) (see Fig. 6 [page 20]). This synthesis was introduced by Kanbe et al. and by Wessling and Zimmerman both in 1968.^{72,73} The precursor polymer is prepared by the reaction of aqueous base with α, α' xylene bis-dialkyl sulfonium halide. It is thought that base acts to abstract a benzylic proton from the bis-salt forming a sulfonium ylid intermediate. The ylid undergoes 1,6 elimination forming a sulfonium quinodimethane species. This latter species is thought to be the monomer which polymerizes by 1,6 addition

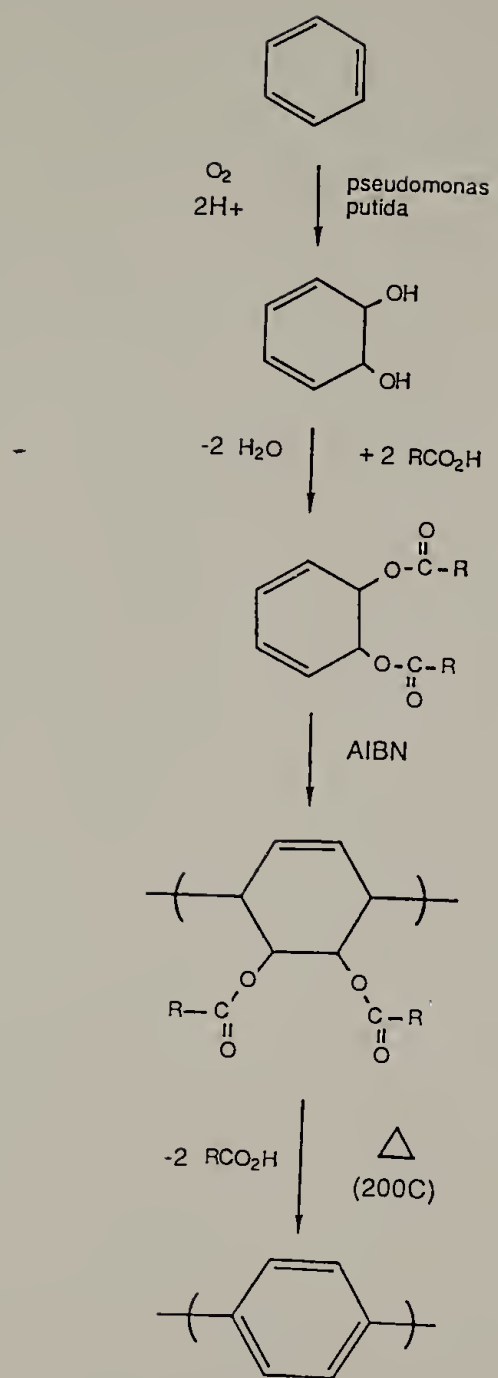


Figure 5. Biotechnological pathway to the poly(p-phenylene) precursor

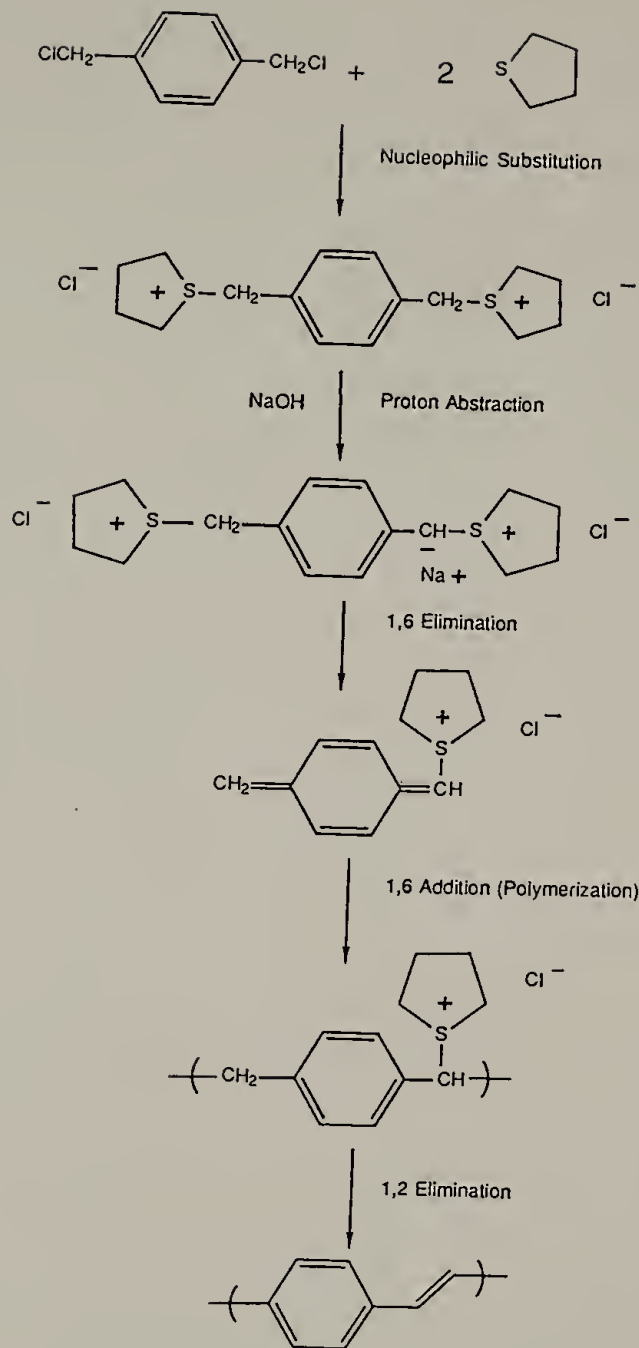


Figure 6. Synthesis of the poly(phenylene vinylene) precursor used in this work

yielding the precursor polymer. No external initiator is added. In fact, the exact nature of the propagating chain end is still under dispute.^{74,75} In any case, the water soluble sulfonium salt precursor can be prepared in high molecular weight and upon removal of solvent forms very strong, clear (somewhat yellow), flexible films. It was recognized that upon heating solution-cast films, the polymer undergoes quantitative elimination yielding the conjugate acid of the anion, the alkyl sulfide, and the conjugated polymer, poly(phenylene vinylene). In 1972 Wessling described the preparation of PPV films, fibers, and foams using the precursor process.⁷⁶ Of course, it was not recognized at that early date that these materials could be rendered conductive by treatment with appropriate chemical dopants. In 1984 independent work by Gagnon et al.⁷⁷ and by Murase et al.⁷⁸ showed that PPV prepared by the sulfonium salt precursor could be rendered highly conducting by treatment with AsF_5 or H_2SO_4 .

Further work by Gagnon showed that a thermally induced elimination/plasticization analogous to that reported for Durham polyacetylene allowed the PPV precursor to be uniaxially stretched to high draw ratios (up to 15). Moreover it was shown that stretching resulted in efficient molecular orientation of PPV chains.⁷⁹ Quantitative characterization of the state of orientation in these materials was reported by Gagnon (WAXD)⁷⁴ and Bradley (I.R. dichroism).⁸⁰ It was shown that molecular orientation profoundly affected the attainable electrical conductivity after chemical doping with AsF_5 .⁷⁹ The conductivity of oriented materials was reported to be highly anisotropic and values up to 2700 S/cm measured parallel to the axis of orientation were reported.^{79,81}

The sulfonium salt precursor route has shown unusual synthetic versatility. Beyond the preparation of poly(phenylene vinylene), it has been used to prepare 2,5 disubstituted PPV (Me, Meo, Br)^{82,83}, the 1,4 and 2,6 isomers of poly(naphthalene vinylene)⁸⁴, heterocyclic analogues such as poly(thiophenylene vinylene)⁸⁵, as well as numerous copolymers among these⁸⁶. Many of these poly(arylene vinylenes) exhibit desirable properties such as low oxidation potentials and improved atmospheric stability⁸⁶. Certainly the synthetic possibilities associated with this system have not been exhausted and this will continue to be a fruitful area of research.

The usefulness of the conducting polymer precursor approach can be viewed from both an applied and fundamental perspective. Technologically, it provides opportunities for the processing, formulation compounding, and shaping operations which will be necessary for the fabrication of useful electronic materials and devices. Scientifically, it provides a means of preparing conducting polymers in a form essentially free of morphological complexities such as interfibrillar contacts, interparticle contacts, or grain boundaries. Moreover, it allows the preparation of materials in forms (generally large area, thin, clear films) amenable to a variety of characterization techniques to probe the optical properties, electronic structure, chemical microstructure, and crystallographic order of these materials. In addition, the acquired processibility permits the continuous variation of morphological features (such as molecular orientation) in order to determine the structure-property relationships in conducting polymers.

With respect to these ideas, the poly(sulfonium salt) system possesses a number of significant advantages over other conducting polymer precursors, chiefly the Durham precursor. First, the aqueous based chemistry is both inexpensive and facile simplifying the preparation of large quantities required for the development of more sophisticated processing techniques. Second, the PPV precursor polymer exhibits good stability at room temperature which facilitates handling. Third, the PPV precursor exhibits more complete elimination after annealing, giving longer conjugation lengths which are reflected in higher attainable electrical conductivities (up to 10^4 S/cm has been achieved). Fourth, the sulfonium salt precursor is sufficiently versatile to allow the preparation of a family of PPV analogues and copolymers thereof. In addition, the nature of the sulfonium moiety and counterion may be varied in order to influence polymer solubility characteristics and the rate of elimination.

The goal of the present study is to expand upon previous efforts involving the PPV precursor and to implement knowledge gained about the chemistry and physics of this material towards the development of improved techniques for the preparation and processing of electroactive PPV. Specifically in terms of processing, a continuous uniaxial stretching device has been fabricated which is capable of preparing continuous quantities of PPV film drawn under precisely controlled conditions of draw ratio, rate, and temperature, where draw ratio has been varied continuously from one to twelve. In addition, two biaxial stretching processes have been developed to further expand the states of molecular orientation in which PPV film can be prepared.

Conducting Polymer Blends

The philosophy of the present work is to exploit advantages associated with the precursor process which may contribute to improved understanding of conducting polymers or to the preparation of improved electroactive materials. One advantage associated with the solubility of the precursor polymer is the ability to disperse additional components into the solution on a molecular level.

Previously there has been interest in the preparation of conducting polymer blends in which the added component is a conventional insulating polymer. Such materials have been prepared in various cases to improve the atmospheric stability⁸⁷, processibility⁸⁸, or mechanical properties⁸⁹ of the conducting materials. However, as a result of the severe processing constraints formerly imposed upon conducting polymers, blend preparation techniques have been largely limited to either the *in situ* polymerization of a conducting polymer within an insulating matrix⁹⁰ or the dispersion of conducting polymer particles within a "binder" matrix⁹¹ (see Fig. 7 [page 25]). In either case, these techniques are limited to the preparation of blends over a rather narrow range of composition and morphology (for instance the conducting polymer is constrained to be the dispersed phase). Thus although significant material improvements have been obtained by blending in specific cases, a complete and systematic study of the effect of composition and structure on electrical properties has not been possible. Greater versatility is gained by preparing blends with the soluble precursor polymer by casting

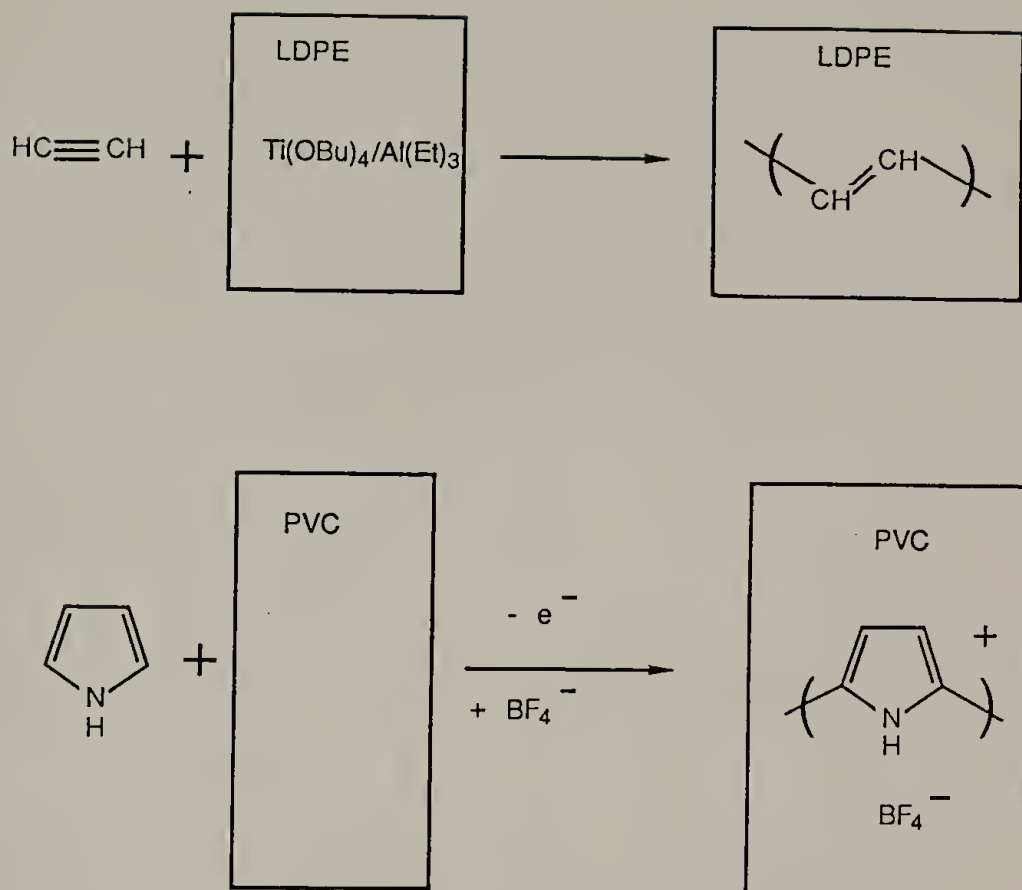


Figure 7. Examples of *in situ* conducting polymer blend preparation techniques.

films from solution in a common solvent. In this way a variety of blend systems can be prepared with access to the full range of composition, allowing an uncompromised and systematic investigation.

The first conducting polymer blends were reported by Galvin and Wnek in 1982.^{87,90} These were prepared by the polymerization of acetylene within a catalyst impregnated LDPE matrix. Polyacetylene contents up to 18 wt % and conductivities up to 5 S/cm after I₂ doping were obtained. Polyacetylene has also been polymerized within matrices of polybutadiene⁹² and Kraton thermoplastic elastomer.⁹³ These blends exhibited conductivities up to 100 S/cm (after I₂ doping) and greatly enhanced flexibility compared to pure polyacetylene. Pyrrole has been chemically polymerized (with FeCl₃) in the presence of methyl cellulose to produce colloidal conducting blend particles.⁹⁴ These particles formed stable suspensions in water which could be cast into coherent films with conductivities up to 0.2 S/cm.

Electrochemical techniques have been widely used to prepare conducting polymer blends by polymerizing a heterocyclic monomer on a polymer coated electrode. In this way polypyrrole blends with polyvinyl chloride, polyvinyl alcohol, polyvinylidene chloride, polystyrene, and polyurethanes^{89,95,96} have been prepared. The reported conductivities range from 1 to 50 S/cm. Pyrrole has also been electrochemically polymerized in solutions containing anionic polyelectrolytes⁹⁷ or anionic latex particles⁹⁸. In either case, deposited films were identified as oxidized polypyrrole in which the added anionic species were incorporated as "dopant" counterions. These blends exhibited greatly enhanced processibility and reasonable conductivity (10^{-3} to 5 S/cm).

Poly(p-phenylene)/poly(phenylene sulfide) composite materials have been made by sintering mixed powders of the two pure components under heat and pressure.⁹¹ After chemical doping (with SbCl₅) conductivities in the range of 1 S/cm were obtained.

Very recently blends between a soluble poly(3-alkyl thiophene) and polystyrene have been prepared by casting films from solutions in chloroform.⁹⁹ The blends were chemically doped by exposure to an acetone solution of NO⁺PF₆⁻. High conductivities were achieved at a composition of electroactive component above 16 volume % as a result of percolation effects. Conductivities in the range of 1-10 S/cm were obtained.

In the present work the poly(sulfonium salt) PPV precursor has been blended with a series of water soluble polymers by casting films from ternary aqueous solutions. Upon annealing at elevated temperatures to complete the elimination, PPV blends are obtained. Subsequent doping by either chemical or electrochemical means resulted in highly conducting materials. The attainable electrical conductivity has been determined with respect to the matrix type (glassy, elastomeric, or semi-crystalline), composition, and morphology. Particular utility in PPV blends has been demonstrated with respect to applications requiring electrochemical activity (e.g. battery electrodes).

CHAPTER III

EXPERIMENTAL PROCEDURES

Preparation and Processing

The initial requirement associated with the development of advanced processing techniques for PPV was the preparation of sufficient quantities of material of reproducible quality. Thus the synthesis of the PPV precursor which has been described elsewhere¹⁰⁰ was scaled up to approximately the one kilogram scale. This required, of course, a number of procedural modifications to facilitate material handling. It is worth noting here also that, in the present work the PPV precursor containing the tetrahydrothiophene based sulfonium group was used, rather than the dimethyl sulfide based sulfonium which had been used in almost all previous work. The change was based upon work by Lenz et al.¹⁰¹ which showed that the PPV precursors containing cyclic sulfonium groups undergo quantitative elimination under milder annealing conditions than the dimethyl sulfonium precursor. The difference is presumably due to the greater resistance to nucleophilic attack (by the anion) at the α -positions of the cyclic sulfoniums relative to the dimethyl sulfonium. The ability to use milder elimination conditions (250°C instead of 300°C) greatly reduced the danger of oxidative degradation during annealing and also expanded the range of blend systems which could be investigated.

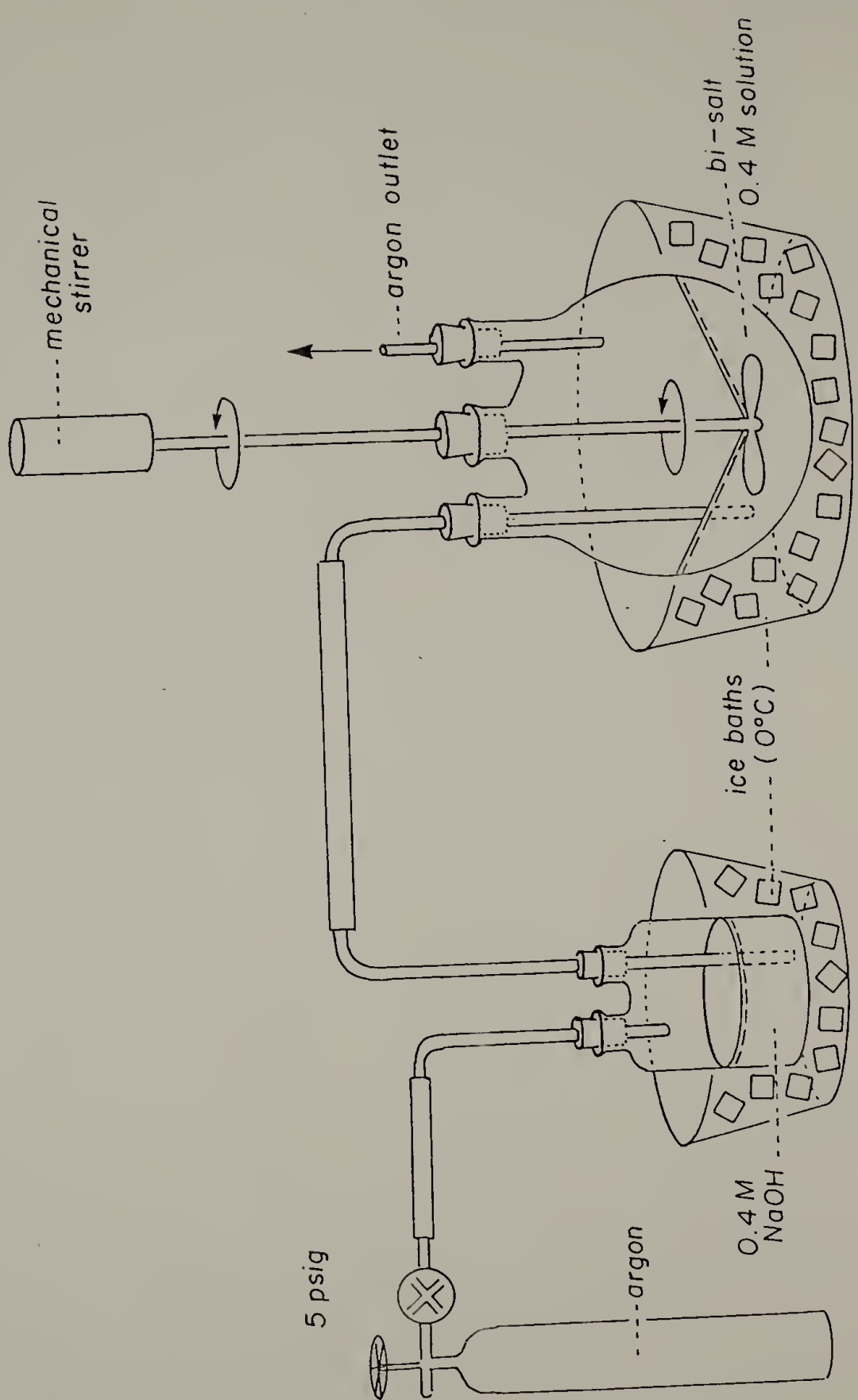
Bis-Sulfonium Monomer Synthesis

1000g (5.71mol) α , α' dichloro-p-xylene (Eastman-Kodak) was added to a 5L round bottom flask containing 2.5L methanol, with stirring at 50°C. To the cloudy suspension 1.3L (14.8mol) tetrahydrothiophene (caution-extreme odor) was added. The solution slowly began to clear and within a few hours a homogeneous solution was obtained. After three hours, the solution was pumped slowly into a 25L round bottom flask containing 15L stirring methylene chloride at room temperature. The product α , α' bis (tetrahydrothiophenium-p-xylene) chloride precipitated out immediately as a white crystalline solid. The precipitate was collected in a large buchner funnel and washed with several liters of cold acetone. The solid was dried under vacuum overnight to yield 1500g dry, very fine powder (~75% yield). The bis-salt decomposed before melting at about 120°C. Typically, the bis-salt monomer was polymerized immediately because it slowly decomposed to starting materials upon standing at room temperature. It could be stored if necessary, however, at ~ -20°C.

Precursor Polymer Synthesis

1500g (4.27mol) bis-sulfonium salt was dissolved in 10.7L distilled water to make a 0.4M solution. The solution was filtered to remove a small amount of beige insoluble material. The solution was charged into a 50L reaction vessel which was cooled to 0°C with ice. The solution was stirred and purged with argon for one hour. A sodium hydroxide solution (10.7L at 0.4M) was prepared and also cooled to 0°C and purged with argon. The base solution was quickly pumped under about 5 psig argon pressure into the reaction vessel (see Fig. 8 [page 31]). The

Figure 8. Apparatus for the synthesis of the poly(sulfonium salt) precursor polymer.



viscosity of the solution increased rapidly. The reaction was allowed to proceed for five minutes at which time the reaction medium was a clear, colorless gel. At this point hydrochloric acid solution (0.4M) was pumped into the reaction vessel to neutralize the solution (desired pH~7) and break the gel. About 7L was required to achieve neutrality. An additional 3L distilled water was added slowly with rapid stirring to fully redissolve the gel.

The PPV precursor polymer, poly(xylylidene tetrahydrothiophenium chloride), was isolated by precipitation. The solution from above was fed in a fine stream into a five-fold excess of rapidly stirring isopropanol. When added in this way, the polymer precipitated into a white fibrous thread which eventually wrapped around the stirring shaft. After precipitation, the crude polymer product, resembling a large ball of white yarn, was further washed with isopropanol and could be stored somewhat wet with alcohol at -20°C indefinitely.

Film Casting

The procedure for converting the precipitated polymer into large-area solution cast films will be described.

The precipitated polymer could easily be redissolved in water, however, the crude precipitate contains a small amount (~2 wt %) of NaCl and unreacted monomer which are entrapped during coagulation. To purify this material, the fibrous precipitate was stirred vigorously in a 3/1 vol/vol isopropanol/water mixture. This mixed solvent is able to swell the polymer slightly and extract the low molecular weight salts and impurities without dissolving the polymer. Subsequently, the precipitate

was washed twice with isopropanol and twice with anhydrous ether. This procedure removed the water and visibly collapsed the precipitate into very fine strands. After the ether rinse, the precipitate is susceptible to discoloration on standing at room temperature due to elimination.

The polymer was then dried overnight under dynamic vacuum at -20°C. The fully dried material was of a fibrous, paper-like consistency with slight discoloration. The dry material was quickly weighed and dissolved in distilled water to a concentration of 4 wt %. Very slow mechanical stirring is required for the preparation of these aqueous casting dopes. Complete dissolution of the polymer requires about 24 hours of stirring and the resulting solutions are extremely thick viscoelastic fluids. Typically two days of stirring was allowed to insure complete homogenization of the transparent, light green solutions. After homogenization the casting dopes could be stored under refrigeration for up to two months without gelation.

Before casting, dopes were typically filtered using a high pressure filtration apparatus (Amicon high pressure cell fitted with a fritted stainless steel disk). For optimum results, the dopes were then degassed by subjecting to a dynamic vacuum for one hour.

Precursor polymer films were prepared by pouring the casting dope (~400 ml) onto a smooth PMMA sheet and slowly passing a "doctor blade" casting knife over the reservoir of solution. Typically a 1.9mm layer of solution was spread over the casting surface covering a 20cm x 100cm area. Films were cast at room temperature by gently passing a filtered air stream over the film surface. After drying the films were slightly

yellow, clear and strong (~60 μm thickness). They could be easily delaminated from the PMMA casting surface (experiments have shown that PMMA sheeting has close to ideal adhesion characteristics; glass and polished metal surfaces resulted in excessive adhesion whereas silane treated glass and teflon surfaces had insufficient wetting characteristics and resulted in film wrinkling during casting.) The free standing PPV precursor films were cut into strips (typically 2-5cm x 100cm) and rolled onto spools for subsequent stretching.

Uniaxial Stretching

A significant element of the present work was the design of an apparatus which would uniaxially stretch continuous films of the PPV precursor in a highly controlled manner. The design which emerged is shown in Fig. 9a (page 35) and a simplified schematic version is shown in Fig. 9b (page 35). The device resembles a calendar and consists of a take-off spool, a pair of nip rolls, two differentially driven heated rolls (for stretching), a second pair of nip rolls and a take-up spool. The feed rolls and first heated roll are synchronously driven to control tension. The 1" nip rolls are polyurethane coated and have adjustable clamping pressure to eliminate upstream tension variability and to insure a smooth feed. The first heated roll is of teflon-coated aluminum construction to allow good heat transfer, low surface friction, and resistance to the corrosive elimination product, HCl vapor. It is heated with an electrical cartridge heater in the center of the roll.

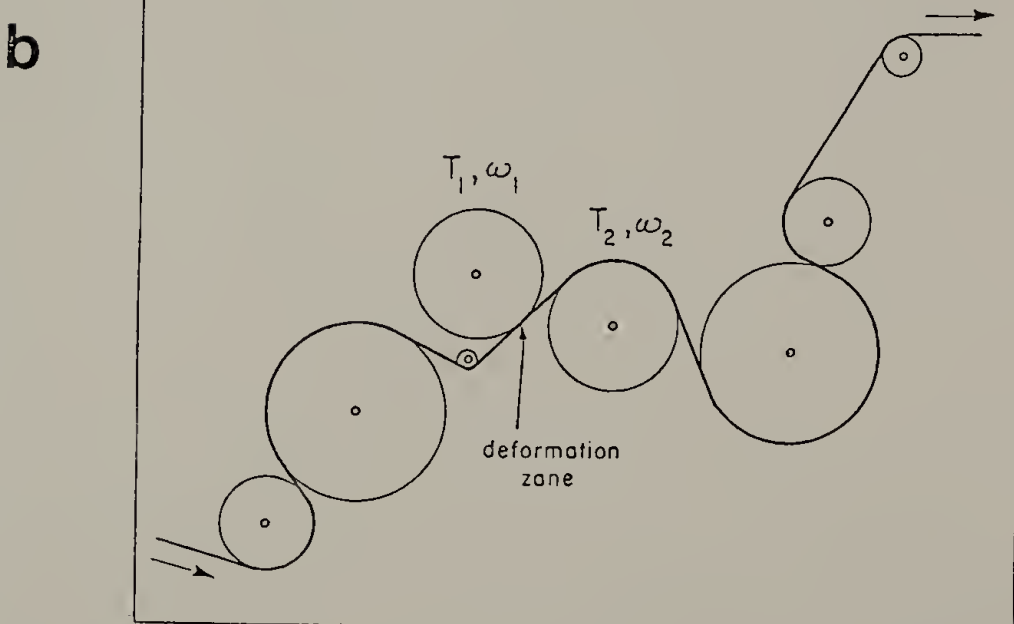
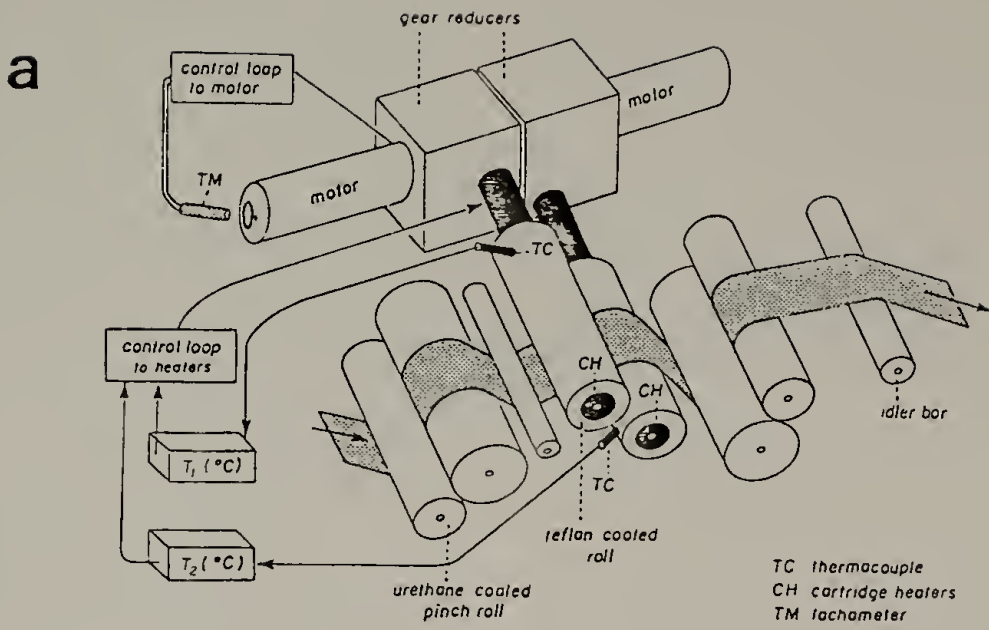


Figure 9 a) Diagram of uniaxial web stretching device used for PPV processing.

b) Simplified schematic diagram of above apparatus emphasizing roll geometry and film path.

Temperature is monitored and controlled through a stationary thermocouple brushing the roll surface. Temperature control of $\pm 1^\circ\text{C}$ is achieved. The second heated roll is of similar design without the teflon coating. The actual stretching process occurs at the surface of the teflon coated roll, nevertheless heating the second roller to 120°C is effective in reducing bowing and wrinkling in the stretched films. The feed system (nip and teflon coated rolls) and take-up system (second heated rolls, nip rolls, and take-up spool) are driven by separate motors at precise rates ($\pm 1\%$) using a closed loop control system. The draw ratio is determined by the ratio of the circumferential velocities of the two heated rolls.

PPV precursor films up to 5 cm in initial width have been stretched easily using this apparatus. The current roller design allows up to 12 cm initial film width material to be stretched. The web stretching apparatus allows considerable variation over roller geometry. The total angle of contact between the film and the heated roll can be varied between 0° and 180° . Other controllable variables include line speed, draw ratio and roll temperature. The device geometry shown in Fig. 9b has been optimized to obtain maximum quality film and the highest attainable draw ratios. An inlet speed of approximately 2.5 cm/min was routinely used. Details of the processing behavior of the PPV precursor will be given in the next chapter.

In order to complete the conversion from PPV precursor to the fully conjugated form the stretched films require annealing at elevated temperatures. In the present study annealing was performed at constant

length (by constraining the film ends) under mild tension, in an air-tight sealed oven (BlueM-DCA-136C) fitted with a nitrogen purge.

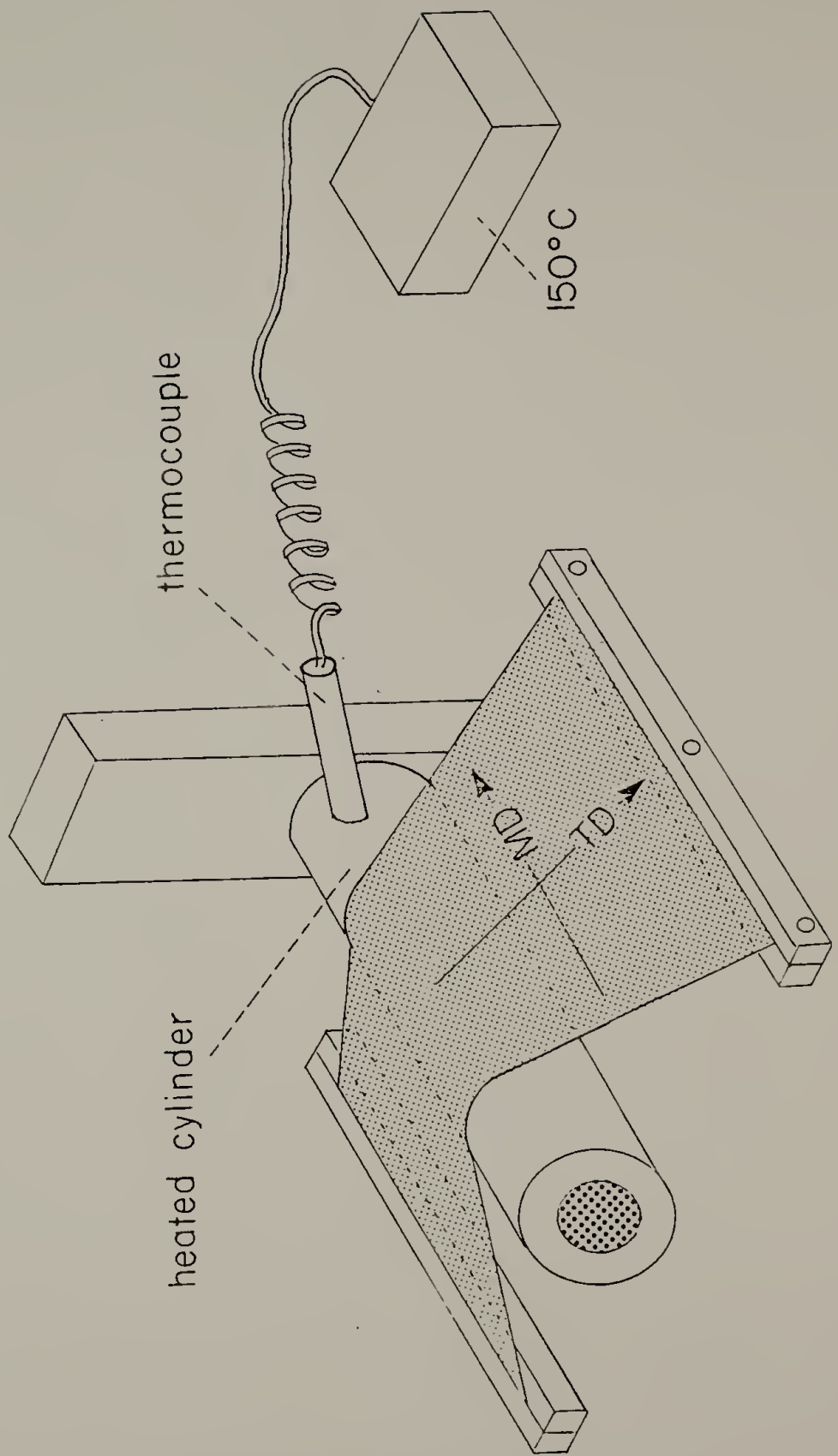
Typical annealing conditions were 250°C for two hours. The optimization of annealing conditions (see Chapter 9) is a compromise between maximizing the extent of thermal elimination and minimizing oxidation of the thermally labile vinylene linkages which are formed. An annealing environment free of oxygen and moisture is essential. Dry nitrogen, argon, or a vacuum better than one millitorr have been used successfully.

Biaxial Stretching

Two techniques were used to prepare biaxially oriented PPV, a two stage sequential stretching procedure and an equibiaxial bubble expansion technique. The two stage process is a modification of the uniaxial process. For two-stage biaxial stretching films were first oriented on the uniaxial web stretching device as detailed previously to a given draw ratio (machine draw ratio). Subsequently, these stretched films, approximately 4 cm in width, were cut into 10 cm lengths. These sections were clamped along the length and then manually stretched in the transverse direction over a teflon coated cylinder heated up to 150°C as shown in Fig. 10 (page 39). Biaxially stretched films were mounted on rigid frames and annealed at 250°C for 2 hours in a sealed oven (Blue M-DCA-136-C) under nitrogen purge to complete the elimination reaction.

For equibiaxial stretching, freshly cast films were secured in a sealed circular clamping device. One side of the film was in contact with the atmosphere, the other side of the film was in contact with a sealed reservoir of air at ambient pressure (see Fig. 11 [page 40]). To effect biaxial stretching, the sample and mount were placed in a vacuum

Figure 10. Diagram of transverse stretching apparatus used for two stage biaxial stretching of PPV film. Here MD is machine direction and TD is transverse direction.



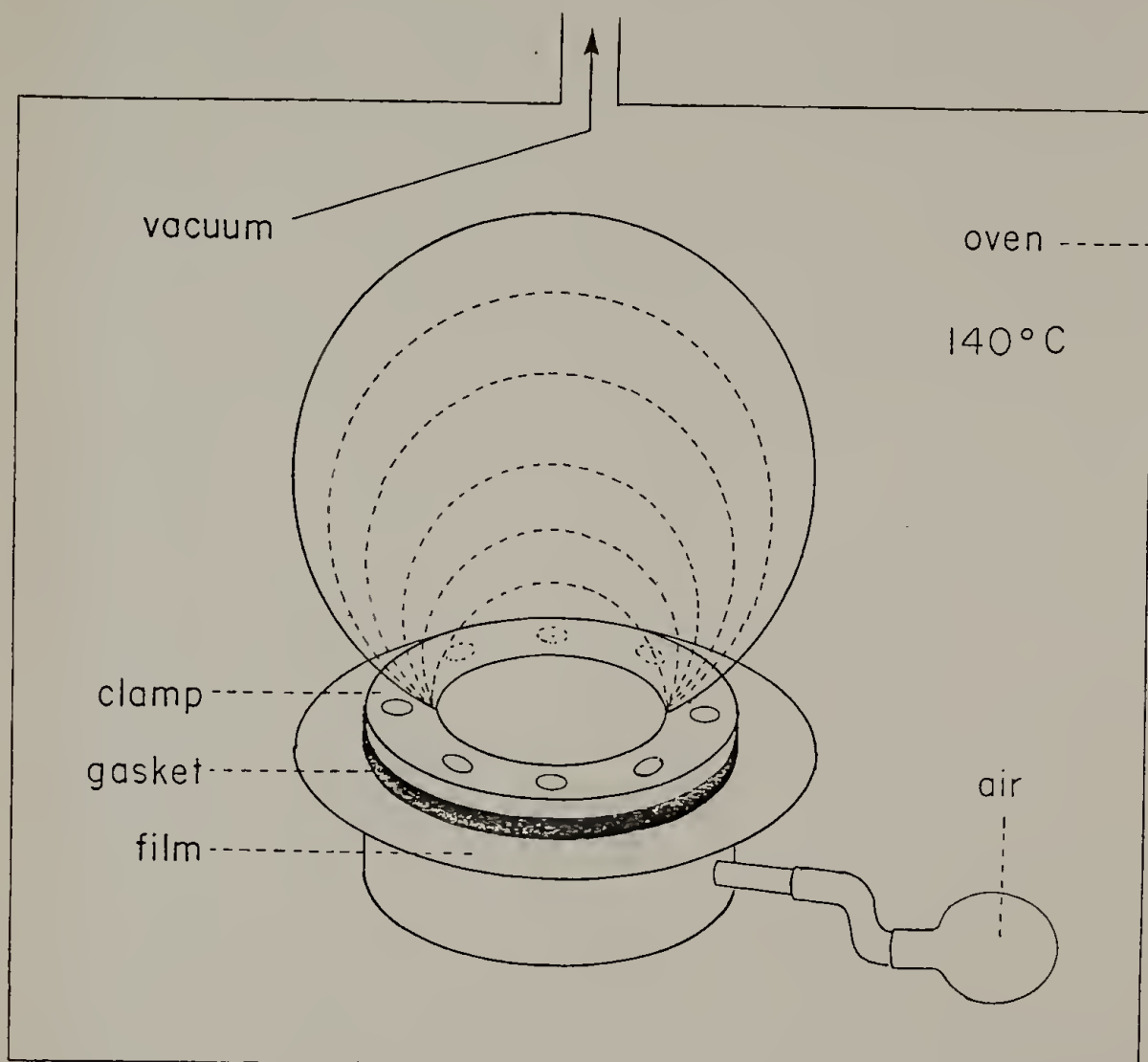


Figure 11. Diagram of bubble expansion process for equibiaxial stretching of PPV precursor.

oven preheated to 140°C and a vacuum was applied. As the film heated and temporarily softened, the pressure gradient caused the film to expand evenly forming a spherical bubble. Such films were annealed as previously described, inflated with a slight positive pressure of nitrogen.

Characterization Techniques

Infrared Dichroism

The degree of molecular orientation in stretched PPV films was determined using infrared dichroism. The measurements were made using a Mattson Cygnus 100 Fourier transform infrared spectrometer fitted with a Harrick Scientific (PWG-U1R) gold wire grid polarizer positioned in the beam path between the source and the sample. The oriented PPV film samples were mounted with the direction of orientation at +45° to the vertical. Spectra were collected with the polarizer electric field vector oriented at +45° and -45° to the vertical which is 0° and 90° respectively to the sample orientation. This procedure is suggested in order to cancel the effect of instrumental vertical polarization of the IR source.¹⁰² Spectra were calculated averaging 50 scans with 2cm⁻¹ resolution using Happ-Genzel apodization.

The molecular orientation function was calculated following the analysis of Bradley et al.⁸⁰ The dichroic ratio (R) of a given absorbance is defined as the ratio of the integrated absorbance with the polarizer oriented respectively perpendicular and parallel to the sample stretching direction (A_{\perp}/A_{\parallel}). The first order orientation function, f,

is defined as $f = (3\langle \cos^2 \gamma \rangle - 1)/2^{103}$, where γ is the angle that the local chain axis makes with the laboratory axis, in this case the sample stretching direction. In the present case, f , for any infrared absorbance, is given by:

$$f = (R-1)/(R-1+1.5 \sin^2 \theta - 3R \cos^2 \theta)$$

where θ is defined as the angle between the transition dipole moment vector of the infrared mode and the chain axis vector. This equality is based only on the assumption of fiber (cylindrical) symmetry of the molecular orientation distribution function and is valid for any (symmetric) orientation distribution.¹⁰² The values of theta for a number of PPV infrared bands have been reported by Bradley et al.⁸⁰

The previous treatment may be shown to be equivalent to the more usual one where the dichroic ratio, D , is defined as A_{\parallel}/A_{\perp} , the inverse of R . In this case, f is given by:

$$f = [(D-1)/(D+2)][(2\cot^2 \theta + 2)/(2\cot^2 \theta - 1)]^{103}$$

Tensile Properties

The tensile properties of oriented PPV films were determined using an Instron Model 4202 universal testing machine. To the extent it was possible, the testing was performed according to ASTM test D882 (standard test for tensile properties of thin plastic sheeting).¹⁰⁴ The mechanical properties of oriented samples were, of course, anisotropic. For the determination of properties parallel to the machine direction (stretching direction), a gauge length of 75mm was used. For transverse property measurement, it was necessary to use a reduced gauge length of

12mm, due to the limited width of stretched films. In either case samples were prepared at a width of 5.1mm. Thickness ($5\mu\text{m}$ to $30\mu\text{m}$) was determined by averaging five micrometer readings. To facilitate proper mounting of thin films, samples were first positioned on cardboard mounts and secured at both ends with epoxy adhesive. The frame-type mount was then positioned properly in the machine grips and the frame was cut away before initiating the test. In all tests a 2 percent/min ($3.3 \times 10^{-4} \text{ sec}^{-1}$) constant strain rate was used. Extension was determined by grip separation. Force was measured using a calibrated 50Kg load cell. For each reported result, five samples were tested, of which three were used to calculate an average.

Chemical Doping Procedures

Chemical doping of PPV samples was performed using the oxidizing agents arsenic pentafluoride (AsF_5) and antimony pentafluoride (SbF_5). The reactivity and toxicity of these dopants as well as the atmospheric instability of the doped polymer necessitate the use of high vacuum line doping procedures. The specification of the glassware used and procedures for dopant manipulation, storage, and purification have been detailed elsewhere.^{105,106}

The electrical conductivity of the sample was monitored during the doping process. Samples were prepared (15mmx5mm) from oriented film and mounted in the four probe configuration as shown in Fig. 12 (page 44). Electrical contacts between the sample and platinum lead wires were made using colloidal graphite conducting adhesive (Electrodag 502). Each sample was mounted in an evacuable vessel. Typically a separate

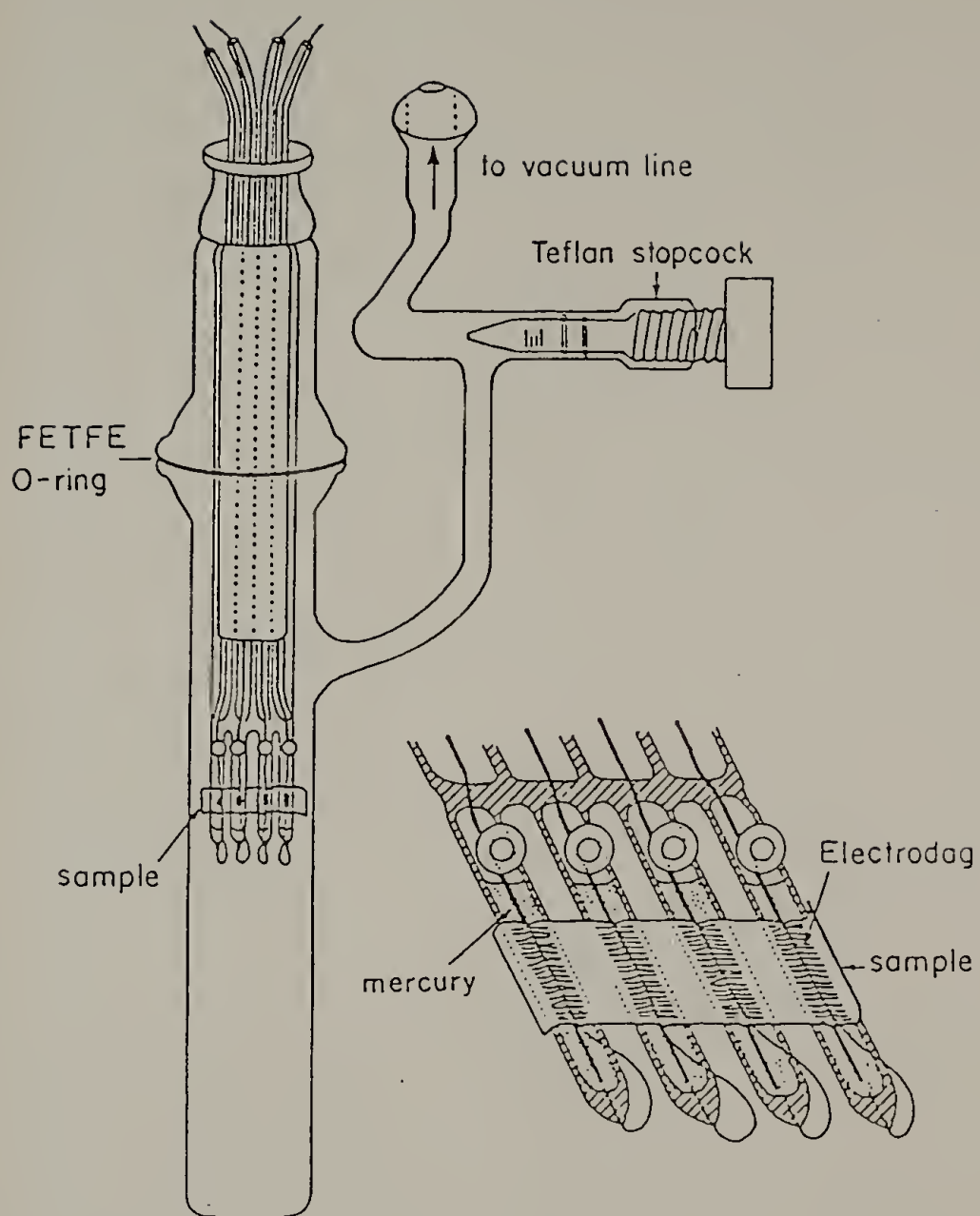


Figure 12. Four-probe apparatus for simultaneous chemical doping and conductivity measurement.

pre-weighed sample (~1 mg) was also placed in this doping vessel for dopant weight uptake determination.

After sample mounting, the doping vessel was placed on a high vacuum line and evacuated for approximately 16 hours to a pressure of less than 10^{-4} torr. At this time, the vessel was closed to the main manifold and exposed to dopant vapor.

In the case of doping with SbF_5 , which is a liquid at room temperatures, exposure was performed by opening the stopcock to a sidearm vessel as shown in Fig. 13a(page 46). Thus the vapor pressure of the liquid dopant at room temperature (4 torr) fills the doping vessel and oxidizes the sample. In the case of doping with AsF_5 , which is a gas at room temperature, the dopant is kept in a storage bulb as shown in Fig. 13b (page 46). The bulb contains a cold finger which is in contact with a methanol bath held at a controlled temperature (Neslab Cryocool-100II immersion cooler). Thus the temperature of the bath is used to control the vapor pressure of dopant in the bulb. To initiate doping, the doping vessel is opened to a submanifold which is also open to the AsF_5 storage bulb (Fig. 13b). The electrical resistance of the samples was monitored using a Kiehley 197 digital multimeter connected to the four-probe apparatus. The resistance is determined by passing a known current through the outer probes, measuring the voltage difference across the inner probes, and applying Ohm's law. The material conductivity (current density/electric field) is calculated by normalizing the resistance by the sample dimensions so that $\sigma = (I1)/(Vwt) = (1/wt)1/R$ (where w and t are the sample width and thickness respectively and l is the distance between the inner electrodes).

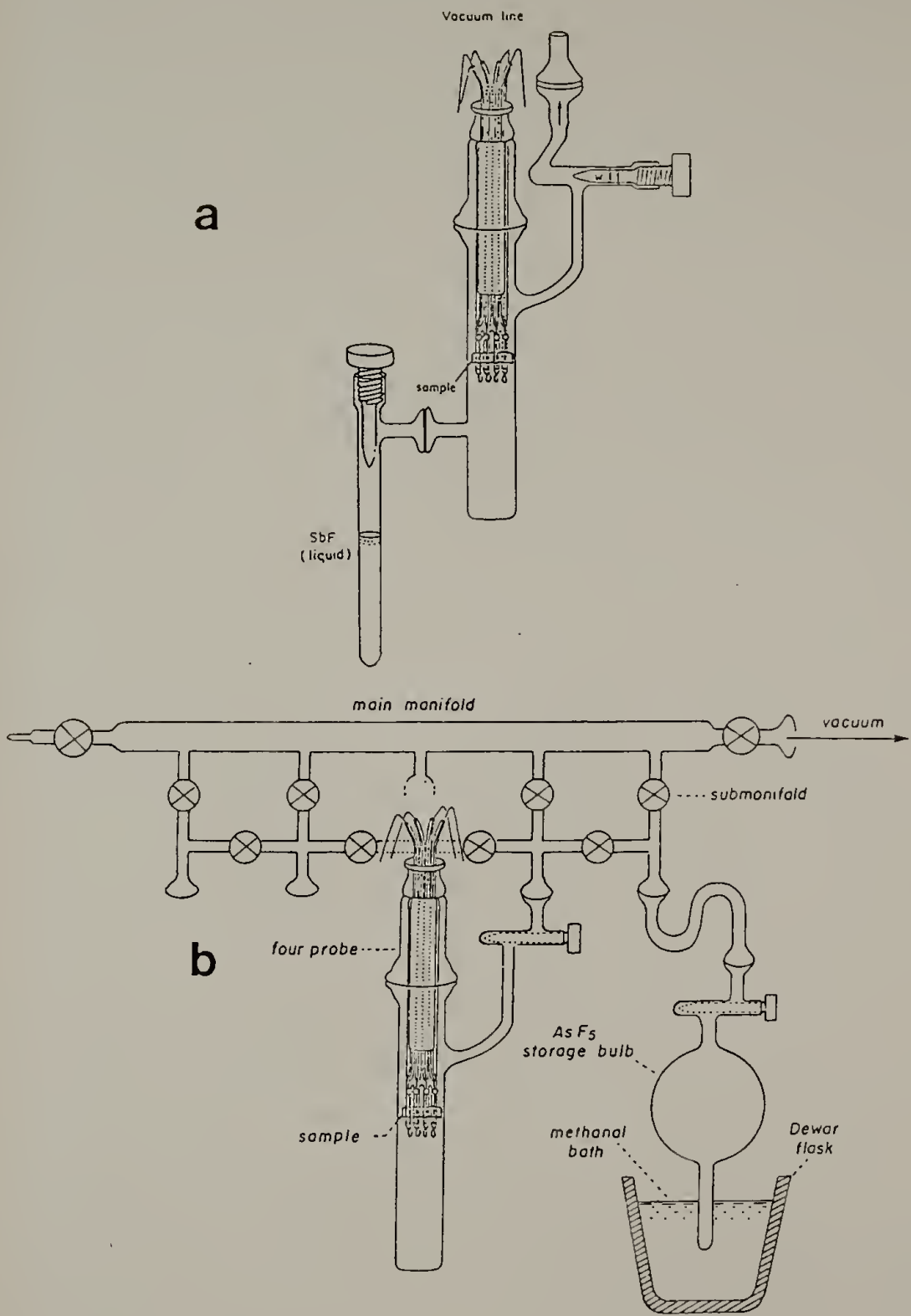


Figure 13. Vacuum line assembly for chemical doping reactions.
a) SbF₅ doping b) AsF₅ doping

Doping was typically allowed to proceed until conductivity reached a maximum. This amount of time varied between six hours and six weeks depending upon the sample type and the doping conditions employed. Doping was terminated by cryogenically removing the dopant vapor, then re-opening the doping vessel to the main manifold and evacuating for at least 24 hours. The final conductivity was then recorded.

Dopant weight uptake was determined by transferring the evacuated vessel to an argon filled Vacuum Atmospheres drybox and weighing the separate uptake sample on a Cahn 31 microbalance. The weight change upon doping was used to calculate the polymer/dopant stoichiometry.

The electrical properties of oriented materials were anisotropic. Thus this procedure was performed separately with samples mounted in the machine and transverse directions.

Blend Studies

Blend Preparation

Blends were prepared between PPV and a series of commercially available water soluble polymers. The procedure for blend preparation is shown schematically in Fig. 14 (page 48). Aqueous stock solutions of the PPV precursor were prepared at concentrations of 0.2 wt % (based upon the final weight of fully eliminated PPV). Similar aqueous stock solutions of the polymers to be blended with PPV were also prepared (polyvinyl methyl ether, polyethylene oxide, polyvinyl pyrrolidone, methyl cellulose, and hydroxypropyl cellulose).

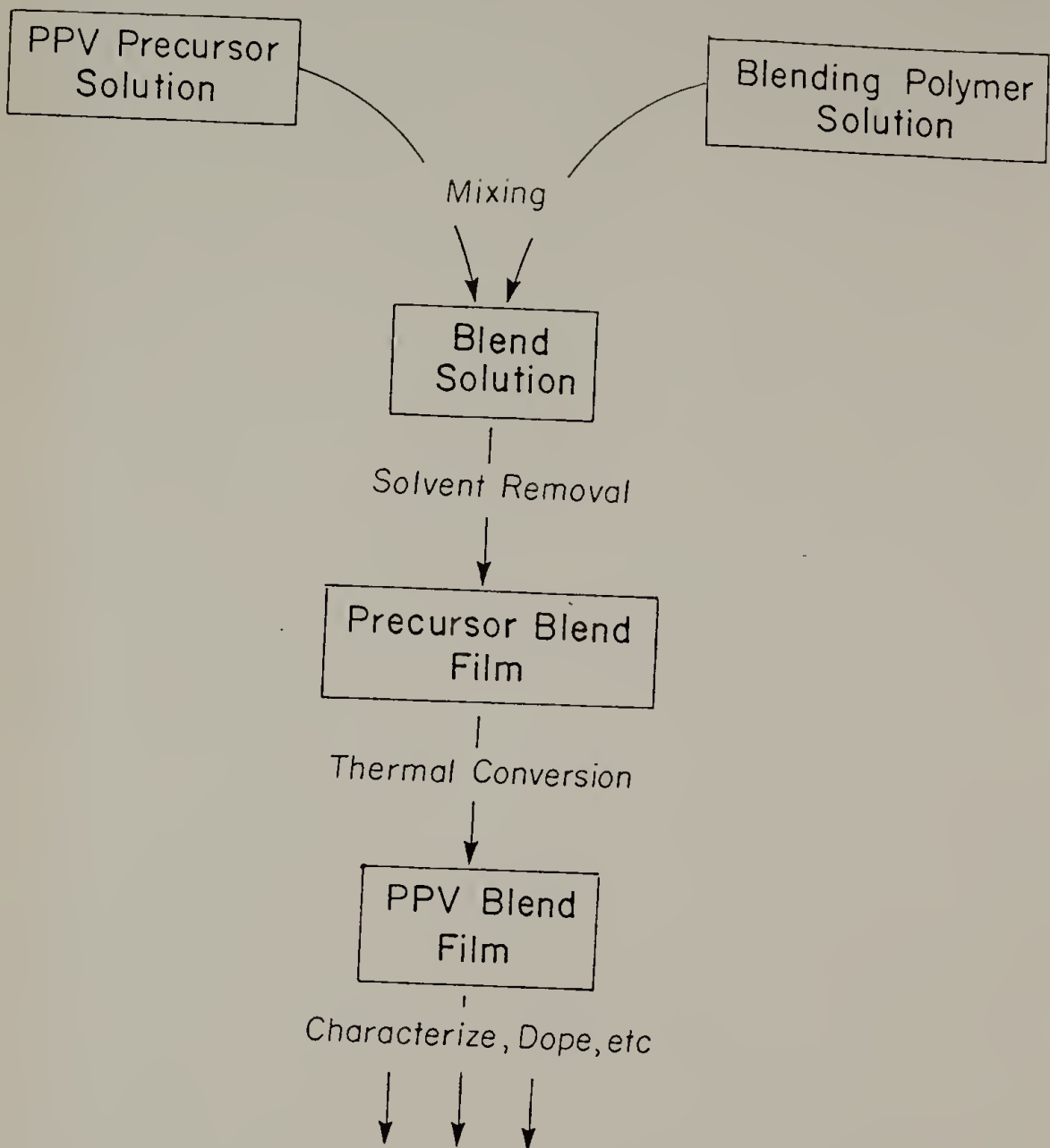


Figure 14. Schematic diagram of blend preparation method.

Blend solutions were prepared by combining aliquots of stock solutions in appropriate quantities. Blend solutions were vigorously stirred for several hours and then poured into silanized glass casting dishes. Films were cast by removing solvent at room temperature under dynamic vacuum. Free standing films 10-50mm thick were obtained. Conversion of the precursor in the blends to fully conjugated PPV was performed by heating the film slowly under vacuum to the desired temperature (typically 200°C) and maintaining this temperature for four hours. Mild annealing conditions were used so as not to cause degradation of the non-PPV constituent. Blend compositions were determined by elemental analysis (University of Massachusetts Microanalytical laboratory) and by infrared spectroscopy using a Mattson Cygnus 100 FTIR spectrometer.

Blend morphology was determined using differential scanning calorimetry, optical microscopy, and solvent extraction techniques. The chemical doping of PPV blends with AsF₅ at 50 torr was performed as described earlier. Blends were also doped electrochemically.

Differential Scanning Calorimetry

The state of dispersion of the blend constituents was examined using differential scanning calorimetry (DSC). Experiments were performed using a Perkin Elmer DSC-4 with helium purge and liquid nitrogen coolant. Heating and cooling rates of 20°C/min were used. Temperature and energy calibrations were performed against cyclohexane and indium standards.

DSC is often a simple and reliable technique for the determination

of polymer miscibility¹⁰⁷. Miscible polymer pairs generally exhibit a composition dependant glass transition temperature intermediate between those of the two pure constituents, whereas immiscible polymer pairs exhibit their glass transitions independently in the blend. Thus for PPV blends the expected lack of mixing on a molecular level was verified by the equivalence of the glass transitions of the non-PPV constituent in its pure state and in its blend with PPV.

For PPV blends with semi-crystalline polymers (PPV/PEO) DSC was also used to examine the melting behavior. The melting temperature was used as a qualitative indication of crystallite size. The area of the melting endotherm was used to calculate the degree of crystallinity of the semi-crystalline component, $X_{\text{cryst.}}$, according to the relation:

$$\Delta H_{\text{exp.}} = X_{\text{PEO}} X_{\text{cryst.}} \Delta H^{\circ}$$

Here, $\Delta H_{\text{exp.}}$ is the measured enthalpy of melting, ΔH° ¹⁰⁸ is the enthalpy of melting of pure crystals, and X_{PEO} is the weight fraction of PEO determined by oxygen analysis.

Optical Microscopy

The morphology of phase separated blends was examined using optical microscopy on a Zeiss Ultraphot II microscope fitted with polarizer, analyser, and 35mm camera attachment. A number of experiments with PPV/PEO blends were performed using the above instrument and a Mettler hot stage with programmable temperature control to examine morphological changes during melting and subsequent recrystallization of the PEO constituent.

Extraction Studies

A series of experiments was performed to determine the extent to which the non-PPV constituent could be extracted in PPV blends. Since fully annealed PPV has no known solvents, this was easily performed by immersing pre-weighed PPV blend samples into a good solvent for the second constituent (typically chloroform). The samples were agitated in the solvent for three days, removed, and thoroughly vacuum dried. The dry, extracted samples were weighed again. The relative weight loss and known initial composition was used to calculate an extraction efficiency.

Electrochemical Doping

Fully dense PPV prepared by the precursor process cannot be doped electrochemically. However, PPV blends exhibited rapid and reversible electroactivity. The electrochemical doping of PPV blends in this study was performed by Dr. J.B. Schlenoff. Experiments were performed in an argon filled Vacuum Atmospheres drybox. A two electrode cell¹⁰⁹ was used with the PPV blend as positive electrode and lithium ribbon (Alfa Ventron) as counter/reference electrode. Doping was performed in 1M LiClO₄ propylene carbonate electrolyte at an applied potential of +4.1V versus Li for approximately six to ten hours. Potential was controlled using a Princeton Applied Research (PAR) 173 potentiostat. The doping level was measured coulometrically using a PAR 179 coulometer. Electrical conductivity was measured by removing the sample from the cell, wiping it dry, and measuring resistance in a four probe configuration with platinum wire pressure contacts.

CHAPTER IV

PROCESSING AND CHARACTERIZATION OF UNIAXIALLY ORIENTED PPV

A major objective of this work was the development of improved processing techniques for poly(phenylene vinylene) prepared by the poly(sulfonium salt) route. This chapter includes the description of a continuous process which has been used to produce oriented films of poly(phenylene vinylene) by simultaneous thermal elimination and uniaxial stretching of the poly(sulfonium salt) precursor polymer. The method provides exceptional control over drawing conditions (temperature, draw ratio, etc.) allowing the preparation of high quality film with draw ratios up to twelve. The evolution of molecular orientation with draw ratio determined using infrared dichroism will be discussed and the results compared to theoretical expectations. Chemical doping results relating the electrical conductivity in both the machine and transverse directions to the draw ratio and degree of orientation will also be presented in this chapter.

Polymer Synthesis and Film Casting

The PPV precursor, poly(xylylidene tetrahydrothiophenium) chloride, has been prepared on a large scale in order to obtain sufficient quantities for subsequent operations. The scaled-up syntheses have proceeded just as the bench scale preparations which have been reported.¹⁰⁰ Monomer yields were typically 75% consistent with previous results for

the bis-tetrahydrothiophenium monomer⁹⁶. The large-scale polymer syntheses typically gave 20% yield compared to 40% from the literature.¹⁰¹ However, the difference probably lies in the method of purification. Previous work has purified the crude polymer from unreacted monomer and low molecular weight by-products using membrane dialysis techniques. However, dialysis on the 25L scale is impractical. Isolation by the precipitation technique used in this study greatly facilitated material storage, handling, and the preparation of high-concentration casting dopes. Molecular weight characterization of the polymer was performed by ion-exchange to the tetrafluoroborate poly(sulfonium salt) followed by GPC in DMF. Various polymerization batches consistently gave $M_N \sim 5 \times 10^5$ and $M_w \sim 10^6$ relative to monodisperse polystyrene standards.¹¹⁰

The film casting technique described in the experimental section produced large-area (20 cm x 100 cm) PPV precursor film of exceptional quality. The plexiglass casting surface had good wetting characteristics with aqueous casting dopes such that no wrinkling occurred during film drying. Variations in film thickness were less than 10% over the full one meter length of cast film. The use of filtered, degassed dopes and a filtered air stream resulted in optically clear films free of particulates. These large, uniform films were required for the uniaxial stretching studies (see Fig. 15a [page 55]).

Figure 15. a) Photograph of film casting apparatus.
b) Photograph of uniaxial web stretching
apparatus in operation (draw ratio = 10.0).



Processing Behavior

The facile stretching of the PPV precursor was originally reported by Wessling⁷⁶ and has been discussed by Gagnon et al.⁷⁹ and Bradley¹¹¹. It is agreed that stretching is facilitated by a temporary plasticization which occurs upon heating as a result of the sudden evolution of elimination products and residual solvent. Elongation to very large strains ($l/l_0 > 10$) is possible under appropriate conditions. In the present study, the film is stretched while in contact with a heated roll. Fig. 15b shows the stretching apparatus in operation. Critical parameters to the success of this process are roll surface friction, roll-film residence time, and temperature.

Initial studies using an aluminum roll surface and large film contact angle ($\sim 60^\circ$) showed that extension did not occur until the heated film had left the roll surface. At this point (~ 1 minute residence time) much of the volatilization/plasticization had already occurred and only moderate draw ratios (up to six) could be achieved. After leaving the roll surface, the film is unconstrained in the transverse direction and thus a considerable reduction in film width (50-70%) accompanied stretching. Better results were obtained by reducing the film contact angle to 2° or 3° (as in Fig. 9) a tangent and applying a teflon coating to the heated roll surface. In this way friction was reduced sufficiently to allow stretching to occur immediately upon heating at the point of maximum softening, thus allowing high draw ratios to be achieved.

Using the apparatus geometry shown in Fig. 9 of Chapter 3 (page 35) which was optimized for the maximum range of draw ratio and film quality, a general relationship between stretching temperature, draw ratio, and film quality was established. The draw ratio, λ_{11} , determines the total imposed strain and the film/roll residence time and the roll temperature, T_1 , determines the rate of volatilization and thus the degree of plasticization. Data were obtained by continuously varying the draw ratio at a given roll temperature and noting changes in film quality. The results, given in Fig. 16 (page 58), allow the establishment of three processing regimes:

- (1) At higher temperatures and lower draw ratios (see Fig. 16), the extent of volatilization is excessive in comparison to the ability of gases to diffuse out of the film. Essentially a mild foaming operation occurs and this region is characterized by the formation of bubbles.
- (2) By either reducing the roll temperature or increasing the draw ratio, a region of clear, high quality film is reached where the degree of plasticization is commensurate with the imposed strain. This region of high quality film is represented in Fig. 16 as solid vertical lines and defines the desirable processing window.
- (3) A decrease in temperature or increase in draw ratio results in increased line stress to a point where the film acquires a white, hazy appearance (resembling the stress-whitening effect in ductile polymers). A further temperature decrease or draw ratio increase results in film fracture due to tensile failure.

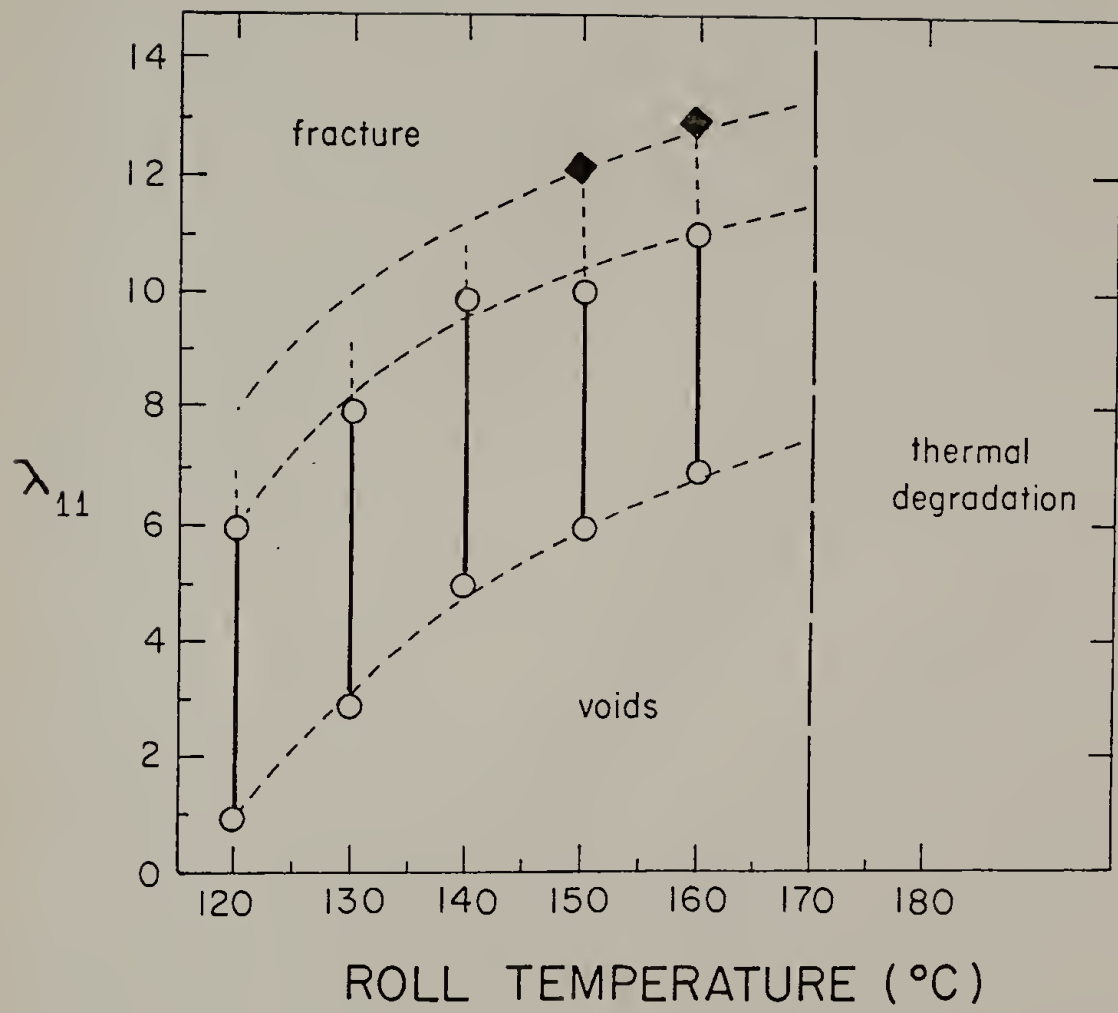


Figure 16. Processing behavior for PPV precursor as a function of heated roll temperature and draw ratio. Solid vertical lines denote region of clear, high quality film, open circles represent transitions to bubbled or hazy film, solid diamonds represent film fracture.

Micrographs of films prepared in the three processing regimes are presented in Fig. 17 (page 61). These were obtained by drawing at 150°C and varying the draw ratio. At low strain ($\lambda_{11} = 2.0$), macroscopic bubbles were formed (Fig. 17a). These bubbles were elongated as a result of stretching, typically to several hundred microns in length and up to one hundred microns in width. At intermediate draw ratios (Fig. 17b; $\lambda_{11}=6.0$), the film was essentially clear and homogeneous, although some striations in the machine direction have been thus far unavoidable. At very high draw ratios (Fig. 17c and 17d; $\lambda_{11} = 11.0$) it was apparent that the observed haziness is a result of scattering from microscopic cracks (~5 μm wide) which are oriented in the transverse direction and distributed uniformly throughout the film. The observed structure is very similar to that reported for polypropylene after micro-cavitation or crazing upon stretching,¹¹² thus it may be attributed to excessive tensile stress (insufficient plasticization) in the film.

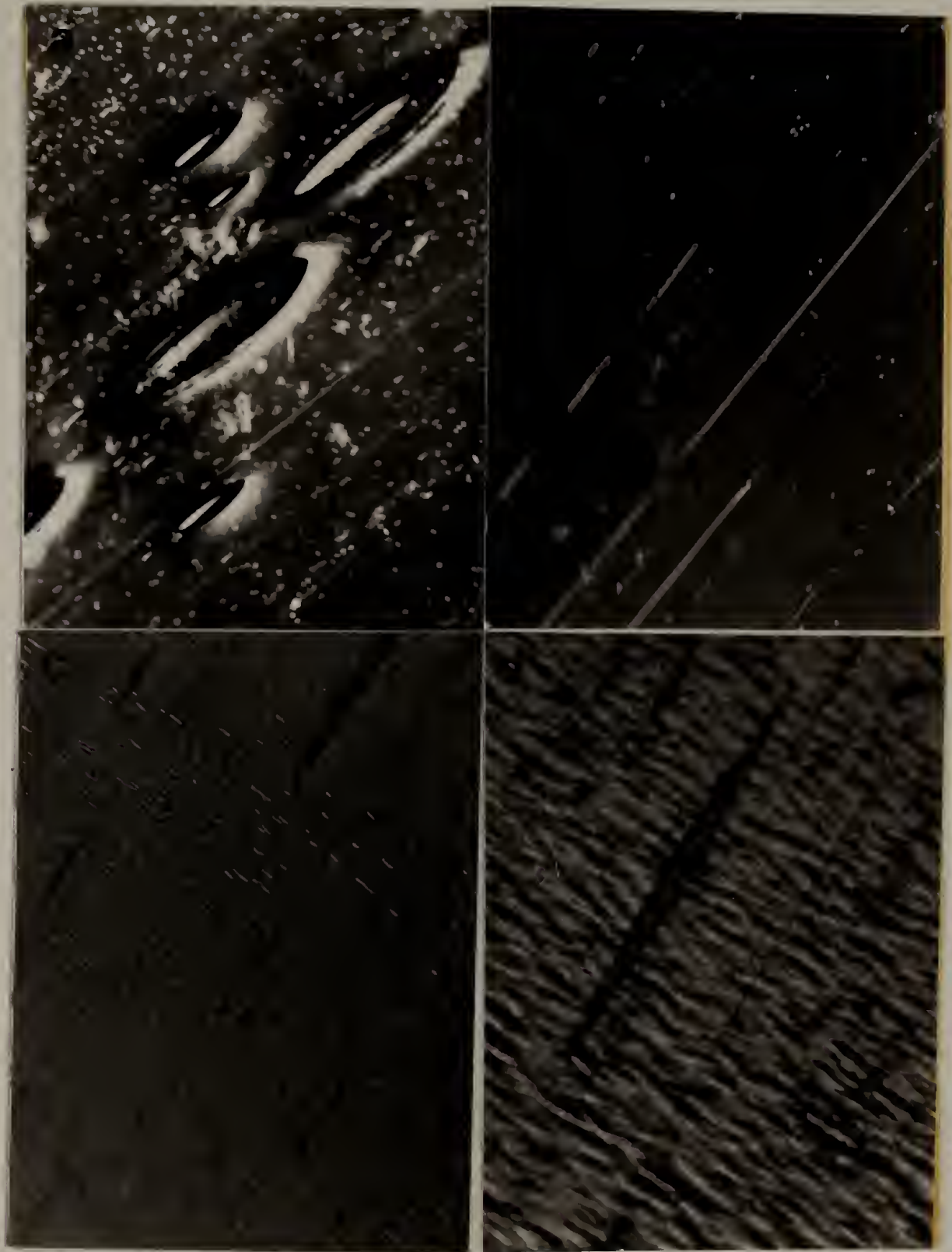
An additional processing constraint is a ceiling temperature of approximately 170°C, above which stretching in the presence of oxygen results in oxidation of the vinylene linkage as determined by elemental analysis and IR spectroscopy.

Deformation Analysis

A complete understanding of the stretching process requires knowledge of the deformation tensor at every point in the film during the process. However, presently an estimation of the uniformity of the

Figure 17. Optical micrographs of oriented PPV film prepared under various processing conditions.

- a) Draw ratio = 2.0; $T_1=150^\circ\text{C}$; 100X
(entrapped volatile bubbles);
- b) Draw ratio = 6.0; $T_1= 150^\circ\text{C}$; 100X (smooth film);
- c) Draw ratio = 11.0; $T_1= 150^\circ\text{C}$; 100X (hazy film;
cavitation)
- d) same as c; 500X.



deformation will prove useful. Ideally, stretching can be modeled as a purely extensional deformation, defined by a deformation tensor, λ_{ij} , where:

$$\lambda_{ij} = \begin{bmatrix} \lambda_{11} & 0 & 0 \\ 0 & \lambda_{22} & 0 \\ 0 & 0 & \lambda_{33} \end{bmatrix}$$

(λ_{ij} relates any material vector, X_j , in the undeformed state to the material vector in the deformed state, X'^j , such that $X_j \lambda_{ij} = X'^j$)

Here, a Cartesian coordinate system is established where direction 1 defines the machine direction, direction 2 defines the transverse direction or direction of film width, and direction 3 defines the direction of film thickness. A homogeneous, isotropic material, under boundary conditions of pure uniaxial tension will deform such that $\lambda_{22} = \lambda_{33}$. However, the roller geometry used imposes a frictional resistance to reduction in film width, but not in the thickness direction.

The normalized macroscopic dimensional changes sustained by the film during the actual stretching operation are plotted in Fig. 18 (page 64). It is apparent that as draw ratio (λ_{11}) increases, the increasing film length is accommodated preferentially by decreasing film thickness, with only small changes in the width. Thus the actual deformation is better approximated by planar extension, in which

$$\lambda_{ij} = \begin{bmatrix} \lambda_{11} & 0 & 0 \\ 0 & 1 & 0 \\ 0 & 0 & \lambda_{33} \end{bmatrix}$$

$$(\lambda_{22} \approx 1; \lambda_{33} \approx \lambda_{11}^{-1})$$

It may be noted from Figure 18 that as the draw ratio increases, the stretched film width actually increases slightly, owing to increased line stress and hence increased frictional forces. This behavior is consistent with the stretching characteristics of many thermoplastic materials oriented by similar means.¹¹³

An unusual characteristic of the present process is the large change in volume which accompanies stretching. In ideal extension, $\lambda_{11}\lambda_{22}\lambda_{33}=1$ (no volume change), and in the drawing of many conventional polymers, strain induced crystallization may reduce the volume by, at most, a few percent. However, in the present case, the chemical conversion from PPV precursor to PPV during stretching results in a volume reduction of nearly 50%. Thus the contribution of shrinkage effects to the deformation process are non-negligible. It may be noted that assuming the deformation, λ_{ij} , arises from an iso-volume planar extension combined with an isotropic volume reduction of 50% due to shrinkage, provides a reasonable agreement with the observed deformation data shown in Fig. 18. A more detailed discussion of the effects of shrinkage is given in the next section (see page 76).

The ability to correlate structural characteristics such as molecular orientation with bulk properties such as electrical conductivity rests on the assumption that the deformation (and hence orientation) is homogeneous throughout the film. The photograph in Fig. 19 (page 66) permits an estimation of the homogeneity of local strain sustained during the stretching process and, moreover, allows estimation of off-diagonal (shear) elements of the deformation tensor, λ_{ij} . The data obtained by passing a film, which had been stamped with a 1/16" square grid, through

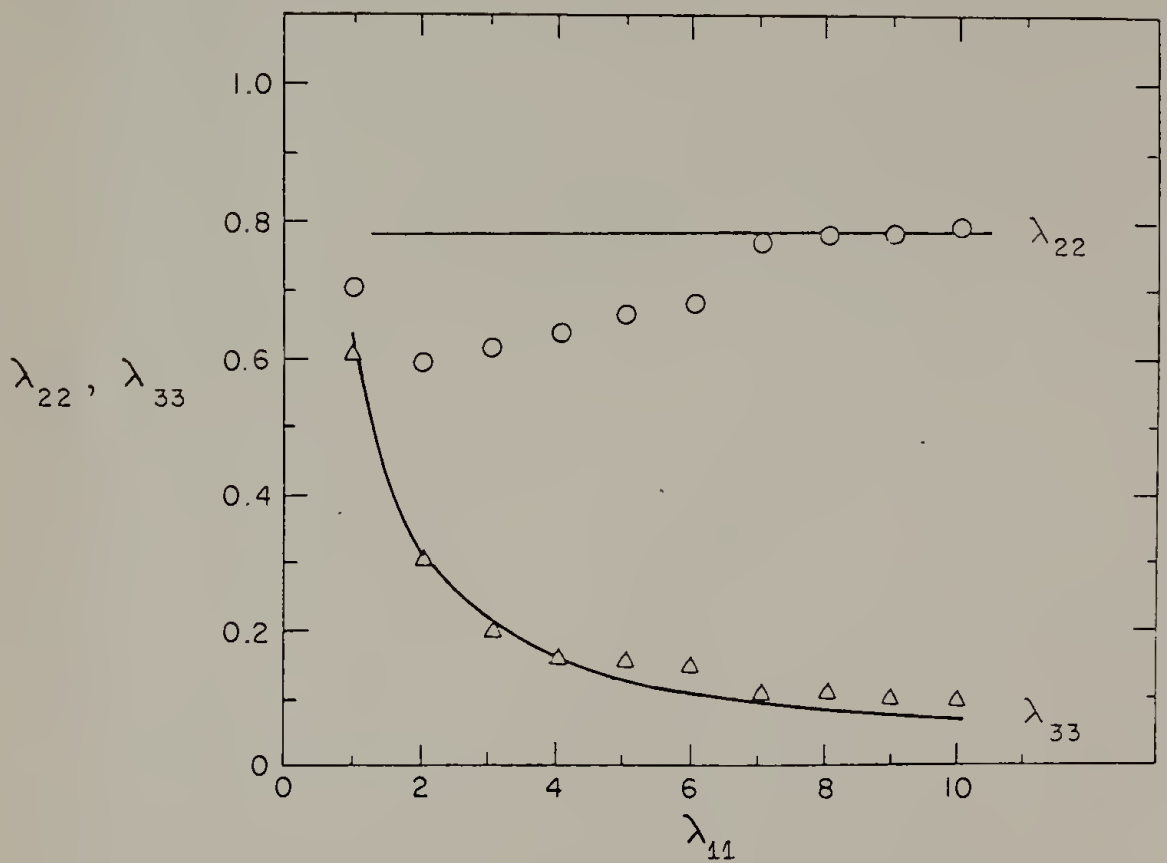
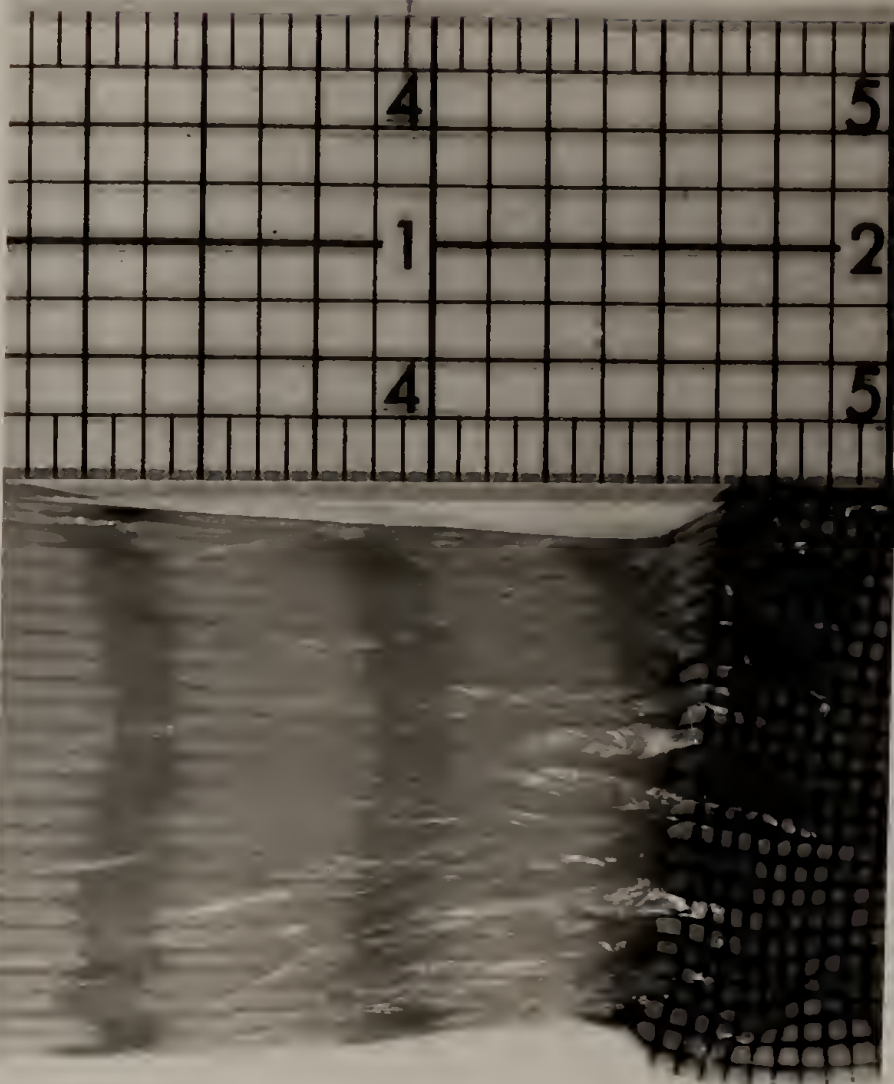


Figure 18. Normalized macroscopic dimensional changes sustained by the film during stretching. λ_{22} (transverse deformation, \circ) and λ_{33} (thickness deformation, \triangle) are plotted a function of λ_{11} , the draw ratio. Solid lines indicate the theoretical prediction of planar extensional flow combines with an isotropic volume reduction of 50%.

Figure 19. Photograph of deformation zone for material stretched at a draw ratio of 10.0. Initial grid is 1/16"; scale shown is in inches.



the stretching apparatus. As the gridded portion passed through the deformation zone, the film was simultaneously cut and removed from the roll. Thus the grid defines surface area elements and provides a means of mapping out the deformation sustained by each element. The sample shown in Fig. 19 has undergone a draw ratio of ten. From this photo, it is apparent squares deform primarily into rectangles as a result of extension. Only at the film edges does the shear component (λ_{21}) become significant so that squares map into elongated parallelopipeds. However, the estimated shear strain at the film edges does not exceed 150% which is small compared to the extensional strain of 900%. Furthermore, shear components are significant only at the outer 10% of the film, otherwise, the deformation is homogeneous and purely extensional. Similar "edge effects" are seen in commercial stretched polymer films.¹¹³ In the present case, film edges were removed prior to subsequent analysis.

Also noteworthy in Fig. 19 is the abruptness of the deformation zone in the machine direction implying a very rapid extensional process. Under steady flow conditions, knowledge of the width of this zone (ΔX), total strain (λ_{11}), and initial line speed (V_0) permits the calculation of an average rate of deformation during stretching. Thus:

$$\left[\frac{d\lambda_{11}}{dt} \right]_{avg} = \frac{\lambda_{11}}{\Delta X} \frac{(V_0 + \lambda_{11}V_0)}{2}$$

For the sample shown in Fig. 19 of the draw ratio ten, this average extensional rate in the neck zone is approximately 7 sec^{-1} . Limitations

in the fineness of the grid which can be prepared on the inlet film, have prevented the determination of the maximum local rate of extension, which is probably considerably higher. In any case, the calculated rate is very large for a solid-state process and would suggest the existence of a truly plasticized, liquid-like or rubbery state.

The magnitude of the deformation rate may explain the differences between the processing behavior reported by Bradley et al. and that observed in the present study. The stretching technique employed by Bradley et al.¹¹¹ is a slower, constant load, creep-type stretching process. They reported a maximum deformation rate occurring at approximately 85°C upon heating and a maximum achievable draw ratio of about six. It was concluded that the primary source of plasticization is the evaporation of residual solvent. The present process, however, employs a rapid heating and deformation rate and significantly higher temperatures (120°C - 160°C) allowing plasticization by both the release of entrapped solvent and the volatile products of elimination. As a result, significantly higher draw ratios can be achieved. High temperatures (~140°C) and rapid manual stretching were also employed by Gagnon to achieve very high draw ratios.^{77,70} Rapid deformation rates and heating rates are required to achieve large strains as a result of the extremely brief period of effective plasticization.

After stretching, films were annealed at elevated temperatures in an inert atmosphere to complete the chemical conversion to PPV. Previous studies have described the sensitivity of final properties to annealing conditions.¹⁰⁰ Most of these studies, which have used the dimethyl

sulfonium derived PPV precursor, have required annealing at temperatures in excess of 300°C for extended periods to achieve complete elimination.^{100,111} Mechanistic investigations have shown that these high temperatures are required for the free radical elimination of neutral thioether pendant groups generated from side reactions of the dimethyl sulfonium moiety.^{100,114} Recent work has shown that cyclic sulfonium precursors do not generate such thioether groups and thus eliminate fully under milder conditions.¹⁰¹ In the present study, the tetrahydrothiophenium chloride based PPV precursor exhibited complete elimination when annealed at 250°C for two hours under nitrogen purge. Oriented samples were annealed at constant length under mild tension. No relaxation of the applied tension was observed during annealing. Typical elemental analysis results for fully converted PPV were:
Anal. Calcd. for C₈H₆: C, 94.12; H, 5.88. Found: C, 92.5; H, 5.66; S, 0.3; Cl, 0.7; O, 0.4. Annealed samples were also characterized by IR spectroscopy and solid-state ¹³C NMR.¹¹⁵

Molecular Orientation

The efficient molecular orientation which accompanies stretching of the PPV precursor has been previously studied using X-ray diffraction⁷⁹ and infrared dichroism.⁸⁰ In the present work, IR dichroism has been used to probe molecular orientation following the analysis of Bradley et al.⁸⁰ The IR spectrum of PPV possesses a number of strong and

narrow bands having transition dipole moments which are either nearly perpendicular or parallel to the chain axis making it an ideal system for dichroism studies. In Fig. 20 (page 72), the dichroic ratios (A_{\perp}/A_{\parallel}) for a number of appropriate bands are plotted as a function of draw ratio. The samples used for these measurements have been stretched under the conditions listed in Table 1.

In agreement with previous data⁸⁰, the largest dichroic ratios were observed for the 558 cm^{-1} absorbance, assigned to a p-phenylene ring bending mode. The dichroic behavior of the remaining strong bands: the 964 cm^{-1} trans-vinylene C-H out of plane bend, 838 cm^{-1} p-phenylene C-H out-of-plane bend, 1518 cm^{-1} p-phenylene ring stretch, and the 3024 cm^{-1} trans-vinylene C-H stretch generate a very consistent picture of the rapid evolution of molecular orientation with extension. Following the analysis of Zbinden¹⁰², the values of θ , defined as the angle which the transition dipole moment vector, M , makes with the chain axis vector, c , for each of the above modes may be calculated from the results in Fig. 20. In Table 2, the values are shown and compared to the results reported in ref. 80. Outstanding agreement is observed confirming the validity of this technique for the PPV system.

Knowledge of the dichroic ratio and θ for a given mode permits the calculation of the first order orientation function, f , which provides a measure of molecular alignment in the material.^{102,103,116}

Table 1. Processing conditions for oriented PPV film used in this study

| Sample | Draw Ratio (W_2/W_1) | Roll Temperature (T_1) |
|--------------------|--------------------------|----------------------------|
| PPV _{iso} | not stretched | -- |
| PPV-1 | 1.0 | 125°C |
| PPV-2 | 2.0 | 125°C |
| PPV-3 | 3.0 | 125°C |
| PPV-4 | 4.0 | 130°C |
| PPV-5 | 5.0 | 130°C |
| PPV-6 | 6.0 | 130°C |
| PPV-8 | 8.0 | 140°C |
| PPV-10 | 10.0 | 145°C |
| PPV-12 | 12.0 | 150°C |

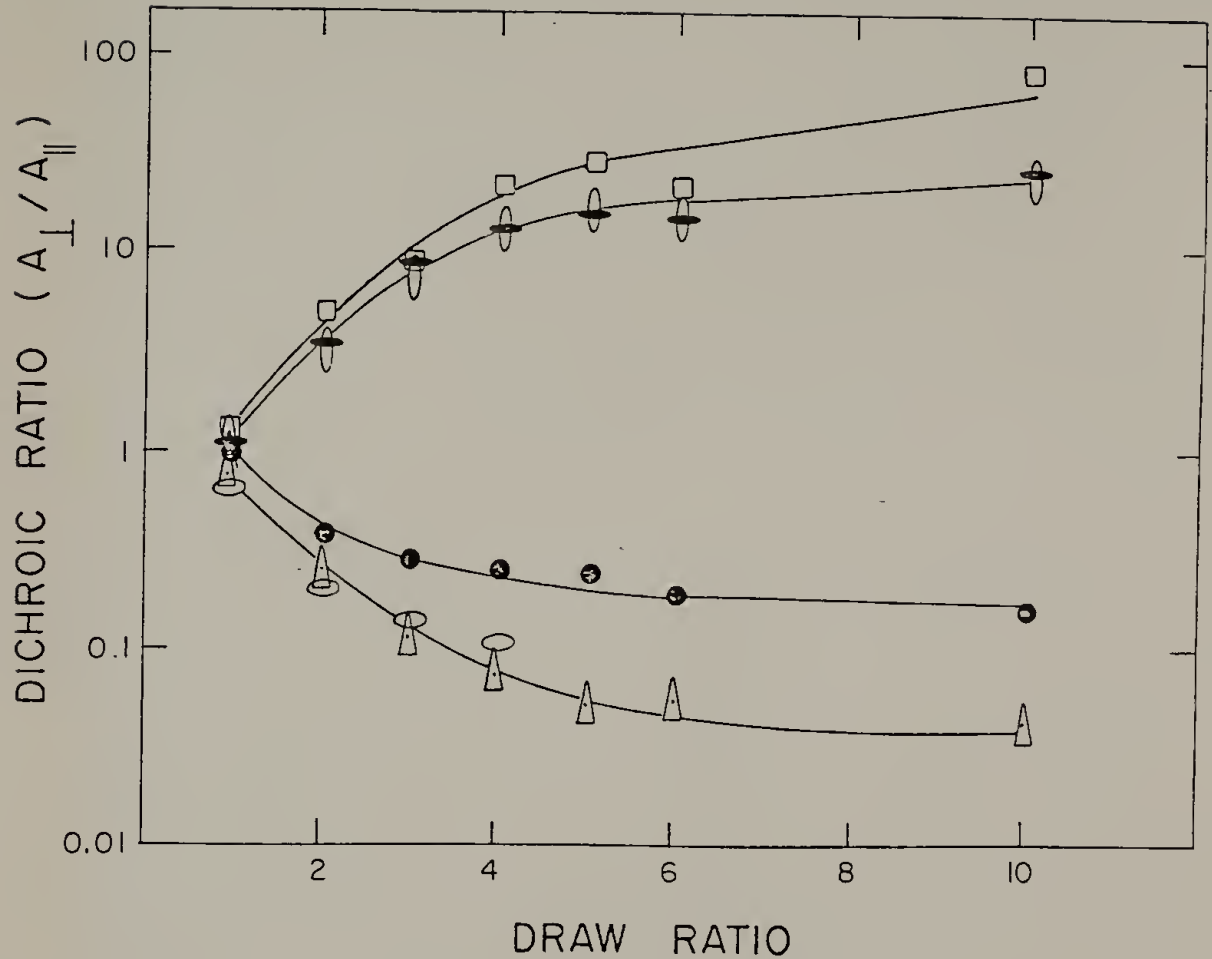


Figure 20. Dichroic ratios of several PPV infrared absorption bands as a function of draw ratio. (\square) 558 cm^{-1} , (\bullet) 964 cm^{-1} , (\circ) 838 cm^{-1} , (\odot) 3024 cm^{-1} , (\blacktriangleleft) 1518 cm^{-1} , (\bigcirc) 2948 cm^{-1} .

Table 2. Calculated values of theta for PPV IR absorbances

| Absorption | θ^* this study | θ from ref. 80 |
|------------------------|--------------------------|--------------------------|
| 558 cm^{-1} | 90° | 90° |
| 838 cm^{-1} | 83° | 83° |
| 964 cm^{-1} | 83° | 84° |
| 1518 cm^{-1} | 14° | 9° |
| 3024 cm^{-1} | 34° | 30° |

*Calculated from dichroic ratios of sample PPV5.

This parameter corresponds to the second moment of the orientation distribution function; however it may also be equated to the fraction of perfectly oriented chains assuming that the remaining chains are randomly oriented. This simplified treatment is justifiable because dichroism provides no information about the functional form of the orientation distribution.¹⁰² Thus, for uniaxial extension, f may assume values between zero and unity.

In Fig. 21 (page 75), the orientation function, calculated from the 558 cm^{-1} dichroic ratio is plotted against draw ratio. Also shown are the theoretical predictions based on a Gaussian chain of 20 Kuhn steps¹¹⁷ and the pseudo-affine deformation scheme of Kratky^{103,118}. Clearly, the Gaussian model is inappropriate for the present case. However, more surprising is the observation also noted previously by Bradley⁸⁰ that the experimentally observed efficiency of molecular orientation exceeds that which is predicted by the pseudo-affine model. This model excludes relaxation effects of any kind and so is frequently considered an upper limit to the development of molecular orientation during stretching.¹⁰³

The observed deviation from the Kratky model may be partially explained by shrinkage effects. As previously noted, the present stretching process is accompanied by a considerable reduction in volume.

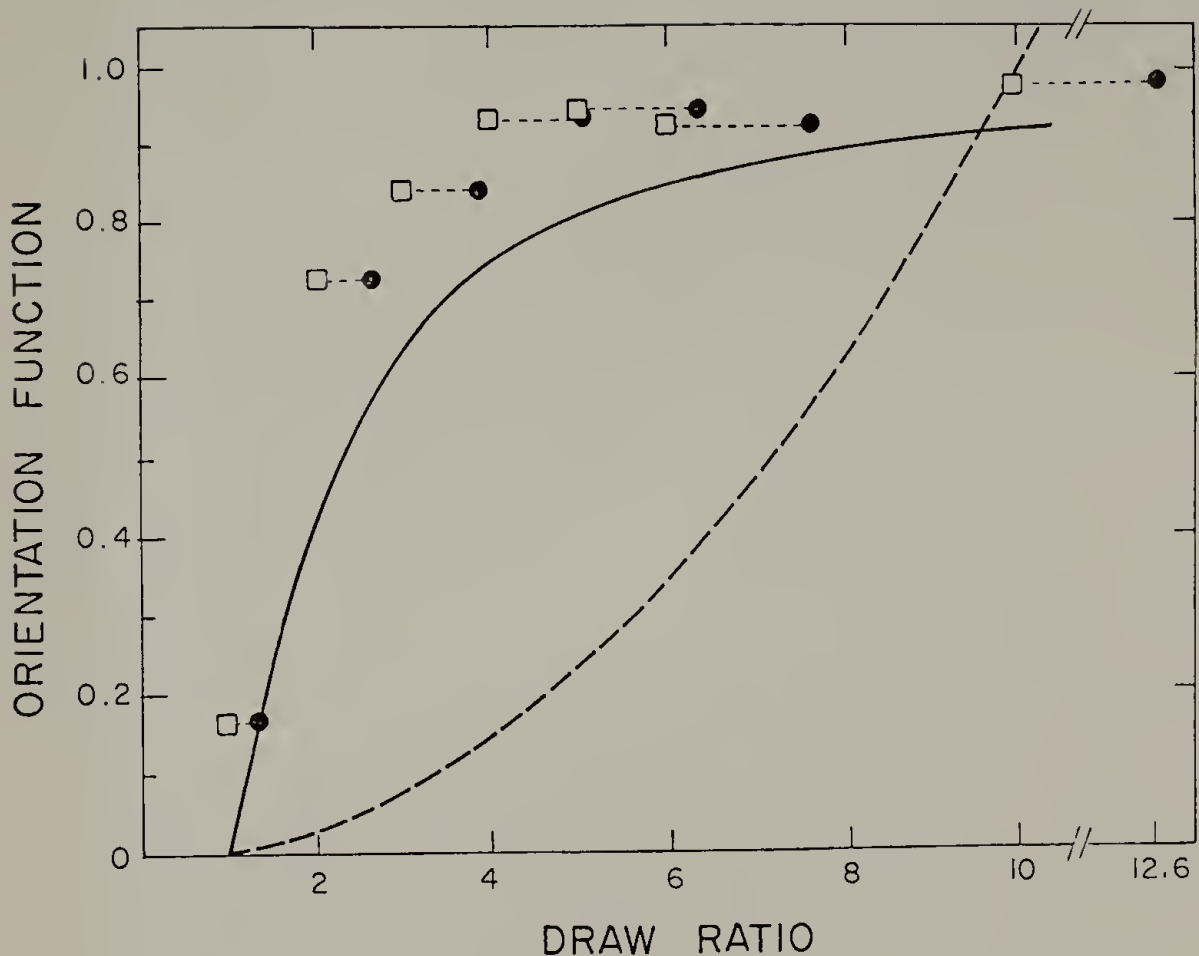


Figure 21. First order orientation function of PPV molecular axis with respect to the machine direction, calculated from the 558 cm^{-1} dichroic ratio, plotted as a function of (□) draw ratio and (●) extensional deformation corrected for volume shrinkage (see text). Dashed line indicates theoretical prediction of Gaussian chain of 20 Kuhn steps; solid line indicates prediction of pseudo-affine deformation model.

Therefore it is not unreasonable to decompose the net deformation tensor into a component arising from isotropic shrinkage and a component, λ'_{ij} , associated with iso-volume extension. Thus

$$\lambda_{ij} = \begin{bmatrix} \lambda_{11} & 0 & 0 \\ 0 & \lambda_{22} & 0 \\ 0 & 0 & \lambda_{33} \end{bmatrix} = (V_f/V_0)^{1/3} \begin{bmatrix} 1 & 0 & 0 \\ 0 & 1 & 0 \\ 0 & 0 & 1 \end{bmatrix} \begin{bmatrix} \lambda_{11} & 0 & 0 \\ 0 & \lambda_{22} & 0 \\ 0 & 0 & \lambda_{33} \end{bmatrix} = (V_f/V_0)^{1/3} \delta_{ik} \lambda'_{kj}$$

where the deformation of material vectors follow: $X_i(V_f/V_0)^{1/3} \delta_{ij} \lambda_{jk} = X'_k$

$$\text{Solving for } \lambda'_{11} : \quad \lambda'_{11} = \lambda_{11} (V_f/V_0)^{-1/3}$$

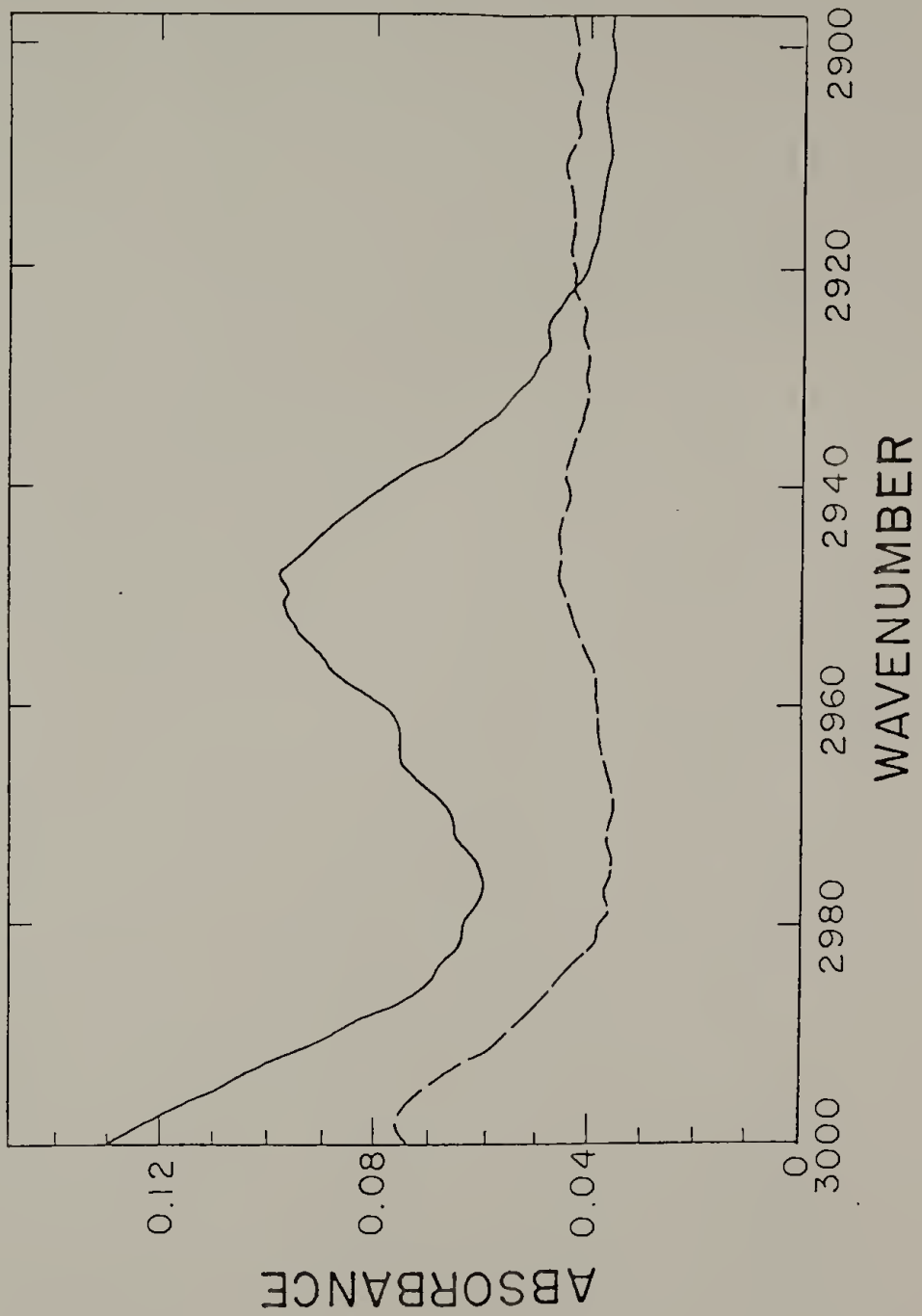
$$\text{Assuming a 50\% volume reduction: } \quad \lambda'_{11} = 1.26 \lambda_{11}$$

Thus the primary extensional deformation sustained by material elements, when referred to their final state, is 26% larger than the nominal draw ratio. The validity of this correction becomes particularly apparent upon noting the observed molecular orientation of material with a nominal draw ratio of one. This sample was passed through the drawing device with equal feed and take-up velocities. However, because it experienced shrinkage at constant length, significant molecular orientation ($f = 0.17$) developed. Correcting the data in Fig. 21 by the calculated factor provides an improved fit to the Kratky model, however, the data still indicate an unusually high orientation efficiency. Thus one must invoke an ordering process which accompanies stretching, analogous to the strain induced crystallization of natural rubber, and which in the present case is associated with the irreversible formation of rigid, linear units during stretching/elimination. Indeed, such a strain induced ordering process has been theoretically predicted to

result in exceptionally efficient orientation¹¹⁹. This suggestion is fully consistent with the frozen-nematic structure of the oriented material as determined by X-ray and electron diffraction studies¹²⁰.

The IR spectrum of PPV cannot be divided into bands associated with the crystalline phase and those associated with the amorphous phase as is possible for many semi-crystalline polymers such as polyethylene.¹²¹ However at least two bands in the PPV spectrum have been assigned to "impurity" absorbances or moieties not associated with the PPV repeat unit⁷⁵. Interest in the nature of structural impurities which limit conjugation length in conducting polymers has increased considerably since the discovery that nearly defect-free "Naarmann" polyacetylene exhibits unusually high conductivity ($>10^5$ S/cm).⁶⁶ In the PPV spectrum, the weak bands at 2948 cm^{-1} and 2850 cm^{-1} can be clearly assigned to the asymmetric and symmetric, respectively, C-H stretching modes of a methylene group.^{80, 102} The magnitude of the dichroic ratios (plotted in Fig. 20) associated with the 2948 cm^{-1} absorbance provides a strong indication that the methylene groups are part of the polymer backbone. However, the observed direction of polarization is initially puzzling. In Fig. 22 (page 79), this band is shown for the cases in which the incoming radiation is polarized respectively, parallel and perpendicular to the direction of draw, for a sample of draw ratio four. It is clear that the 2948 cm^{-1} aliphatic C-H asymmetric stretching mode exhibits strong polarization parallel to the machine direction. However,

Figure 22. The 2948 cm^{-1} PPV "impurity" infrared band for sample PPV-4 with incoming radiation polarized (—) in the machine direction and (---) in the transverse direction.



the majority of studies of oriented polymers possessing backbone methylene groups have shown that backbone C-H stretching modes invariably exhibit significant polarization perpendicular to the chain axis.^{102,122,123}

Thus we propose that these methylene moieties are associated with topological impurities for which the local chain axis prefers a transverse orientation. This hypothesis rests upon previous work, which has shown that the thermal elimination reaction proceeds regiospecifically resulting in all-trans vinylene linkages.^{80,100} However, in the solid state a finite fraction of repeat units will be topologically prevented from attaining the trans configuration. In the absence of cis elimination, this reaction will likely be superceded by nucleophilic substitution by the anion (at the benzylic position); the expected result being saturated -- CH₂CHCl -- units in the polymer backbone. These flexible units are likely to be associated with chain bends or folds; i.e. topological impurities, along the backbone having a local chain axis which is perpendicular to the average chain axis of the rigid, unsaturated units, thus giving rise to the unexpected direction of polarization. Analogous results have been reported in IR dichroism studies of oriented PET in which absorbances associated specifically with the gauche conformer of the ethylene glycol residue indicate that these units tend to orient perpendicular to the draw direction.^{119,120} In the present case the weakness of the impurity bands (low concentration of defects) has prevented the verification of the above hypothesis by analysis of other expected bands (CH₂ bend, C-Cl stretch) which are intrinsically weaker and thus cannot be unambiguously assigned. Solid-state NMR experiments currently in progress are expected to provide further elucidation.¹¹⁵

Doping Studies

The significant property of PPV is its high attainable electrical conductivity. The materials thus far described are electrical insulators, but are readily converted to the conducting form by exposure to strong oxidizing agents, which upon accepting electrons from the conjugated π system are said to "dope" the chain. The resultant conducting materials are well-ordered macromolecular charge transfer salts which may possess electrical conductivities of up to 10^4 S/cm. The crystallographic structure of these doped materials is currently under investigation.¹²⁶

In the present study samples were doped with AsF_5 and SbF_5 to maximum conductivity. Upon doping, the materials assume a highly reflective metallic luster which, in the case of SbF_5 doping, has the appearance of copper, and in the case of AsF_5 doping, has the appearance of gold. The electrical conductivity of oriented samples is highly anisotropic. In Fig. 23 (page 82), the electrical conductivities (after SbF_5 doping) measured in the machine direction and transverse direction are plotted as a function of draw ratio. In the machine direction conductivity increases from about 30 S/cm for isotropic (unstretched) material to nearly 2500 S/cm in the fully oriented state. Conductivity increases very rapidly with draw ratio initially, then levels off at the point where molecular orientation becomes nearly perfect. This is in agreement with the results of Gagnon et al. for AsF_5 doping of manually stretched materials.⁷⁹

Transverse conductivity is unexpectedly insensitive to the degree of orientation. The transverse conductivities of isotropic PPV and PPV

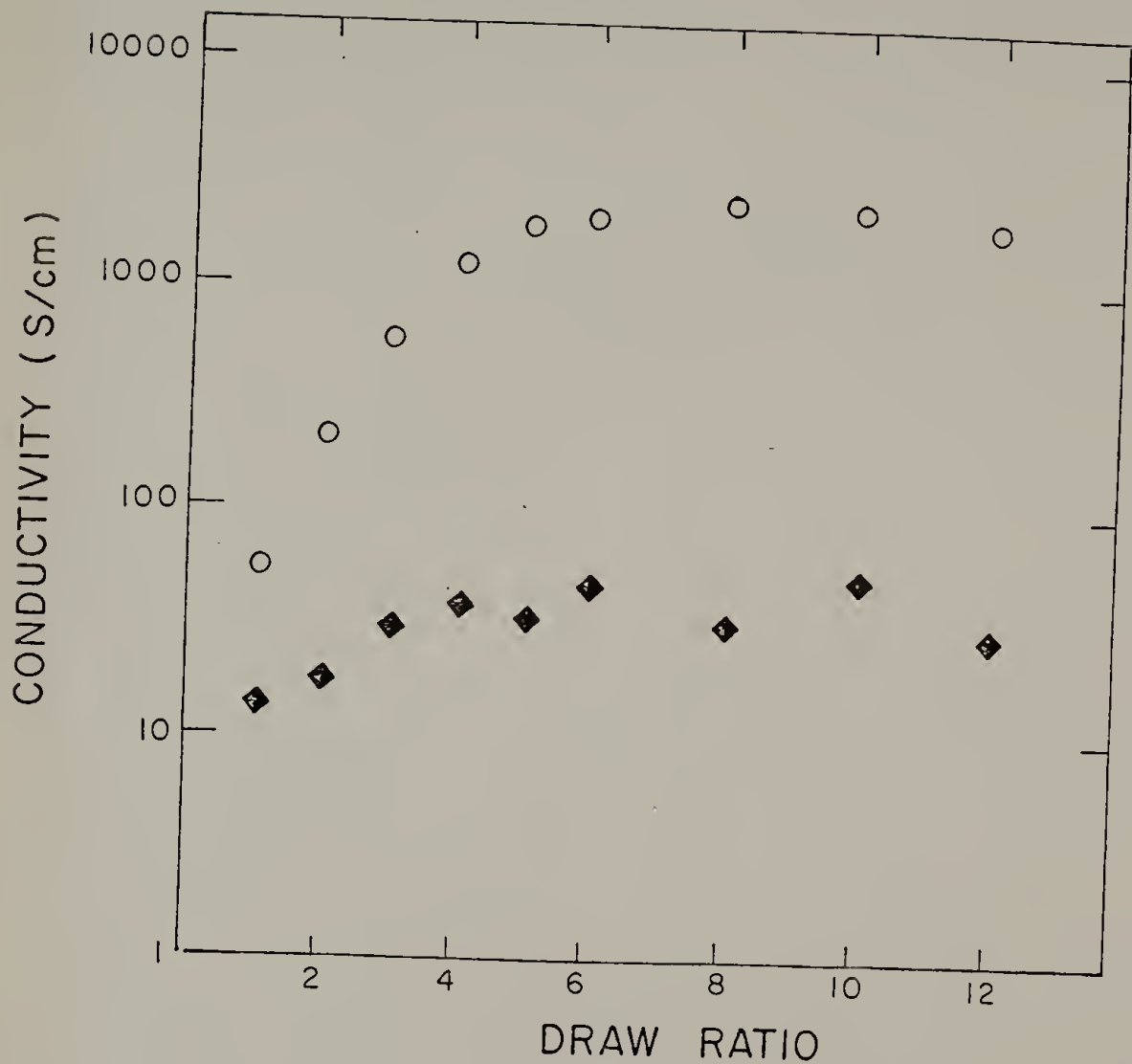


Figure 23. Electrical conductivity of oriented PPV, after SbF_5 doping, measured (○) in the machine direction and (◆) in the transverse direction plotted as a function of draw ratio.

with a draw ratio of twelve were 33 S/cm and 28 S/cm respectively (identical within the limits of experimental error). These results are in apparent contradiction with previous data for manually stretched samples, for which transverse conductivity significantly decreased with draw ratio.⁷⁹ The discrepancy is possibly a result of differences in the stretching processes. The present process produces materials with high mechanical integrity and physical continuity in the transverse direction, whereas manual stretching processes are known to produce microfibrillated materials which are fragile and sensitive to tear propagation during handling.^{79,113} Thus the results of Fig. 23 may be considered to more closely reflect the intrinsic transverse properties of the material.

The anisotropy of conductivity, listed in Table 3, has been used to provide some indication of the relative contribution of inter- and intra-molecular charge transport in polymeric conductors.^{79,111} The large anisotropies (up to 80) which are observed presently for well oriented samples reflect the quasi-one-dimensional (preferred intra-chain) nature of transport in doped PPV. The apparent lack of dependence of transverse conductivity upon draw ratio in the present study is attributed to competing effects arising from increased molecular alignment and improved crystalline ordering with draw ratio.⁶²

The final electrical properties of the doped material depend not only on the processing conditions and state of order before doping but also upon the doping protocol which is used. Table 3 lists results for identical samples doped under various conditions. For example, sample PPV-5 doped with a low vapor pressure of AsF₅ (60 torr) attained a

Table 3. Electrical conductivity and molar dopant uptake for chemically doped PPV film.

| Sample | Draw Ratio | Dopant | σ_{\parallel} (S/cm) | σ_{\perp} (S/cm) | $\sigma_{\parallel}/\sigma_{\perp}$ | Dopant Mole Fraction |
|------------|------------|-----------------------------|--------------------------------|----------------------------|-------------------------------------|----------------------|
| PPV-FM-iso | not drawn | SbF ₅ (4 torr) | - | 32.7 | - | 1.0 |
| PPV-FM-5 | 5.0 | SbF ₅ (4 torr) | 1850 | 31.7 | 58 | 1.90 |
| PPV-FM-5 | 5.0 | AsF ₅ (60 torr) | 593 | 18.7 | 32 | 0.18 |
| PPV-FM-5 | 5.0 | AsF ₅ (300 torr) | 5000 | 129 | 39 | 0.90 |
| PPV-FM-8 | 8.0 | SbF ₅ (4 torr) | 2360 | 30.5 | 77 | 1.08 |
| PPV-FM-10 | 10.0 | SbF ₅ (4 torr) | 2320 | 39.1 | 59 | 1.01 |
| PPV-FM-10 | 10.0 | AsF ₅ (300 torr) | 6390 | 89.3 | 72 | 0.87 |
| PPV-FM-10 | 10.0 | AsF ₅ (610 torr) | 10,800 | -- | - | -- |

parallel conductivity of approximately 600 S/cm, an electrical anisotropy of 30 and a doping level of about one charge carrier per five repeat units (by weight uptake). These results are in excellent agreement with the similarly doped materials of Gagnon et al.⁷⁹ However, by increasing the dopant vapor pressure (300 torr), the required dopant exposure time was reduced, the parallel conductivity was substantially increased to 5000 S/cm at essentially constant anisotropy, and the extent of doping increased to one charge carrier per repeat unit. The same sample doped with SbF₅ attained a conductivity of nearly 2000 S/cm. The unusually large weight uptake often observed during SbF₅ doping is probably related to the low volatility of the disproportionation product SbF₃.¹²⁷ It may be noted that a sample of draw ratio ten doped with AsF₅ at nearly one atmosphere vapor pressure achieved an electrical conductivity of 10⁴S/cm measured in the machine direction.

The increased conductivity for the oriented materials in the present study ($2-10 \times 10^3$ S/cm) compared to previous studies ($1-3 \times 10^3$ S/cm)^{77,78,79} is attributed to the controlled stretching and improved annealing processes which minimize degradation (oxidation) during processing, as well as to optimized doping techniques which provide maximum doping levels.

CHAPTER V

MECHANICAL PROPERTIES OF ORIENTED PPV

Most studies of electrically conducting polymers have been appropriately concerned with understanding the unique electrical, electrochemical, and optical properties of these materials. However, as more applications begin to arise, it is expected that the mechanical behavior of these materials will also gain relevance. The ability to prepare PPV in the form of continuous, well ordered, fully oriented film, as described previously, may provide an advantage in the development of high strength conducting polymeric materials in applications which require load bearing ability. Thus in this chapter, the tensile properties of uniaxially oriented PPV, measured in both the machine and transverse directions, at a series of draw ratios, will be presented.

Background

The reported tensile properties for materials such as polyacetylene^{128,129} and polypyrrole^{130,131} are somewhat disappointing in comparison to what might be expected for a fully conjugated, rigid, linear macromolecule. Clearly, the mechanical performance of these materials is limited by their morphological structure. For instance Shirakawa polyacetylene films are entangled mats of microfibrils¹³² and electrochemically polymerized heterocycles form very grainy films of irregular topology.¹¹ In contrast outstanding mechanical properties

have been reported for solid-state polymerized poly(diacetylenes).¹³³ Correspondingly, these materials possess a very highly ordered single crystalline morphology. However, the degree of order in these single crystals is such that it has entirely prevented chemical "doping" which is necessary to impart high conductivity to this class of materials.⁸

"As Stretched" Films

In investigating the tensile properties of PPV, initial efforts were aimed at determining the "green" strength of the oriented films. That is, the mechanical behavior of the films obtained directly after thermal stretching and prior to annealing. Elemental analysis and spectroscopic studies indicate that these materials are at an intermediate stage of conversion and are adequately described by the structure shown in Fig. 24 (page 88) of the approximate composition $x/y/z$ equals 1/2.25/0.75.

Typical stress-strain curves for these materials measured parallel to the machine direction are given in Fig. 25 (page 89) for various draw ratios; additional data are listed in Table 4. The "as stretched" materials exhibit classical yield behavior at low and intermediate draw ratios. At draw ratios greater than five however, purely elastic deformation is observed. The yield stress increased with draw ratio from 45 MPa for the unstretched (isotropic) material up to 150 MPa for a draw ratio of five. The attainable strain decreased very rapidly with draw ratio from 50% to 2% upon increasing draw ratio from one to ten. The tensile modulus increased substantially as a result of orientation, from 2.7 GPa for isotropic film to 16 GPa for film which had been stretched

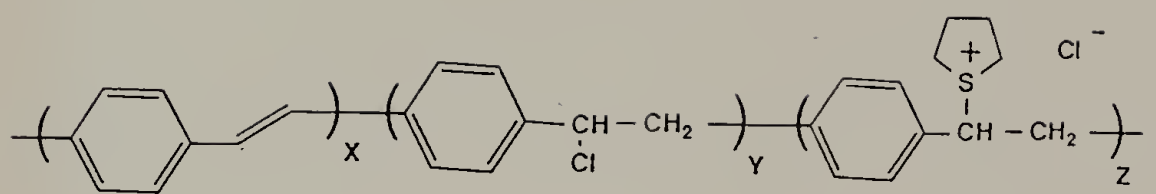


Figure 24. Chemical structure of partially converted PPV precursor directly after stretching process.

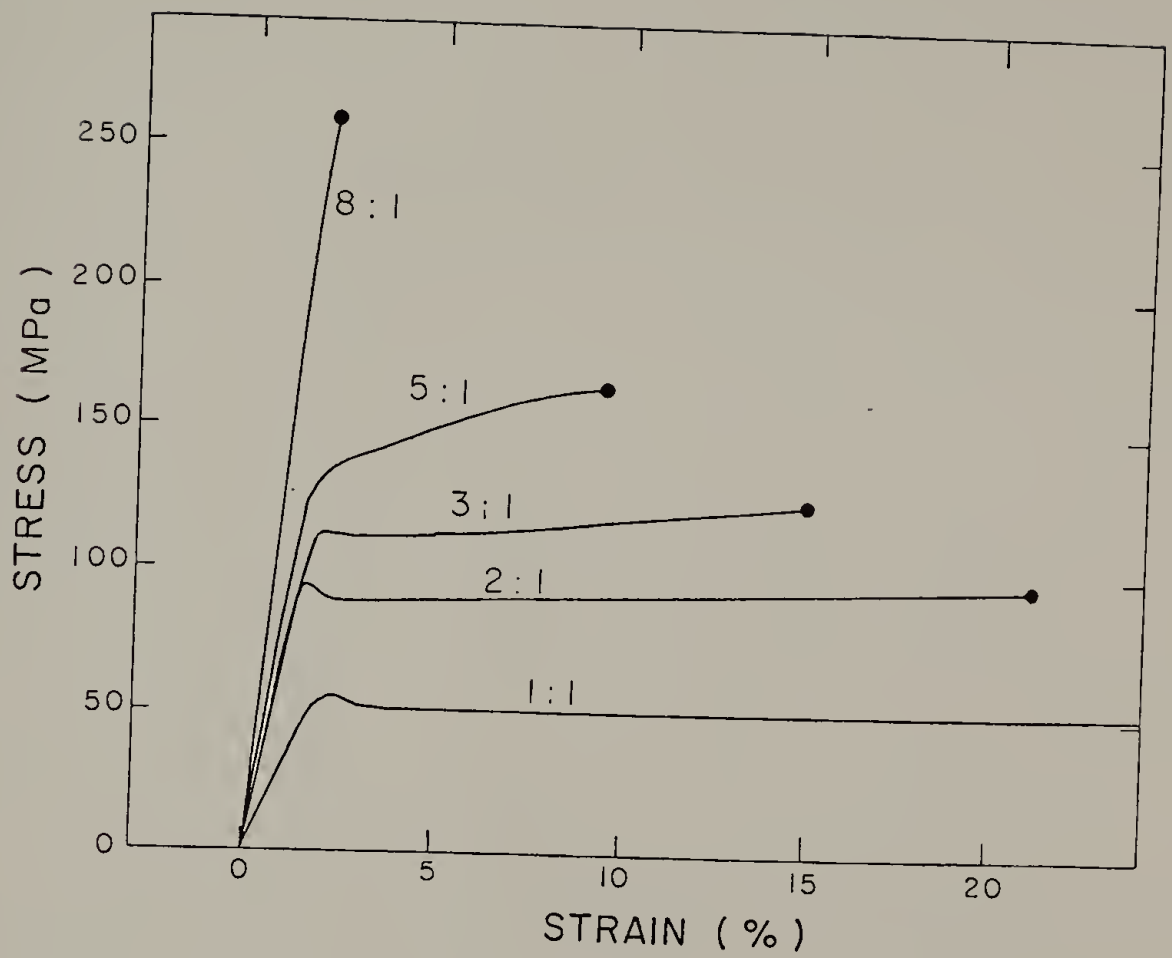


Figure 25. Stress-strain curves for "as-stretched" (unannealed) PPV precursor stretched to a series of draw ratios. Measurements were made in the machine direction.

Table 4. Tensile properties of "as stretched" PPV film measured in the machine direction.

| <u>Draw Ratio</u> | <u>Modulus</u> | <u>Yield Stress</u> | <u>Yield Strain</u> | <u>Tensile Strength</u> | <u>Elongation</u> |
|-------------------|----------------|---------------------|---------------------|-------------------------|-------------------|
| | (GPa) | (MPa) | (%) | (MPa) | (%) |
| isotropic | 2.7 | 45.2 | 3.3 | 48.2 | 38 |
| 1* | 3.5 | 60 | 2.5 | -- | 53 |
| 2 | 8.1 | 114 | 1.8 | 116 | 20 |
| 3 | 9.1 | 129 | 1.9 | 140 | 14 |
| 4 | 8.6 | 112 | 1.4 | 157 | 13 |
| 5 | 10.6 | 152 | 1.4 | 181 | 9.3 |
| 6 | 11.8 | -- | -- | 223 | 2.9 |
| 8 | 14.2 | -- | -- | 256 | 2.1 |
| 10 | 15.5 | -- | -- | 271 | 2.1 |

*Materials of draw ratio one are not isotropic because the precursor elimination/stretching process involves a substantial volume change (~50%) and these materials are converted at constant length.

its initial length. It may be noted that low draw ratio materials yielded with the formation of a stable neck, which propagated at constant rate and constant stress until reaching the grips and fracturing.

"As stretched" materials also exhibited yield behavior when stressed in the transverse direction. The anisotropy of yield stress was as high as six. In general, the tensile behavior of these materials, particularly the dependence of yield stress upon draw ratio, is quite similar to that reported for other oriented ductile polymers such as polypropylene¹³⁴ and polyethylene terephthalate.¹³⁵

Oriented and Annealed PPV

In the preparation of conducting poly(p-phenylene vinylene) annealing is required in order to fully convert the polymer to its conjugated form. In the present case, annealing was performed as discussed earlier.

In terms of mechanical behavior, the effect of annealing was substantial. Annealed materials did not exhibit sharp yield points. They did, however, exhibit some plastic deformation which decreased with increasing draw ratio (see Fig. 26[page 92]). Moduli and tensile strengths increased significantly as a result of annealing; attainable elongation however was greatly reduced.

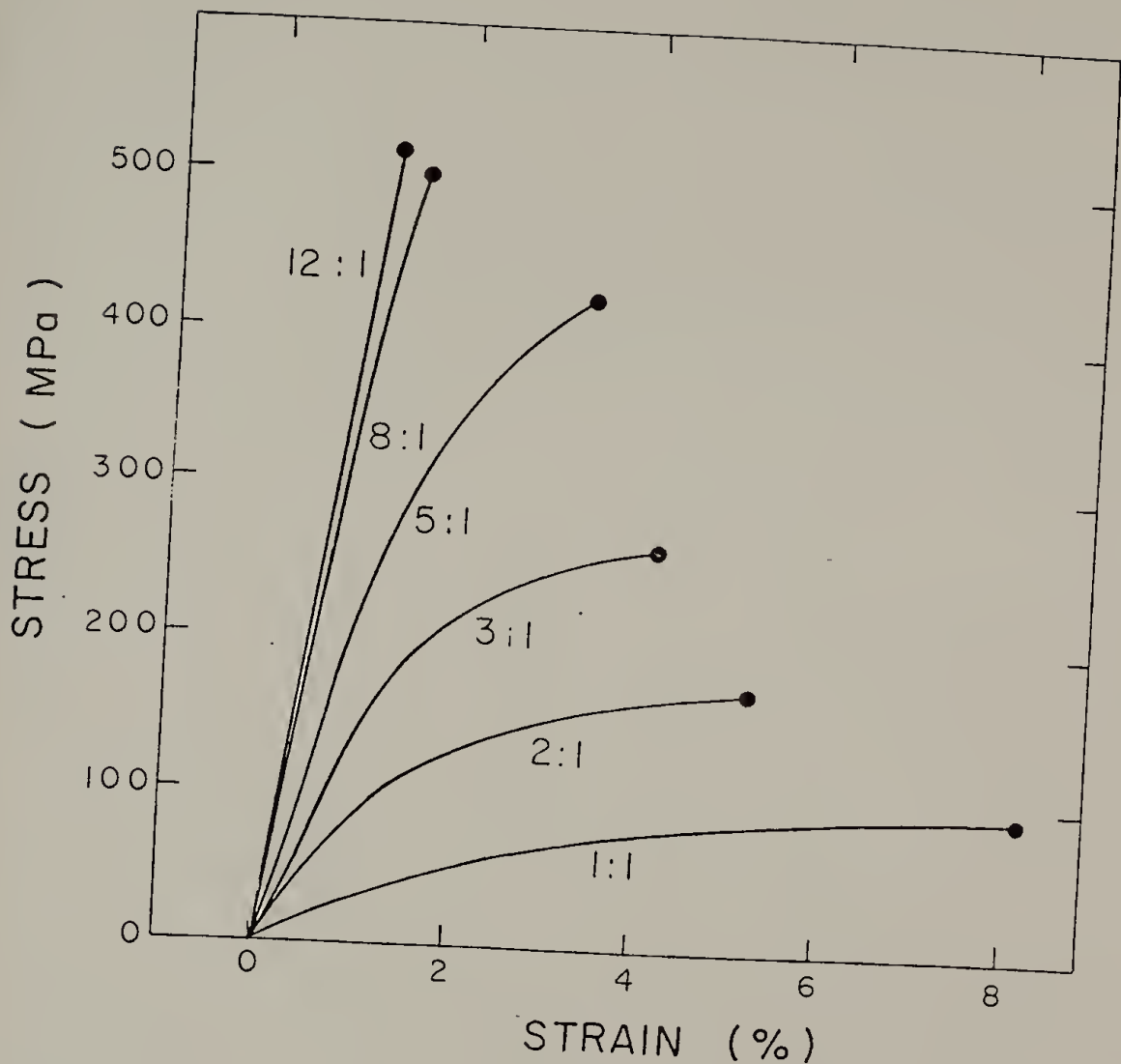


Figure 26. Stress-strain curves for fully annealed PPV stretched to a series of draw ratios. Measurements were made in the machine direction.

For measurements parallel to the machine direction, typical stress-strain curves are shown in Fig. 26 and averaged results are plotted in Figs. 27 (page 94) and 28 (page 96). The increase in modulus with draw ratio is considerably more rapid, particularly at low and intermediate draw ratios, than has been commonly observed for various oriented commercial polymers (PET, PP, PE, Nylon).¹³⁶ This is attributed to the unusually high efficiency of molecular orientation characteristic of the PPV stretching process. For PPV, Young's modulus increased from 2.3 GPa for unstretched material to 37 GPa in the highly oriented case. For comparison, this latter value is intermediate between 4.6 GPa typical for highly drawn Nylon 6,6 fibers¹³⁶ and 150 GPa typical of high performance polyaramid fibers (Kevlar).¹³⁷

For polyacetylene prepared by the Shirakawa method a tensile modulus of 0.2 GPa has been reported.¹²⁸ Presumably, this value increases somewhat with cis-to-trans isomerization and/or partial stretch alignment, however, no details have been given. For polypyrrole prepared electrochemically, the mechanical properties have been shown to depend a great deal upon the method of preparation¹³⁰, however, the highest reported modulus for this polymer is 2.4 GPa which is equivalent to that of unstretched PPV in the present study. The properties of highly oriented PPV correspond most closely to those of single crystalline poly(diacetylene) for which a tensile modulus of 42 GPa has been reported.¹³³ These latter materials, however, are much more difficult

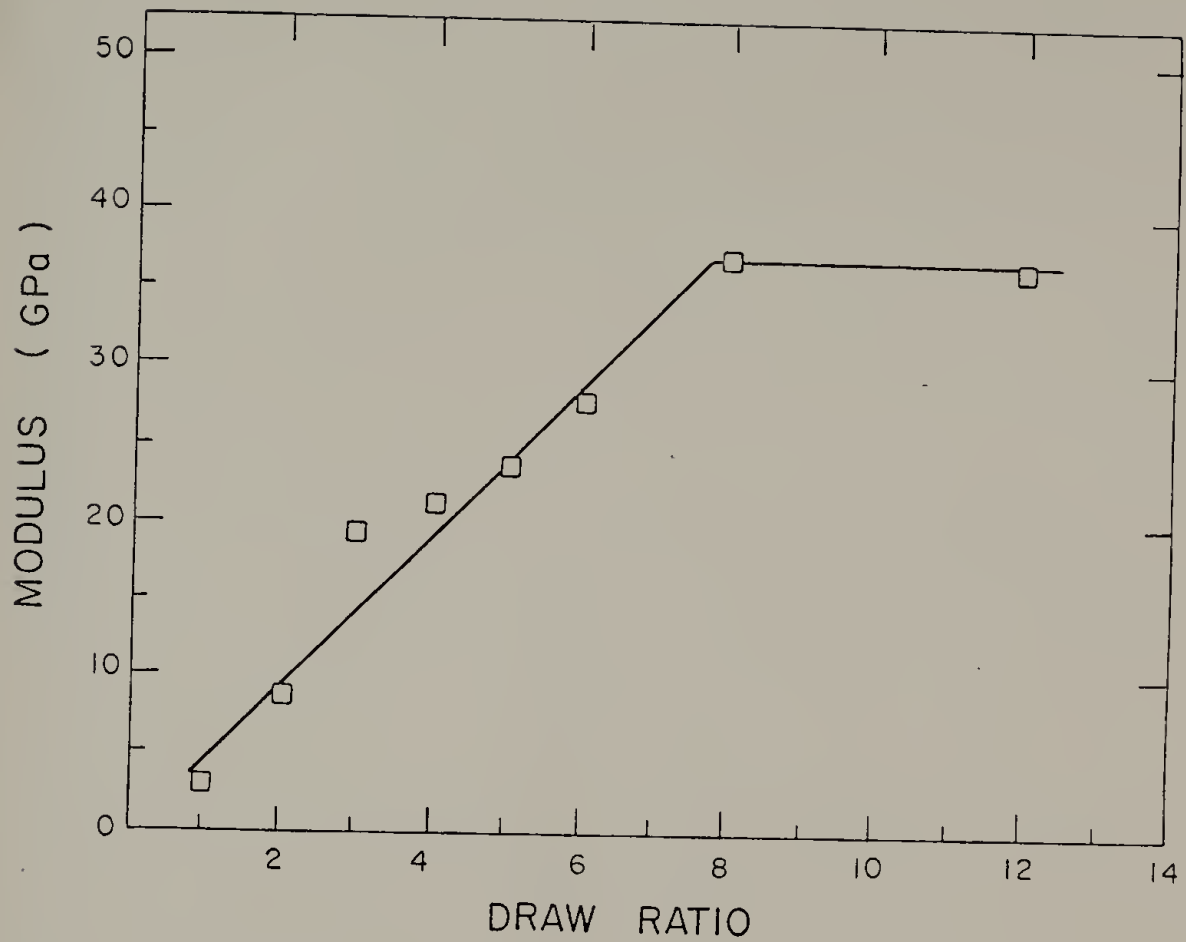
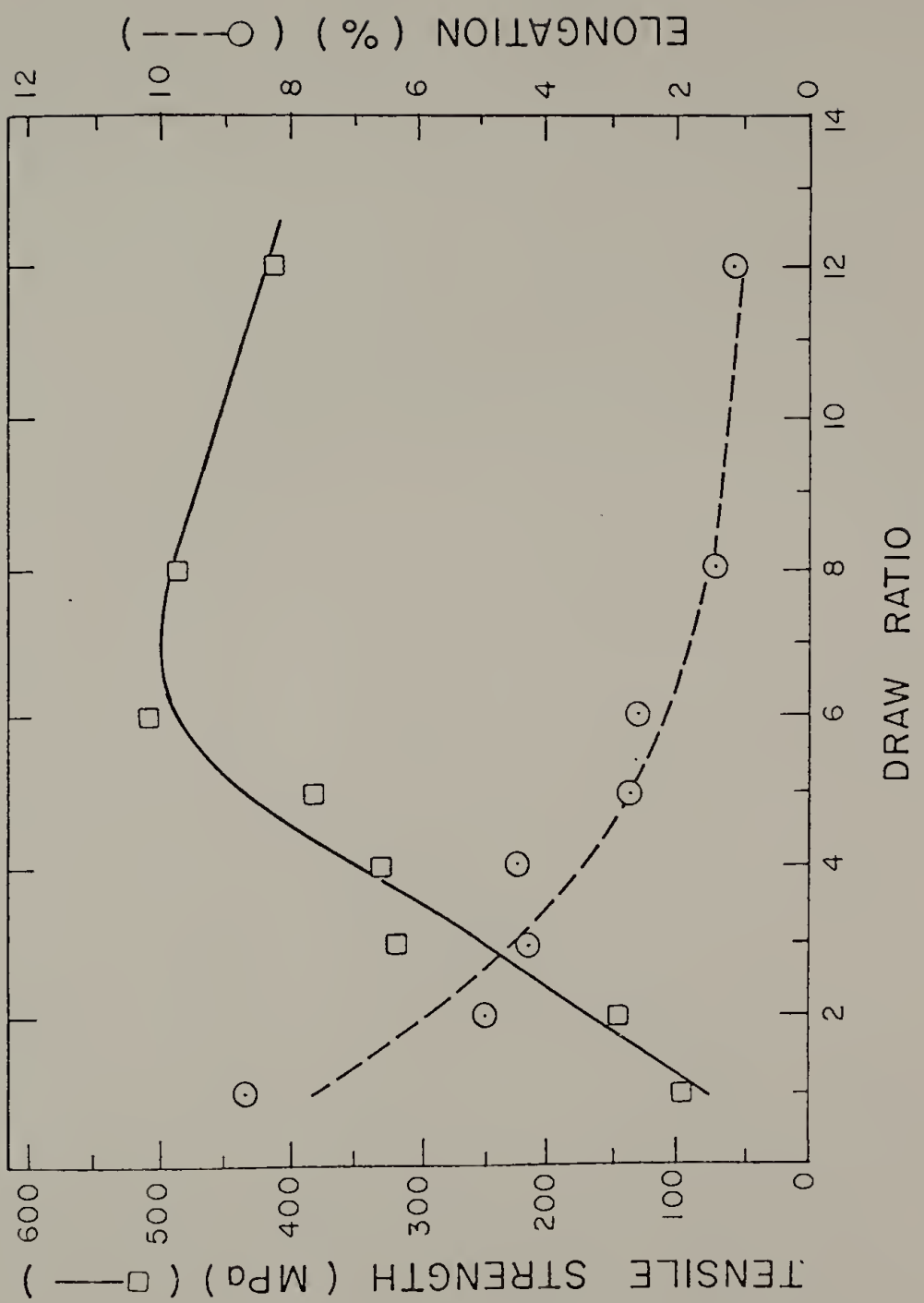


Figure 27. Young's modulus measured in the machine direction for annealed PPV plotted as a function of draw ratio.

Figure 28. Tensile strength (\square) and ultimate elongation (\circ) measured in the machine direction for annealed PPV plotted as a function of draw ratio.



to prepare and handle than PPV. It may also be interesting to note that oriented PPV exhibited significantly better mechanical properties than those reported for electrically conducting nickel phthalocyanine/Kevlar composite fibers.¹³⁸

In Fig 28, the stress and strain at failure are plotted for annealed PPV as a function of draw ratio. The ultimate strain decreases from about nine to one percent with increasing draw ratio. The tensile strength however exhibits a maximum value of about 500 MPa occurring at a draw ratio of six.

The transverse properties of oriented PPV have also been measured. Previous studies of PPV oriented manually¹⁰⁰ or by a hanging weight¹¹¹ have reported tendencies of the oriented materials to fibrillate reflecting poor transverse properties. However, the heated roll stretching process used in the present study has produced materials with improved transverse integrity. Stress-strain curves obtained in the transverse direction are given in Fig. 29 (page 98) and calculated properties are listed in Table 5. Young's modulus decreased with draw ratio from 2.3 GPa in the undrawn state to 0.5 GPa at a draw ratio of five. Tensile strength decreased only slightly, maintaining a value of about 30 MPa at a draw ratio of five; elongation increased slightly with draw ratio. It may be noted that the transverse properties of oriented PPV although inferior to the machine direction properties, are comparable to those of many commodity polymeric materials.

The anisotropy of mechanical properties may be compared to the anisotropy of electrical properties observed for identical samples.

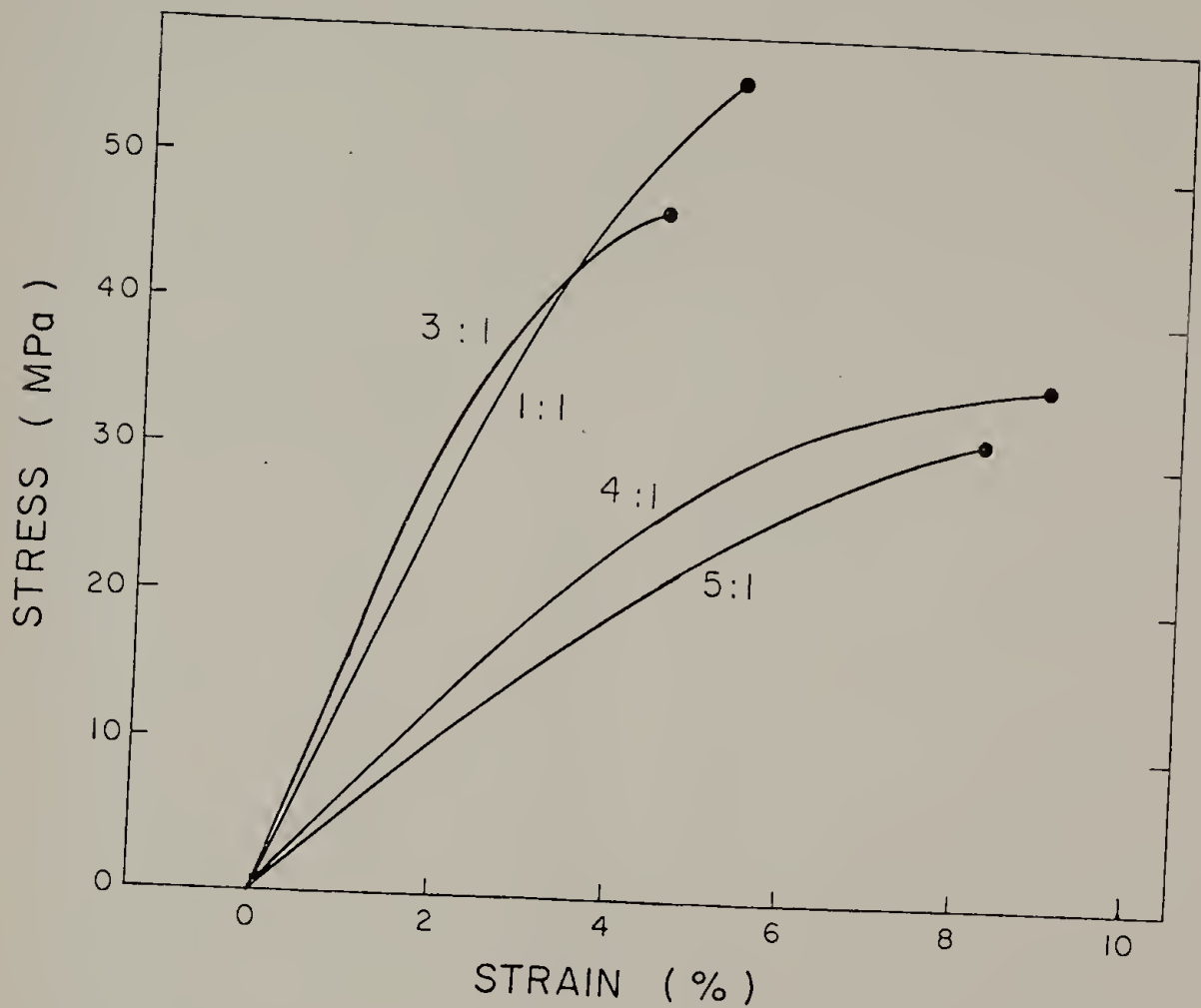


Figure 29. Stress-strain curves for fully annealed PPV stretched to a series of draw ratios. Measurements were made in the transverse direction.

Table 5. Tensile properties of annealed PPV film measured
in the transverse direction

| <u>Draw Ratio</u> | <u>Modulus</u> (GPa) | <u>Tensile Strength</u> (MPa) | <u>Elongation</u> (%) |
|-------------------|-------------------------|----------------------------------|--------------------------|
| isotropic | 2.33 | 41.2 | 2.1 |
| 1 | 1.49 | 51.1 | 4.6 |
| 2 | 0.83 | 30.1 | 3.9 |
| 3 | 1.23 | 37.4 | 4.0 |
| 4 | 0.54 | 36.0 | 6.0 |
| 5 | 0.47 | 31.7 | 7.7 |

In Table 6, the Hermans orientation function determined from the infrared dichroism of the 558 cm^{-1} infrared absorbance (from Chapter IV), is given for PPV at a series of draw ratios. Also shown are the mechanical anisotropy before doping (ratio of moduli in the machine and transverse directions) and the electrical anisotropy after SbF_5 doping (ratio of conductivities in the machine and transverse directions). The similar values for these two types of anisotropy over a range of draw ratios may suggest that in the present case they arise from similar structural features (e.g. orientation, crystallite size, shape and perfection, inter-chain interactions) and may provide a clue in determining structure-property relationships.

In summary, like the electrical properties, the mechanical properties of PPV can be varied over a wide range through control of molecular orientation. Young's modulus as high as 37 GPa and tensile strength up to 500 MPa have been measured. It is expected that the available range of mechanical properties for PPV can be further expanded by the preparation of polymer blends which are discussed in Chapter 7.

Table 6. Mechanical anisotropy and electrical anisotropy of oriented PPV film

| Draw Ratio | Orientation Function ^a | E_{\parallel}/E_{\perp} ^b | $\sigma_{\parallel}/\sigma_{\perp}$ ^c |
|------------|-----------------------------------|--|--|
| isotropic | 0 | 1 | 1 |
| 1 | 0.17 | 1.9 | 4.1 |
| 2 | 0.73 | 11 | 12 |
| 3 | 0.84 | 16 | 20 |
| 4 | 0.94 | 39 | 34 |
| 5 | 0.95 | 50 | 58 |

a) determined from IR dichroism of PPV 558 cm^{-1} absorbance

b) Young's Moduli of annealed sample before doping

c) Electrical conductivity after SbF_5 doping to maximum conductivity

CHAPTER VI

BIAXIALLY ORIENTED PPV

Biaxial orientation has been used to improve properties such as the tensile strength, oxygen barrier capability, and puncture resistance of polymeric materials. Commercial processes include tentering, blow molding, and thermoforming. Novel biaxial processing techniques (e.g. counter rotating dies) have also been developed to reduce the inherent mechanical anisotropy of liquid crystalline polymer films.^{139,140} However, biaxial orientation has not yet been used to influence the electrical properties of conducting polymers.

Previous chapters have shown the utility of preparing uniaxially oriented PPV. In this chapter two processes are discussed by which the poly(sulfonium salt) PPV precursor can be oriented biaxially. The first is a two-stage sequential stretching operation which is a modification of the uniaxial stretching process. This process allows non-equibiaxial stretching over a wide range of deformation ratios. The second process is a film blowing technique which involves equibiaxial planar extension.

The purpose of this work is to further establish the unique processing advantages associated with the conducting polymer "precursor technique", to introduce biaxial orientation as a means of controlling and improving electrical properties in conducting polymers, and to provide additional information contributing to the establishment of structure-property relationships for electrically conducting polymers.

Processing

It has been shown that uniaxial stretching of the PPV precursor is facilitated by temporary plasticization associated with the rapid evolution of volatiles which accompanies thermal elimination. This plasticization effect has been controlled as discussed in Chapter 4 to prepare continuous film of 12:1 draw ratio. This high degree of stretching is accompanied by nearly perfect molecular orientation and maximized electrical conductivity. This same effect has been used to produce biaxially oriented film. Freshly cast films were first stretched uniaxially (λ_1) at a relatively low temperature in order to minimize the extent of conversion which accompanies the initial stretch. The transverse stretch (λ_2) was performed at a higher temperature and was facilitated by a brief softening associated with the elimination of precursor units remaining after the first stretch. The amount of transverse draw attainable is quite significant. In Fig 30 (page 104), the maximum attained transverse draw ratio for a number of samples is plotted against the initial machine draw ratio. The shaded area defines the available deformation window for PPV biaxial stretching. Biaxial deformation up to 6X7 have been obtained in this way. The magnitude of the transverse "second stage" draw ratios which are attainable may suggest that the maximum attainable uniaxial draw ratios (~12) have been limited not by the exhaustion of available volatile "plasticizer" but perhaps by the complete extension of chain segments between entanglements.

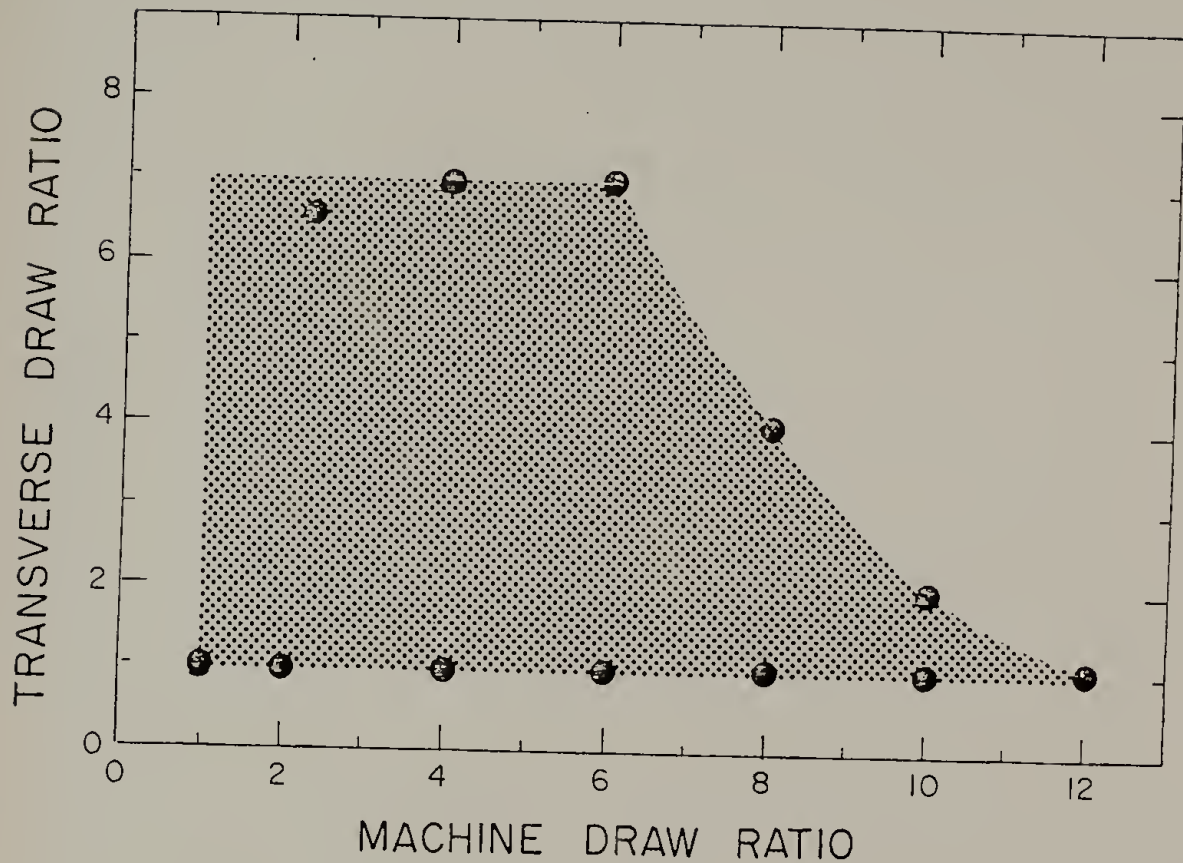


Figure 30. Attainable deformation window using two-stage biaxial stretching.

Of critical interest in this work was the homogeneity of strain sustained during transverse stretching. In Chapter 4 it was shown that the uniaxial web stretching apparatus (machine draw) imposes a homogeneous extensional deformation. To determine local strain a 1/16" grid was stamped upon samples prior to transverse stretching. The observed deformation of the grid established the strain sustained by the material. Results showed that the transverse strain variations were acceptably small ($\pm 15\%$) except in the vicinity of the clamps where the film was restrained from contracting in the machine direction.

Of course the manual technique used for transverse stretching does not allow optimum control over the desired draw ratio nor does it allow the development of steady flow conditions required for homogeneous strain. However, the present work demonstrates the application of biaxial stretching techniques towards the PPV precursor. In light of the present results, it is expected that the application of a continuous tentering process with the PPV precursor would be both straightforward and worthwhile.

Equibiaxial extension was achieved by inflating a bubble of freshly cast film as depicted in Fig 11 (Chapter 3). Again, the thermally induced plasticization allows large deformations. Thus far, a linear draw ratio of three (3X3) has been obtained using this technique. Good homogeneity of strain was confirmed by the nearly perfect spherical shape of the expanding bubble. It is expected that higher draw ratios can be obtained with improvements in this process. With control over internal bubble pressure and more rapid, even heating of the film, bubble expansion can be optimized and precisely controlled.

Structural Characterization

The X-ray diffraction patterns of biaxially stretched films are shown in Fig 31 (page 108). The quantitative measurement and description of multiaxial molecular orientation using X-ray diffraction and dichroism methods have been reviewed.^{141,142,143} In the present contribution, however, purely qualitative observations will be made.

In the case of uniaxially oriented PPV, it was shown that the chain axis assumes nearly perfect alignment in the machine direction (for $\lambda_1 > 5$, $f_c > 0.95$). Figure 31a shows the x-ray diffraction pattern of PPV uniaxially drawn to $\lambda_1=10$. The pattern is characteristic of highly oriented crystallites possessing a cylindrically symmetric distribution of orientations about the draw direction.¹⁴⁴ For biaxial films at low transverse draw ratios strong orientation in the machine direction persists. Figure 31b shows the diffraction pattern for a film with $\lambda_1=10$ and $\lambda_2=2$. This pattern is very similar to the one obtained from the uniaxially drawn sample. As the transverse deformation becomes comparable to the draw ratio in the machine direction the chain axis orientation distribution is broadened into a planar distribution. This is evidenced by a smearing of the (110) equatorial reflection intensity over all azimuthal angles as is apparent in the biaxial sample with $\lambda_1=6$ and $\lambda_2=5$ (see Figure 31c). With further increase of the transverse draw ratio the chain axis orientation assumes an increasingly transverse preference evidenced by the sharpening of the (110) equatorial reflection at 90 degrees to its initial position (Fig. 31d).

Figure 31. X-ray diffraction patterns of biaxially stretched PPV.
Samples are positioned such that the machine direction
is vertical and the transverse direction is horizontal.
a) $\lambda_1=10$ (uniaxial); b) $\lambda_1=10, \lambda_2=2$; c) $\lambda_1=6, \lambda_2=5$;
d) $\lambda_1=2, \lambda_2=6.5$.

a

(110)

**b**

(110)

**c**

(110)

**d**

(110)



Previous work involving polypropylene biaxially stretched by a very similar two stage process showed that the second-stage (transverse) stretch is more influential than the first-stage stretch in determining the final state of the material.¹⁴⁵ Thus the material will achieve a biaxially balanced molecular orientation under conditions where $\lambda_2 < \lambda_1$. Similar results were obtained in this work as evidenced by Fig 31c, where material stretched to $\lambda_1=6$ and $\lambda_2=5$ has already attained a preferentially transverse orientation.

It may be noted that in all biaxially oriented films only one preferential orientation direction exists. The orientation distribution appears unimodal in all films. This demonstrates that regions oriented by the first stretch are subsequently reoriented by the second implying that the materials retains some flexibility on a molecular scale after the first stretch despite the degree of conversion from flexible precursor to rigid PPV which has already occurred.

As a result of the symmetry of planar extension during the equibiaxial stretching process (inflated film), the resulting diffraction patterns indicate an isotropic distribution of orientation in the plane of the film. Future efforts may be aimed at quantifying the state of biaxial orientation in these materials.

Electrical Conductivity

Uniaxial and biaxial samples were doped with SbF₅ and their electrical conductivity was measured both in the machine and in the transverse

directions. Results for uniaxial samples are given in Table 7 (data from Chapter 4) and those for biaxial materials are given in Table 8. The utility of orientation arises from the inherently anisotropic nature of charge transport in conducting polymers with transport occurring preferentially along the molecular axis. The incentive for biaxial stretching lies in the ability to vary electrical anisotropy over a wide range (.05 - 80) and moreover, given a desired anisotropy, to maximize total conductivity.

For example, a comparison may be made between the biaxial sample where $\lambda_1=10$ and $\lambda_2=2$ and the uniaxial sample from which it was derived ($\lambda_1=10$) (See Tables 7 and 8). The biaxial sample had a machine direction conductivity which was 2.5 times lower than the uniaxial sample but a transverse conductivity which was more than five times greater; thus the process may possess some engineering utility.

Viewed another way, the $\lambda_1=10$, $\lambda_2=2$ sample exhibits a conductivity anisotropy of 4.5 and a machine direction conductivity of 928 S/cm. If the same anisotropy were desired by purely uniaxial stretching, it is estimated (by extrapolation from Table 1) that a uniaxial draw ratio (λ_1) of about 1.3 would be required, which would produce a material with a machine direction conductivity of only about 100 S/cm.

The conductivity data in Table 8 are fully consistent with expectations based upon the previous structural data. For example, the sample where $\lambda_1=8$, $\lambda_2=4$ appeared to possess nearly equibiaxial orientation by X-ray diffraction. After doping this sample exhibited electrical anisotropy near unity (0.6). Moreover in comparison to the

"parent" uniaxial sample ($\lambda_1=8$), the machine direction conductivity was decreased by a factor of eleven and the transverse conductivity was increased by a factor of eleven. Based upon this data it is estimated that at the "ideal" equibiaxial point (the biaxially balanced state) using this process, planar isotropic conductivity would be about 300 S/cm (compared to 33 S/cm for 3D isotropic material).

For equibiaxially expanded films, conductivity was, of course, isotropic in the plane of the film. At a linear draw ratio of three ($A_f/A_0 = 9$) a doped conductivity of 85 S/cm was obtained, corresponding to a 2.5 fold increase compared to unstretched material. It is expected that this value can be increased with improvements in the processing method.

In summary, biaxial stretching processes introduce a degree of control over electrical properties through processing which cannot be otherwise obtained in electronic materials. The full range of possibilities and applications has yet to be explored.

Table 7. Electrical conductivity and electrical anisotropy
of SbF₅ doped, uniaxially oriented PPV film

| λ_1 | σ_1 (S/cm) | σ_2 (S/cm) | σ_1/σ_2 |
|-------------|-------------------|-------------------|---------------------|
| 2 | 210 | 18 | 12 |
| 4 | 1240 | 37 | 34 |
| 6 | 2020 | 46 | 44 |
| 8 | 2360 | 31 | 76 |
| 10 | 2320 | 39 | 59 |
| 12 | 2310 | 28 | 83 |

Table 8. Electrical conductivity and electrical anisotropy of SbF_5 doped biaxially oriented PPV of machine draw ratio, λ_1 , and transverse draw ratio, λ_2 .

| λ_1 | λ_2 | $\sigma_1 (\text{S/cm})$ | $\sigma_2 (\text{S/cm})$ | σ_1/σ_2 |
|-------------|-------------|--------------------------|--------------------------|---------------------|
| 2 | 6.5 | 17 | 339 | 0.05 |
| 4 | 7 | 63 | 1020 | 0.06 |
| 6 | 7 | 142 | 448 | 0.32 |
| 8 | 4 | 219 | 342 | 0.64 |
| 10 | 2 | 928 | 208 | 4.5 |

CHAPTER VII

POLY(PHENYLENE VINYLENE) BLENDS

The use of the water soluble PPV precursor provides a unique opportunity to prepare conducting polymer blends by casting from solution. This allows an additional degree of control over morphology which may find particular utility in applications requiring large or controlled surface areas (e.g. electrodes, chemical sensors). Blending may also be envisioned as a means of controlling mechanical properties, improving atmosphere stability, or improving processing characteristics.

In this chapter, results will be presented from an initial survey study in which PPV was blended with a series of commercially available water soluble polymers. The added polymers were chosen to represent three general types:

- 1) poly(ethylene oxide) (PEO) is a semi-crystalline polymer;
- 2) poly(vinyl methyl ether) (PVME) is an elastomeric material at room temperature;
- 3) poly(vinyl pyrrolidone) (PVP), methyl (cellulose) (MC), and hydroxypropyl cellulose (HPC) are glassy materials at room temperature.

Thus the effect of matrix type on blend properties will be addressed.

Blend Characterization

For this study nominally 50/50 wt % blends were prepared as detailed in Chapter 3 (Experimental). All of the blends supported clear, homogeneous aqueous solutions (by contrast, blending the PPV precursor with water soluble anionic polyelectrolytes, such as polyacrylic acid, caused immediate precipitation upon combining the aqueous stock solutions). After casting PPV/PVP, PPV/MC, and PPV/HPC formed very clear, glassy (not very flexible) films. PPV/PVME films were clear and flexible but possessed a very tacky surface. These blends did not exhibit the large extensibility of an elastomer. PPV/PEO blends were less clear as a result of PEO crystallinity. However, these compositions were strong, tough, and flexible.

The blends were annealed at 200°C for four hours under vacuum. Relatively mild elimination conditions were used in order to minimize thermal degradation of the added components. The chemical microstructure of the annealed blends was examined using IR spectroscopy and elemental analysis. Only the PPV/PVME blend showed any evidence of degradation under the conditions employed. For the other systems the infrared spectra of the blends corresponded almost exactly to a summation of the spectra of the pure components with no changes in the relative intensities, positions, or line shapes of the major bands. The PPV/PVME blend showed the emergence of new medium strength bands at 1720 cm^{-1} , 1690 cm^{-1} , and 1595 cm^{-1} which may be attributed to carbonyl groups and backbone unsaturation generated as a result of thermal degradation of PVME during annealing.

The elemental analysis results for each of the blends and for the pure components are given in Table 9 (page 117). The agreement of experimental and theoretical results provides further evidence that thermal elimination proceeds clearly and unperturbed in the blends. The oxygen assay was used to calculate the actual composition for the nominally 50/50 wt % blends (also in Table 9).

Miscibility in the blends was examined using differential scanning calorimetry. In the present case, the unlikelihood of molecular miscibility would be accompanied by a significant increase in the glass transition of the blend compared to that of the pure added component because PPV is a fully extended rigid rod macromolecule. DSC thermograms given in Figure 32 (page 118) clearly show that no shift in the glass transition is found upon blending PPV with PEO, PVME and PVP, indicating independent thermal responses and thus phase separated materials. For the modified cellulosic constituents, no unambiguous glass transition could be detected even for the pure components. In the PPV/PEO blend, a large melting endotherm at 61°C was also detected indicating a crystalline PEO phase. A detailed analysis of the morphology of PPV/PEO blends will be presented in the next chapter.

Table 9. Elemental analysis results for a series of PPV blends and the pure constituents

| Sample | Carbon Found (Theoretical) | Hydrogen | Oxygen | Nitrogen Composition (Calculated) ^a |
|----------|----------------------------------|-------------------------|--------------|--|
| PPV | 93.67(94.11) | 5.96(5.88) | 0.58(0) | 0(0) PPV |
| PEO | 53.50(54.55) | 8.87(9.09) | 36.80(36.36) | 0(0) PEO |
| PPV/PEO | 70.29(71.17) | 7.64(7.74) | 21.29(21.09) | 0(0) 42/58 PPV/PEO |
| PVME | 61.20(62.07) | 11.10(10.34) | 27.93(27.59) | 0(0) PVME |
| PPV/PVME | 74.47(74.89) | 8.09(8.56) | 16.74(16.55) | 0(0) 40/60 PPV/PVME |
| PVP | 63.42(64.86) | 8.27(8.11) | 15.88(14.41) | 12.33 PVP |
| PPV/PVP | 71.76(82.66) | 6.66(7.27) | 9.16(6.92) | (12.51) 52/48 PPV/PVP |
| HPC | 53.28(-) ^b | 8.86 (-) | 37.00(-) | 0(-) HPC |
| PPV/HPC | 72.05(73.70) | 7.11(7.37) ^c | 18.33(18.50) | 0(0) 50/50 PPV/HPC |
| MC | 47.32(-) | 6.97(-) | 44.16(-) | 0(0) MC |
| PPV/MC | 70.28(71.18) | 6.58(6.41) | 21.49(21.64) | 0(0) 51/49 PPV/MC |

a Actual composition is calculated from the oxygen content in the blends or in the case of PPV/PVP the nitrogen content.

b No theoretical values for modified celluloses were calculated because the extent of modification is not precisely known.

c Theoretical values are calculated using the found values from the pure modified celluloses.

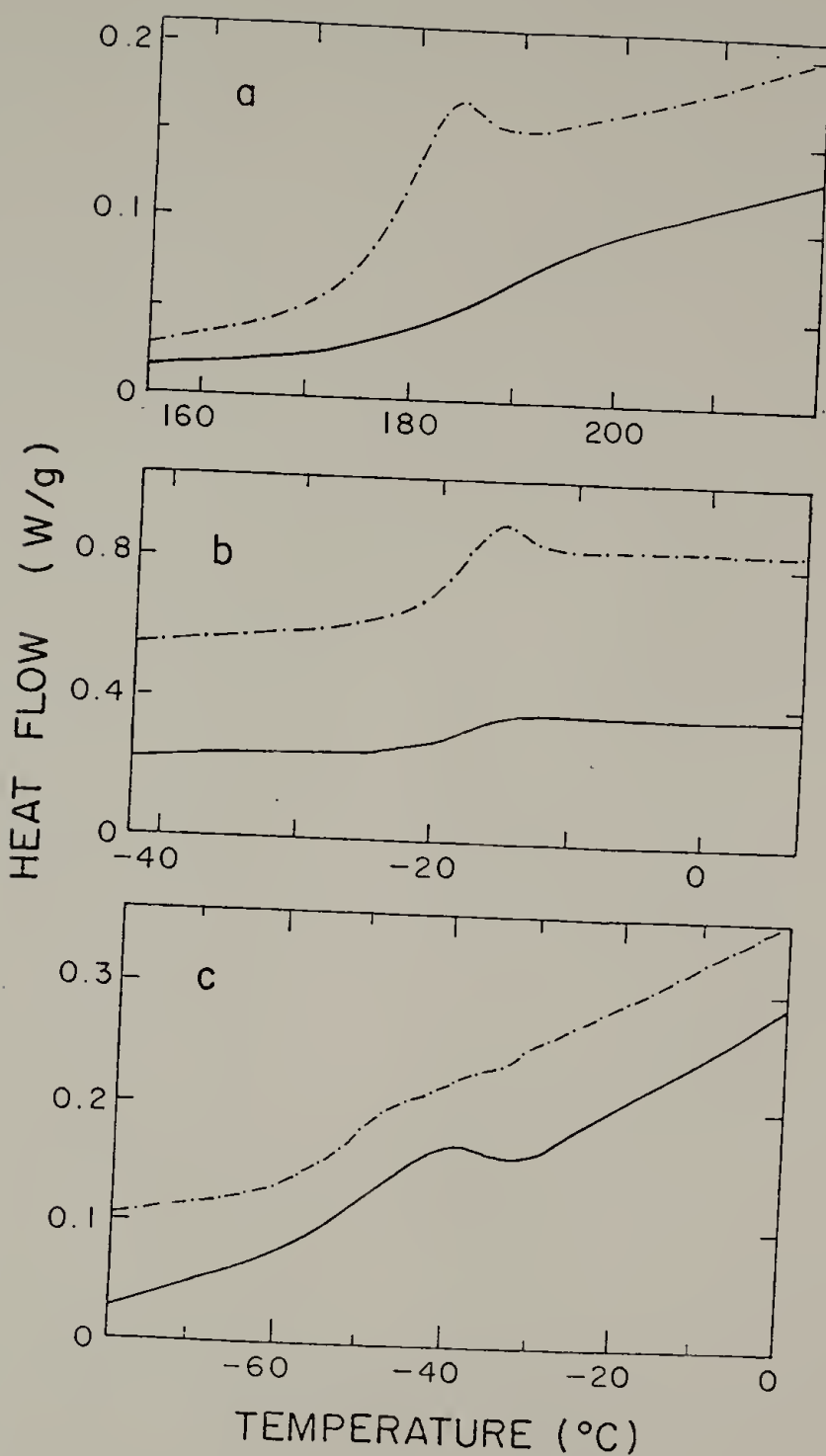


Figure 32. Normalized DSC thermograms of pure components and blends:
 a) Poly(vinyl pyrrolidone) (upper) and 50/50 PPV/PVP (lower);
 b) Poly(vinyl methyl ether) (upper) and 50/50 PPV/PVP (lower);
 c) Poly(ethylene oxide) (upper) and 50/50 PPV/PEO (lower).

Chemical Doping Studies

Some of the blends exhibited significantly enhanced doping rates with chemical dopants. In Fig. 33 (page 120) the conductivity is plotted as a function of time of exposure to AsF₅ vapor (50 torr) for pure PPV and the nominally 50/50 blends. Pure PPV, like Durham polyacetylene, dopes very slowly as a result of its continuous morphology of densely packed rigid rods. In Fig. 33, pure PPV does not reach its limiting value of conductivity within the time scale shown (~2 weeks). Blends with PVP and MC show very similar doping rates although conductivity is lower as a result of dilution of the electroactive phase. However, PPV blends with PEO and PVME exhibited a greatly enhanced rate of doping. It may be noted in Fig. 33 that PPV/PEO and PPV/PVME blends achieved a maximum conductivity within two days of dopant exposure and furthermore, that these blends attained a final conductivity which exceeded that of the pure PPV sample. The PPV/HPC blend showed intermediate behavior.

The greatly accelerated doping observed for blends with PEO and PVME is attributed to the fact that these polymers are well above their glass transition temperatures at room temperature (see Fig. 32). Thus the diffusion of dopant vapor through the amorphous domains of these polymers is rapid, facilitating dopant access to the bulk of the film and improving the overall doping rate of the conducting material. Decreases in conductivity after the maximum value are probably a result of degradative side reactions (e.g. crosslinking) frequently associated with strong Lewis acid dopants.¹⁴⁶ It is not clear, however, whether

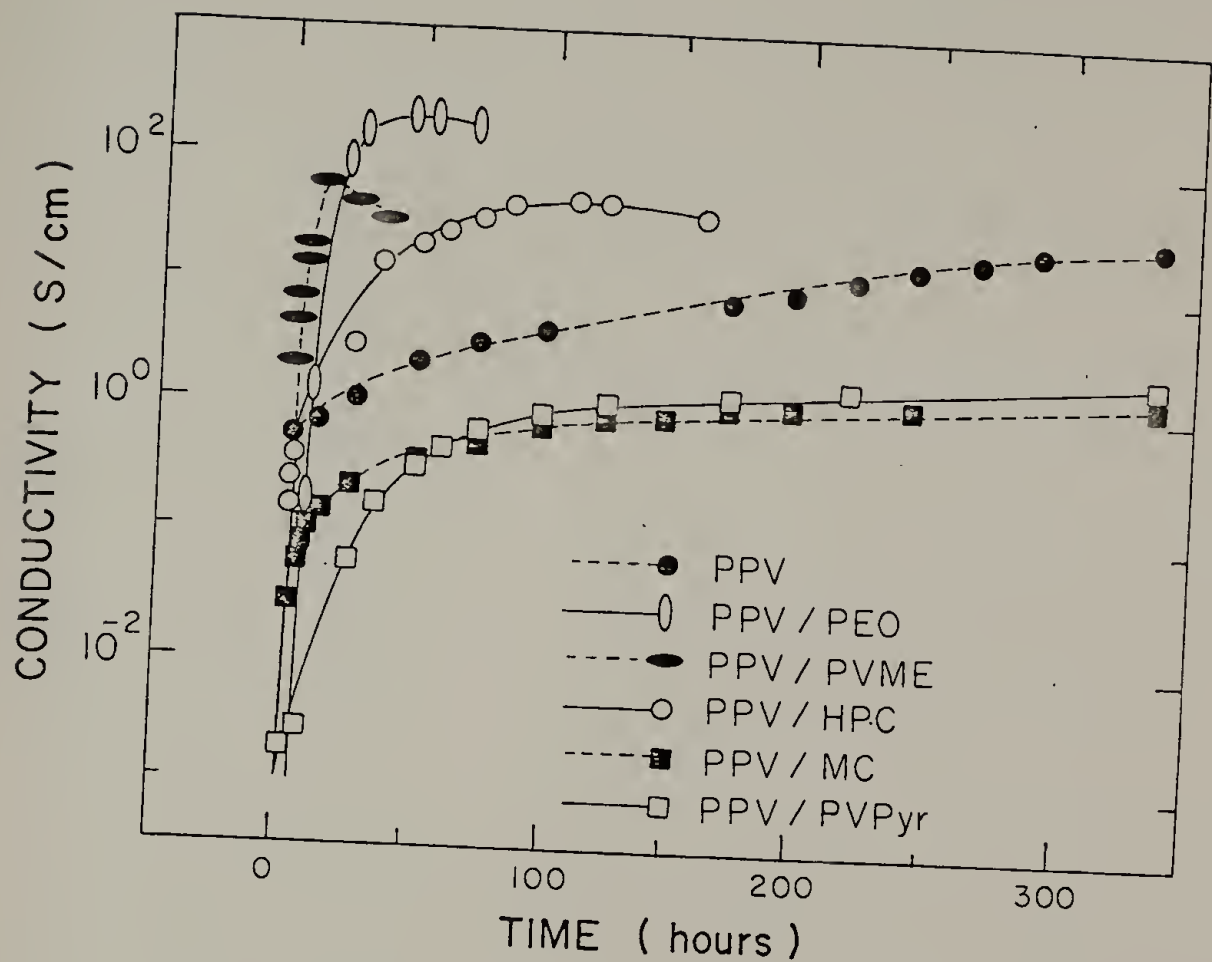


Figure 33. Conductivity as a function of time for PPV and nominal 50/50 blends upon exposure to 50 torr AsF_5 vapor.

these side reactions which destroy charge carriers in the blends are merely a result of overexposure of PPV domains to the dopant or whether they involve fragments generated by reactions of the dopant with the added constituents.

Table 10 lists the final conductivity achieved for each of the samples from Fig. 33 as well as the weight uptake of dopant. The final conductivity of the blends varies by two orders of magnitude (1.6 to 166 S/cm) depending on the nature of the blended polymer. In general, samples exhibiting the highest conductivities also show the largest dopant uptakes. Of course, the pure added constituents did not become conducting when exposed to dopant vapor. However, as Table 10 shows these materials did contribute significantly to dopant uptake (particularly PEO which absorbed over 600% by weight of dopant). This is not surprising since AsF_5 is an extremely reactive compound.

It may be noted that the PPV/PEO blend attained a conductivity of 166 S/cm whereas pure PPV doped under the same conditions reached only 26 S/cm. The higher conductivity of the blend must be attributed to a higher level of doping of the PPV constituent in the blend arising from improved dopant transport.

Electrochemical Doping

Pure PPV prepared from the poly(sulfonium salt) precursor cannot be doped electrochemically except in the form of extremely thin films (<100nm thick).¹⁴⁷ This is considered a serious deficiency for the material since many proposed applications require rapid electrochemical

Table 10. Electrical conductivity and dopant weight uptake for AsF_5 doped PPV blends and pure constituents.

| Composition (nominal) | Conductivity (S/cm) | Dopant Uptake (wt %) |
|--------------------------|------------------------|-------------------------|
| PPV | 26 | 11% |
| 50/50 PPV/PEO | 166 | 265% |
| 50/50 PPV/PVME | 57 | 99% |
| 50/50 PPV/HPC | 36.1 | 175% |
| 50/50 PPV/PVP | 2.1 | 6% |
| 50/50 PPV/MC | 1.6 | 33% |
| PEO | | 644% |
| PVME | | 24% |
| PVP | | 4% |
| HPC | | 36% |
| MC | | 6% |

activity. Its inactivity is due to the prohibitively slow rate of diffusion of counterions through the bulk of the material. It was found in this study that blending may be an effective method for providing electrochemical activity to PPV.

In Fig. 34 (page 124) the degree of doping at constant potential (+4.1V vs. Li) is plotted as a function of time for a series of PPV blends. Pure PPV and its blend with poly(vinyl pyrrolidone) show no evidence of doping under the conditions used. However, PPV blends with PEO, PVME, MC, and HPC (all of which swell to some extent in the electrolyte) dope very rapidly under these conditions, reaching saturation within 1-2 hours. Doping of these compositions is readily reversible. Experiments show that there is a net loss of weight upon doping these electroactive compositions suggesting that the added component is actually extracted by the electrolyte during doping, leaving pores for effective ion infiltration. This idea is further supported by data in Table 11 where the initial current density (rate of doping) is given for each of the blends upon first and second charging cycles. For each sample, the second charge exhibits a higher current density than the first indicating that the added component has been replaced by electrolyte solution.

Since battery electrodes are one of the most immediate areas of application for conducting polymers, PPV blends were evaluated in this respect. For a 50/50 PPV/PEO film of 20um thickness discharged at a constant current density of 340 A/Kg, a charge density of 80 A·hr/Kg could be obtained. These results are comparable to the electrochemical discharge characteristics reported for polyacetylene.¹⁴⁸

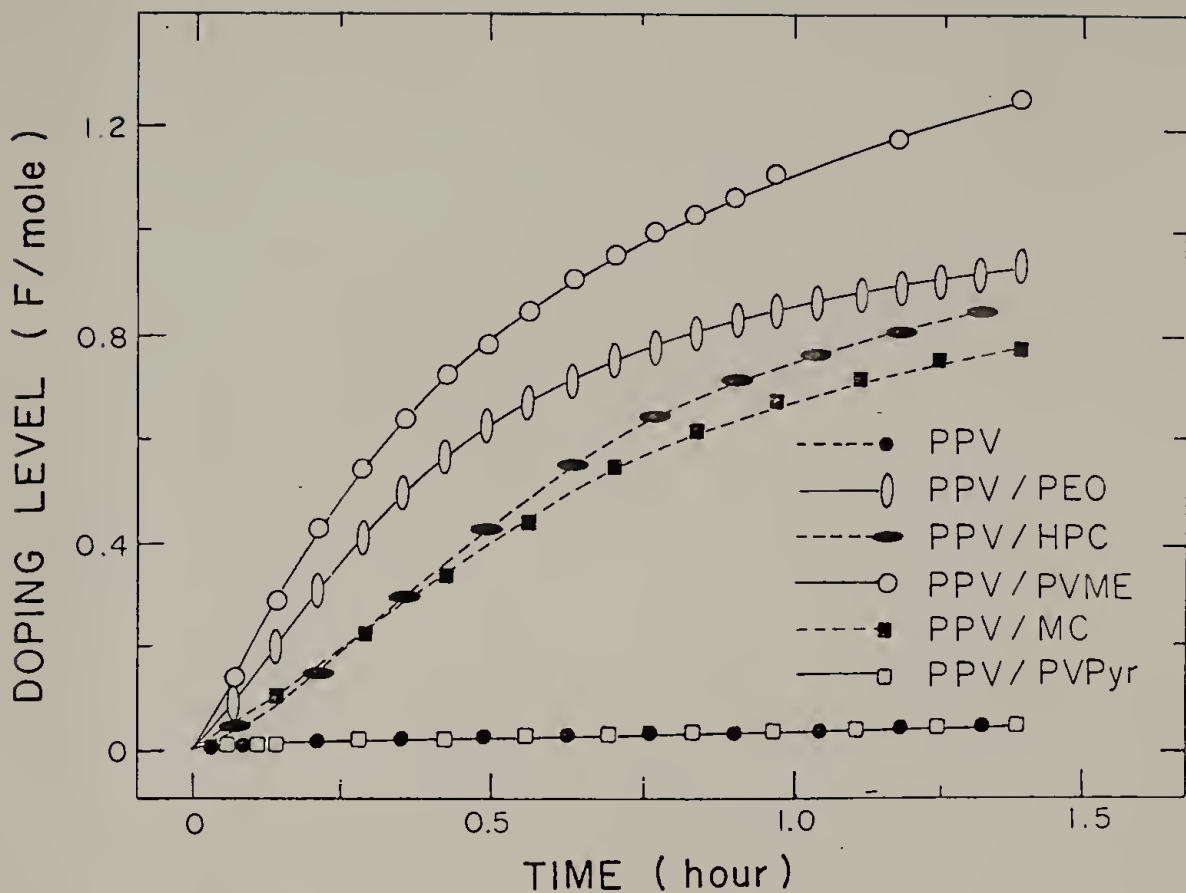


Figure 34. Doping level as a function of time for PPV and nominal 50/50 blends doped electrochemically at +4.1 V versus Li in 1M LiClO₄/propylene carbonate electrolyte.

Table 11. Initial current density for the first and second charging cycles upon electrochemical doping of PPV blends

| Composition (nominal) | Initial current density(mA/cm ²) | |
|--------------------------|--|------------|
| | 1st charge | 2nd charge |
| PPV | <0.05 | ---- |
| 50/50 PPV/PEO | 0.48 | 0.83 |
| 50/50 PPV/PVME | 0.64 | 1.0 |
| 50/50 PPV/HPC | 0.17 | 0.65 |
| 50/50 PPV/MC | 0.13 | 0.51 |
| 50/50 PPV/PVP | <0.05 | ---- |

In summary blending the soluble precursor of a conducting polymer has been shown to be an effective technique for accelerating both chemical and electrochemical doping processes. Blending is effective by improving the net transport of dopant to the electroactive constituent.

CHAPTER VIII

POLY(PHENYLENE VINYLENE)/POLY(ETHYLENE OXIDE) BLENDS

In the previous chapter, a variety of PPV blend systems were investigated with respect to their effect upon chemical and electrochemical doping. Of these the PPV/PEO system was most attractive because it exhibited accelerated chemical and electrochemical doping, good thermal stability (during PPV precursor elimination), and good mechanical strength and flexibility. In addition, the use of a semi-crystalline polymer as the added component allows the attainment of various morphological features (e.g. spherulites) which may depend upon composition, casting conditions, thermal history, etc..

Thus a comprehensive study of the PPV/PEO system was undertaken with respect to morphology and attainable electrical properties after chemical and electrochemical doping. Blends were prepared as described in Chapter 3. The effects of blend composition, PEO molecular weight (M_w of 2×10^5 and 4×10^6 were used), blend casting conditions (room temperature and 90°C), casting solvent (H_2O , DMF, acetonitrile), and PPV precursor elimination conditions were studied. The results are presented in this chapter.

Optimization of Elimination

An essential element of the conducting polymer precursor process is the conversion or elimination of the precursor polymer, PXD, to the

fully conjugated product, PPV. Previous studies of the PPV precursor have demonstrated the sensitivity of the ultimate conductivity to the conditions of conversion.¹⁰⁰ In the present case of PPV/PEO blends, the optimization of PPV precursor conversion is complicated by the presence of the poly(ethylene oxide) constituent which is susceptible to thermal degradation under severe elimination conditions. Therefore, an initial study was undertaken to determine the optimum elimination conditions for this system with regard to the electrical conductivity and chemical microstructure of the blends.

For this optimization study 50/50 wt % PPV/PEO material was used. Samples of this blend were annealed at a series of temperatures and maintained at the given temperature for a series of times. The samples were then electrochemically doped at an applied potential of +4.1 V vs Li for nine hours. The infrared spectrum of the undoped blend and the electrical conductivity after doping were obtained for samples subjected to each set of elimination conditions. The conductivities of these samples are plotted in Figure 35 (page 129) where it can be seen that the conductivity is greatly affected by the conditions of elimination. The data indicate that, in terms of obtaining maximum conductivity, there is a compromise between driving the thermal elimination reaction to completion and minimizing thermal degradation. At lower annealing temperatures (150 - 200°C) long annealing times (~ 12 hours) are needed to achieve maximum conductivities. At high temperatures (250 - 300 °C) maximum conductivities are reached at shorter times (one hour). In general, conductivities in excess of 200 S/cm were reproducibly obtained

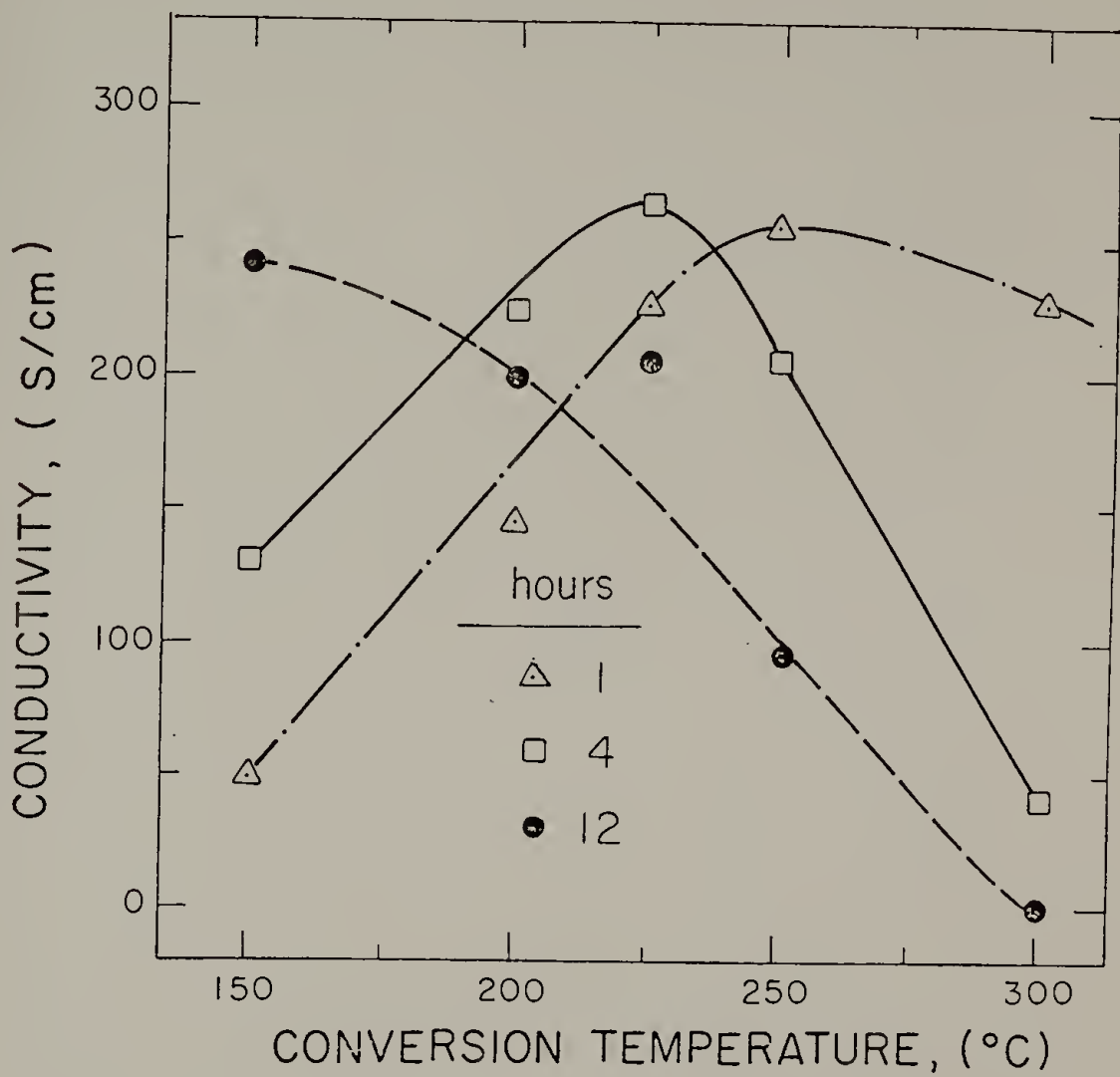


Figure 35. Conductivity of electrochemically doped 50/50 wt % PPV/PEO blends as a function of elimination temperature for a series of annealing times.

with conversion temperatures between 200 and 250°C maintained for several hours. Thus, the conditions adopted as standard for subsequent PPV/PEO blend studies were annealing at 225°C for four hours.

The effect of various elimination conditions upon the chemical microstructure of the blends could be observed directly using infrared spectroscopy. In Figure 36 (page 131), relevant portions of the IR spectra are displayed for some of the blends depicted in Figure 35. It may be noted that the absorption at 631 cm⁻¹, indicative of uneliminated units,⁸⁰ is still present for material annealed at 150°C for one hour. However, it disappears when the temperature is raised (200°C; one hour) or the time extended (150°C; 12 hours). At the other extreme of thermal treatment, spectroscopic evidence for thermal degradation (the emergence of a carbonyl absorbance at 1687 cm⁻¹ and disappearance of the PEO 1463 cm⁻¹ absorbance) begins to occur for annealing temperatures of 250°C and becomes severe at 300°C. The IR spectrum of optimized material (225°C, 4 hours) shows no evidence for the presence of either uneliminated units or thermal degradation.

Chemical Microstructure

Using optimized conversion conditions for this system, the chemical microstructure of the converted material was studied. Elemental analysis results for a series of PPV/PEO blends are displayed in Table 12. The oxygen content has been used to evaluate the blend composition which is also shown. The agreement between experimentally determined and calculated results supports clean elimination without observable chemical modification of PEO in these blends. Additional support for this

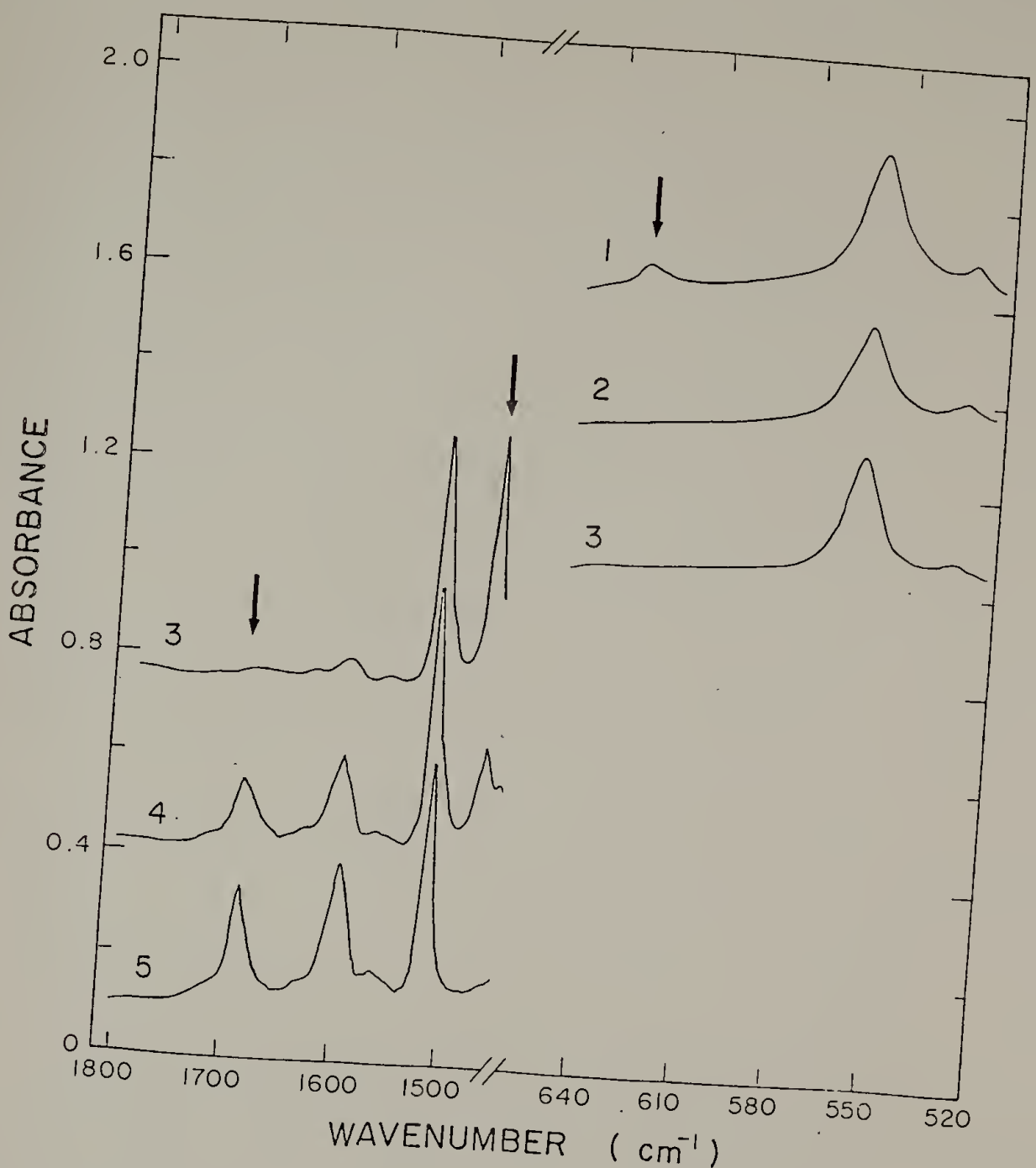


Figure 36. Regions of the infrared spectra of 50/50 wt % PPV/PEO blends annealed under various conditions. 1) 150°C, 1 hour; 2) 200°C, 1 hour; 3) 225°C, 4 hours; 4) 250°C, 12 hours; 5) 300°C, 12 hours.

Table 12. Elemental analysis results for a series of PPV/PEO blends

| <u>Composition</u> (wt/wt % PPV/PEO) | <u>Experimental</u> | | | <u>Theoretical</u> | | |
|---|---------------------|------|-------|--------------------|------|-------|
| | C | H | O | C | H | O |
| 0/100 | 53.30 | 8.87 | 36.80 | 54.55 | 9.09 | 36.36 |
| 10/90 | 55.83 | 8.72 | 32.79 | 58.71 | 8.77 | 32.72 |
| 16/84 | 57.80 | 8.59 | 30.84 | 60.88 | 8.58 | 30.54 |
| 21/79 | 61.3 | 8.57 | 29.0 | 62.86 | 8.42 | 28.72 |
| 42/58 | 71.03 | 7.43 | 21.48 | 71.17 | 7.74 | 21.09 |
| 58/42 | 77.29 | 6.78 | 15.63 | 77.50 | 7.23 | 15.27 |
| 82/18 | 86.30 | 6.43 | 6.58 | 87.00 | 6.46 | 6.54 |
| 87/13 | 87.25 | 5.98 | 4.70 | 88.97 | 6.30 | 4.73 |
| 100/0 | 93.67 | 5.96 | 0.58 | 94.12 | 5.88 | 0 |

conclusion is gained from the IR spectra. The spectra of various PPV/PEO blends were compared with the calculated spectra obtained by addition of the spectra of the two pure components. The equivalence of these spectra strongly indicates that the blends can be viewed as physical mixtures of pure poly(phenylene vinylene) and poly(ethylene oxide), without significant side reactions.

Thermal Properties

In the previous chapter it was demonstrated that PPV and PEO are immiscible both in the precursor and fully eliminated forms, as shown by a constant PEO glass transition temperature (-55°C) independent of blend composition. A PEO crystalline phase is readily identified in the blends by a melting endotherm in the region of 60°C. Pure PEO, prepared under similar conditions has a T_m of 66°C, and thus a significant melting point depression is observed in the blends. Figure 37 (page 134) displays T_m as a function of composition for a series of PPV/PEO blends. Although large melting point depressions are usually characteristic of miscible systems, this kind of behavior has also been observed in a number of immiscible crystalline polymer blends and has been attributed to a reduction in the average crystallite size as a result of blending.^{149,150}

The measured enthalpy of melting for each of the blends has been related to the degree of crystallinity of the PEO component using the relation:

$$\Delta H = X_C X_{PEO} \Delta H_0$$

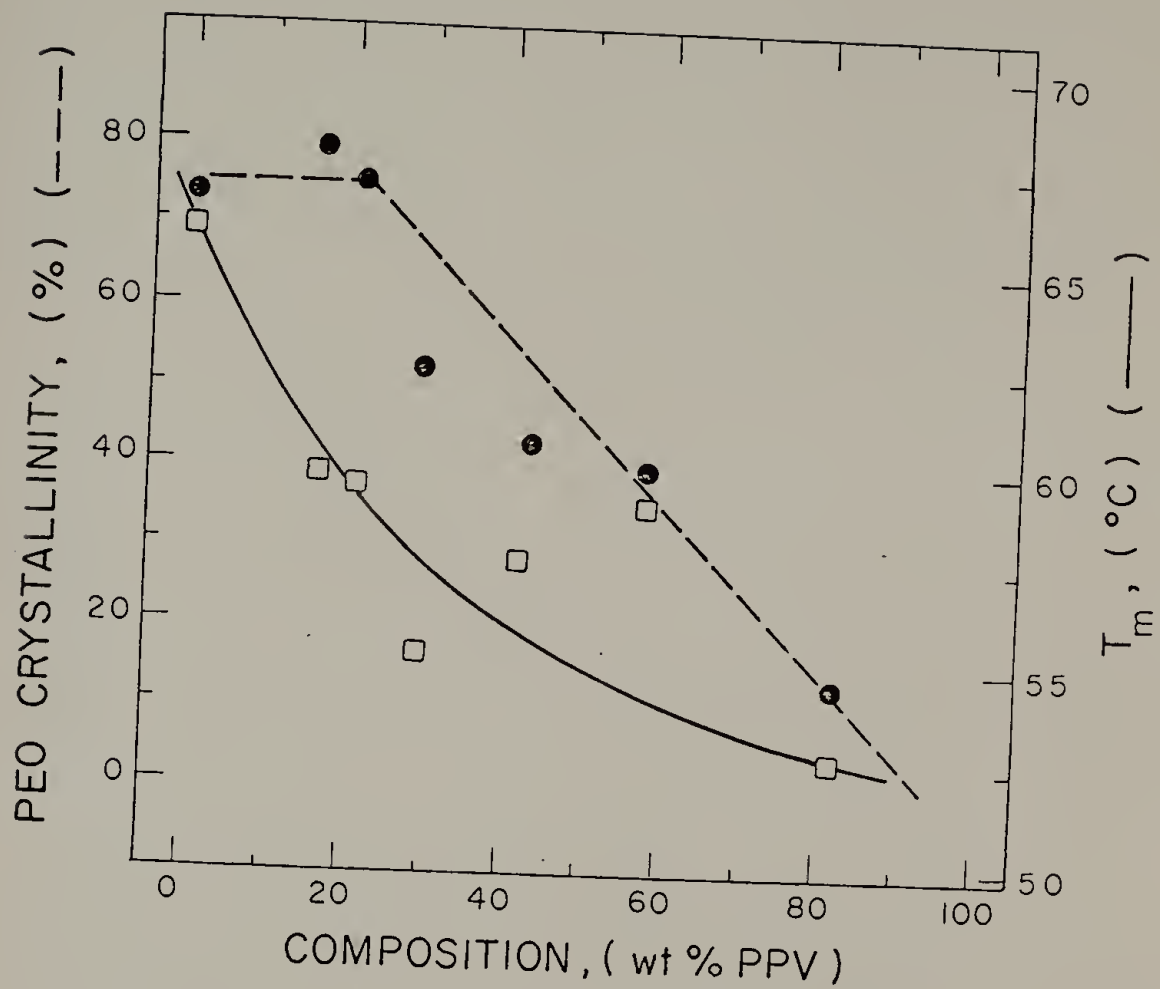


Figure 37. Melting point (\square) and degree of crystallinity (\bullet) of the PEO component as a function of the blend composition in PPV/PEO blends.

The enthalpy of melting of pure PEO crystals, ΔH_0 , was taken from Mandelkern as 45 cal/g.¹⁰⁸ In Figure 37, X_C is plotted against blend composition. It may be noted that the degree of crystallinity of PEO remains rather constant up to about 30 wt % PPV content at which point crystallinity decreases markedly with increasing PPV content. The suppression of PEO crystallinity at higher PPV contents affects the resulting blend morphology and the subsequent doping behavior as will be discussed below. Similar reductions in crystallinity have been reported for a number of blend systems including PEO/PMMA¹⁵¹ and polyacetylene composites.^{90,92}

Morphology

The morphology of the "as cast" PXD/PEO system is composition dependent. Blends rich in PEO (>~40 wt %) crystallize into spherulites when cast from solution at room temperature. The spherulites are large (100-500 μm diameter), birefringent, and volume filling (see Figure 38 [page 137]). The resulting samples are mechanically rather fragile. For blends rich in the PPV precursor, PXD, (>~60 wt %) spherulites do not form. These films are transparent, flexible, and tough. They are featureless in the optical microscope indicating highly dispersed phases, consistent with the observed melting point depressions shown in Figure 37.

Figure 38. Optical micrographs of spherulites in "as cast" PXD/PEO blends showing decreasing birefringence with increasing PXD contents: a) pure PEO; b) 10/90 wt % PXD/PEO; c) 21/79 wt % PXD/PEO; d) 42/58 wt % PXD/PEO.

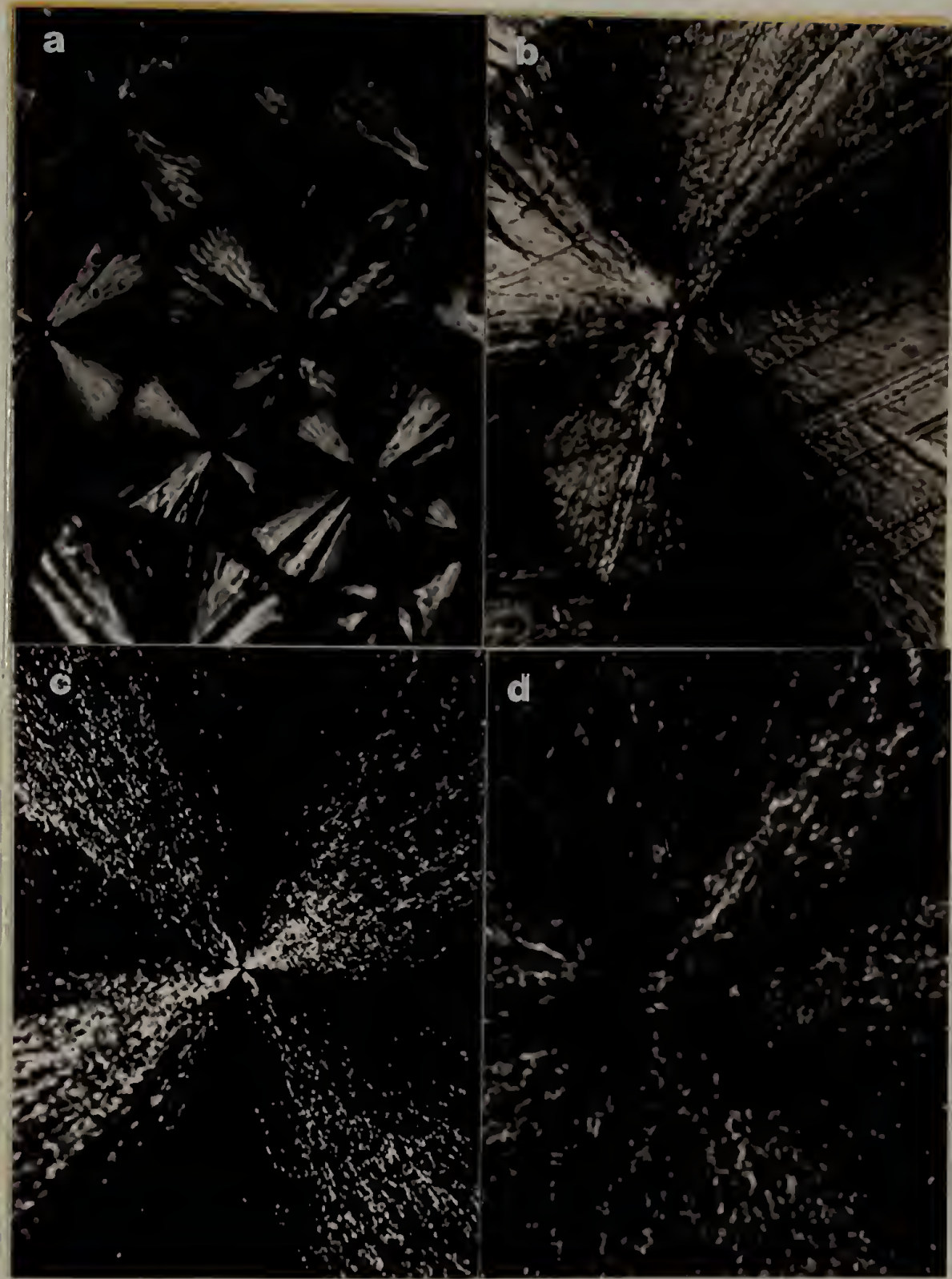


Figure 38 demonstrates that the total birefringence of the spherulites decreases with increasing PXD content, concommittant with the reduction in crystallinity measured by calorimetry (Figure 37). Thus the absence of spherulites at still higher PPV contents may be attributed to the reduction of crystallinity below some threshold level required for spherulite growth.

The morphology of crystalline polymer blends has been well studied experimentally and theoretically and several reviews are available.^{152,153} For systems in which one component crystallizes, three types of spherulite formation have been observed. The non-crystalline component may be excluded into the interlamellar regions of growing crystallites, forming amorphous domains with dimensions on the order of the lamellar thickness (~ 10nm), or the non-crystalline component may be excluded into regions between growing crystalline fibrils forming domains with dimensions of the order of fibrillar width (~ 1μm). A third possibility is that the non-crystalline component may be excluded completely from the growing spherulite, forming inter-spherulitic domains of the order of 100μm in size.

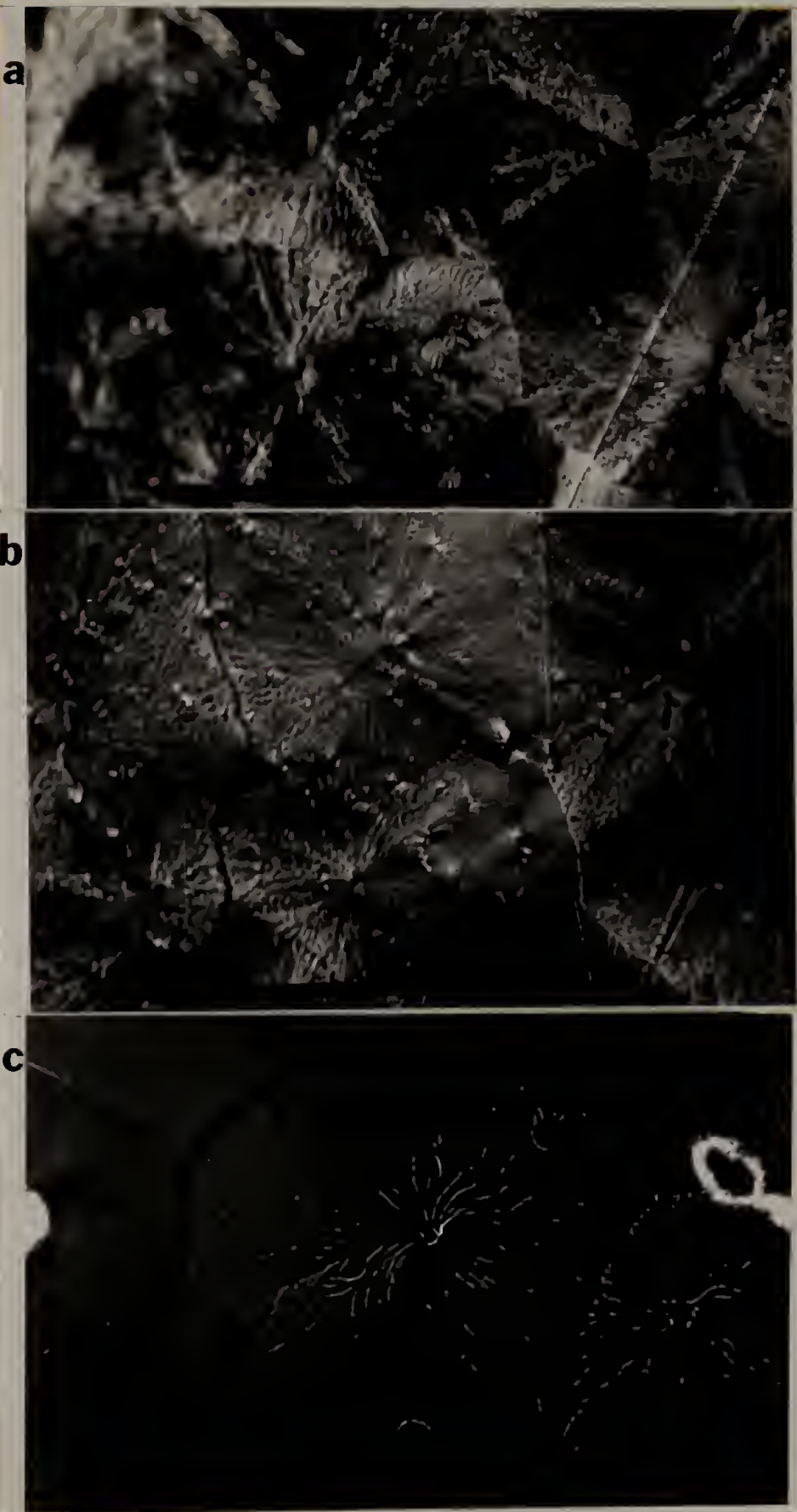
Interlamellar segregation has been verified in the poly(ϵ -caprolactone)/PVC and PEO/PMMA systems using SAXS techniques.^{154,155} Interfibrillar segregation has been observed in a number of systems, for example blends of trans- and cis-polyisoprene.¹⁵⁶ Interspherulitic segregation is commonly encountered upon crystallizing from heterogeneous melts, for example in PEO/PS and PP/LDPE immiscible blends.¹⁵⁷

In the present system, segregation on the interfibrillar scale can be directly observed using hot stage microscopy. The spherulites are completely volume filling, even up to a PXD content of 50 wt %. The boundaries

between impinged spherulites are sharp and well defined. Therefore the PPV precursor domains must be included within the spherulite structure. The implication is that during film casting, the spherulitic linear growth rate surpasses the diffusion rate of excluded material so that PXD domains are entrapped within the spherulite.

Evidence for interfibrillar segregation is presented in Figure 39 (page 141). An "as cast" 30/70 PXD/PEO film at room temperature is shown in Figure 39a. This sample was heated to 60°C at which point the melting of PEO crystallites was evidenced by a sudden reduction in birefringence. However the spherulitic texture remained otherwise intact. Of course, pure PEO when melted suffers complete extinction of light between crossed polars because no optically anisotropic species remain. However, the weak birefringent pattern which persists in the blends is attributable to "form" birefringence associated with the anisotropy of shape of the dispersed domains.¹⁵⁸ The sample in Figure 39a was further heated to temperatures where the conversion of PPV precursor to PPV proceeds. Figure 39b shows the sample held at 150°C. In this micrograph one can discern the meandering domains of PPV in the molten PEO matrix. These domains appear to be fibrils which extend radially with an average width of several microns. This radiating fibrillar structure is even more evident in Figure 39c, which shows a 50/50 PPV/PEO blend also held above the PEO melting point. From these micrographs the conclusion may be drawn that the morphology obtained during the casting of PXD/PEO films from solution is largely maintained throughout the PXD elimination to PPV at elevated temperatures. This is a result of the infusibility of PXD and PPV domains. It is expected that the resulting bicontinuous morphology is a desirable one for conducting polymers

Figure 39. Optical micrographs of PPV/PEO blends showing separate PPV and PEO domains upon melting. a) 30/70 PPV/PEO blend "as cast" at R.T.; b) the same sample held at 150°C; c) 50/50 PPV/PEO blend held at 150°C (showing radiating fibrillar domains).

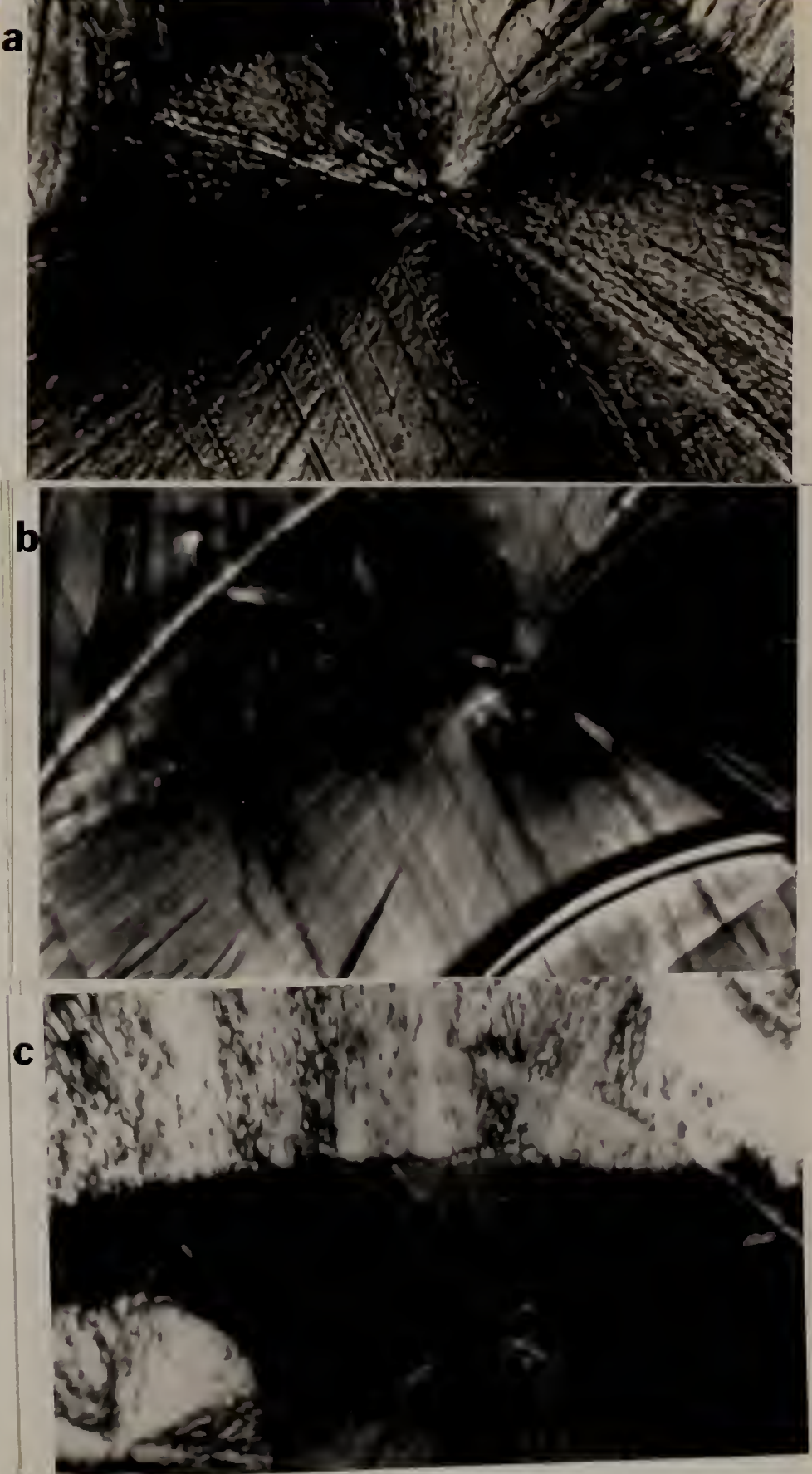


because it results in a highly connected (and hence conductive) electroactive phase which is still relatively "open" allowing rapid diffusion of dopant into the material (c.f. Shirakawa polyacetylene).¹³²

Additional hot stage microscopy showed that the persistence of spherulitic texture after PEO melting was observed at PXD contents as low as 10 wt %. In Figure 40a (page 144) a micrograph of a 10/90 PXD/PEO "as cast" blend shows the strongly birefringent (high crystalline) extinction pattern. In Figure 40b, the same spherulite is held at 150°C (90°C above T_m). The birefringence is of course greatly diminished; however, the texture of radiating fibrils persists, strongly suggesting a continuous PPV phase even at this loading. Upon cooling again to room temperature, the PEO melt phase crystallizes over the surface of the material; the advancing crystallization front is shown in Figure 40c. The result is a layer of pure PEO coating the fully converted blend. The presence of this layer affects subsequent chemical doping, resulting in an induction period which will be discussed in the next section.

Non-spherulitic textures could be observed if films were cast by removing the solvent at a temperature above the PEO melting point. A series of films was cast from aqueous solutions at 90°C to dryness. After casting the films were cooled rapidly to room temperature. For these films, PEO crystallization does not occur during the film casting process. Instead liquid-liquid phase separation occurs followed by vitrification of the amorphous PPV precursor phase. When the film is cooled, PEO crystallizes out of droplets of pure melt. The resulting morphology, shown in Figure 41 (page 147), is a grainy micro-crystalline

Figure 40. Optical micrographs of a 10/90 PXD/PEO blend at various temperatures. a) "as cast" at R.T.; b) held at 150°C; c) upon cooling to R.T. (showing crystallization front).

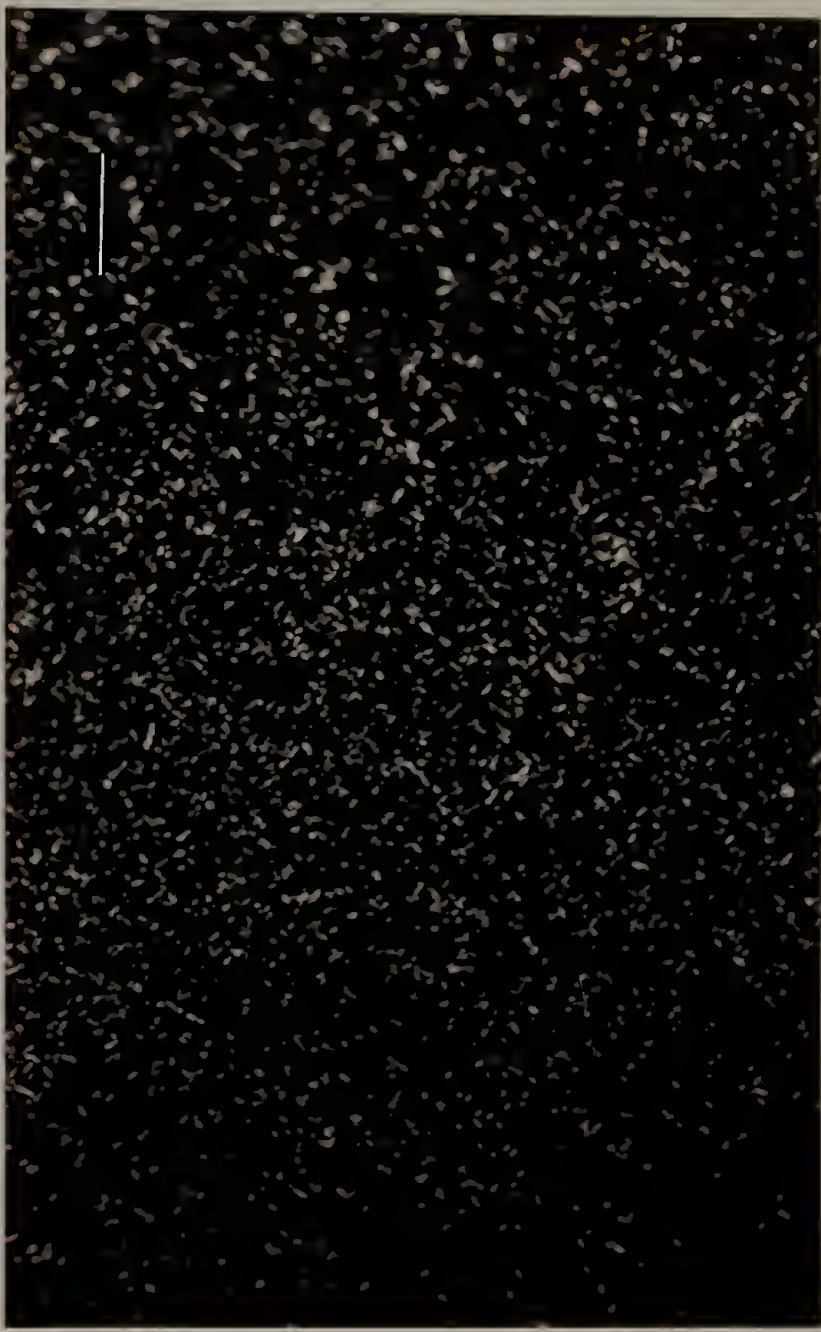


structure with irregular domains on the order of several microns in size. The materials prepared in this way were decidedly tougher and stronger than room temperature cast film, (particularly for PEO-rich formulations) and showed improved doping characteristics to be discussed in the next section.

Experiments were performed to determine the extent to which the PEO component could be extracted out of the blends by a good solvent. This study was stimulated by results on electrochemical doping, discussed in Chapter 7, where the blend is exposed to electrolyte solution and introduction of dopant and extraction of PEO occur simultaneously. Chloroform was used because of its high volatility and strong solvating power for PEO. Figure 42 (page 148) shows the extraction efficiency or fraction of material extracted compared to the composition of PEO in the blend. (Previous work has shown that fully eliminated PPV is insoluble in all common solvents.).¹⁵⁹ It may be noted in Figure 42 that for PEO-rich (spherulitic) blends nearly all (80-90%) of the PEO is extractable. As the PPV content increases, progressively less of the PEO can be extracted, presumably because PEO becomes the dispersed (and thus less solvent-accessible) phase. This effect has relevance for electrochemical doping because electroactivity is achieved as a result of infiltration of electrolyte into the material through interaction with the PEO phase. To obtain facile and complete charge storage, channels for such infiltration must be present throughout the material.

At extremely low PPV contents (2 wt % and 4 wt % PPV), extraction resulted in complete disruption of the film leaving micron size particles of PPV. However, a 10/90 wt% PPV/PEO blend could be fully

Figure 41. Optical micrograph of 30/70 wt % PXD/PEO blend cast under vacuum at 90°C and quenched to R.T. showing grainy morphology.



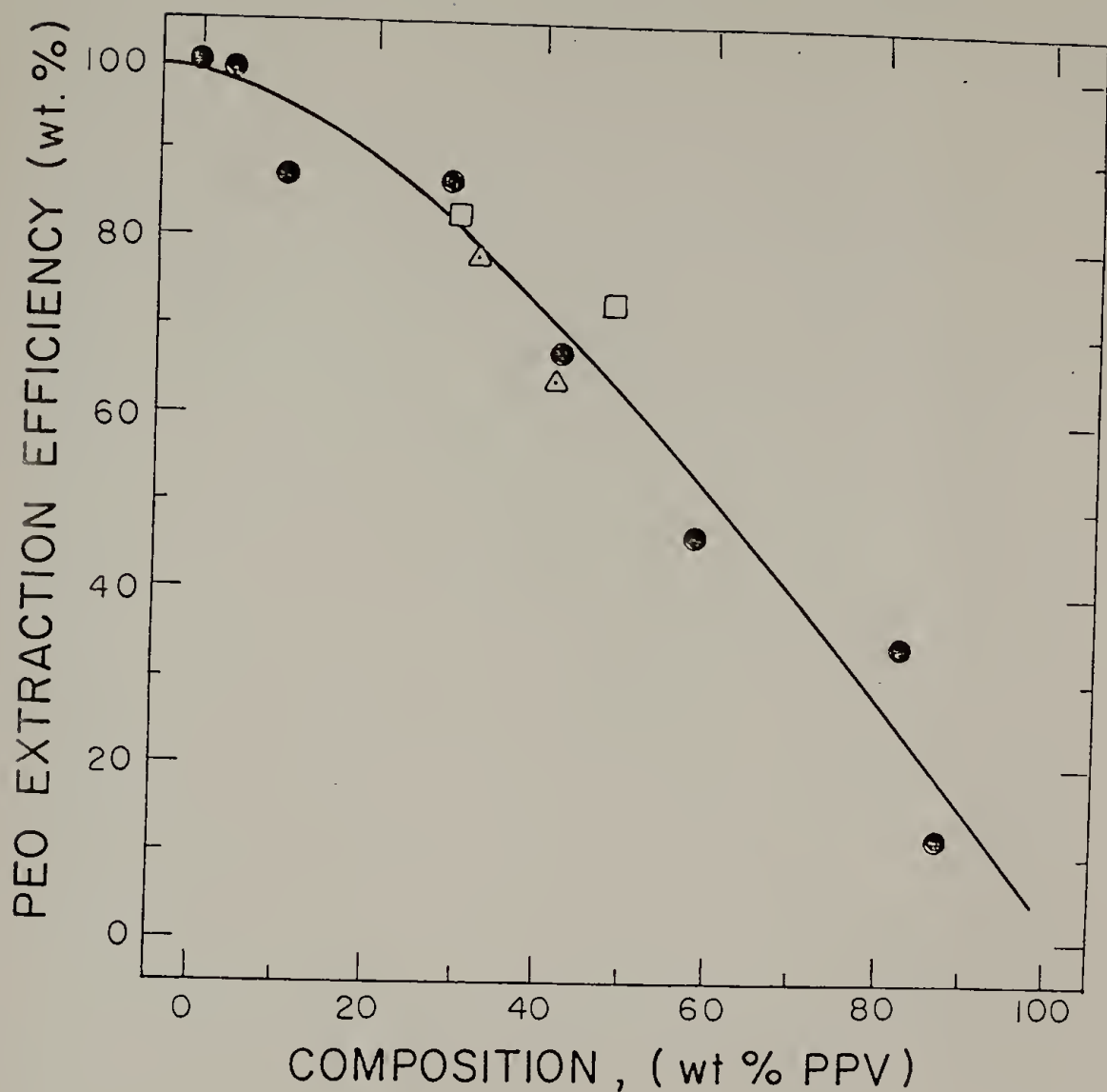


Figure 42. The weight fraction of PEO which could be extracted with chloroform for PPV/PEO blends as a function of blend composition.

● : PEO MW 2×10^5 , cast at R.T.;

△ : PEO MW 4×10^6 , cast at R.T.;

□ : PEO MW 2×10^5 , cast at 90°C.

extracted leaving a continuous, although fragile film, implying a continuous PPV phase at this loading. Optical microscopy revealed that extracted films retained their spherulitic texture with the expected greatly weakened birefringence. Chemical and electrochemical doping of extracted films was performed and will be discussed subsequently.

In general, spherulitic morphologies could be associated with high extraction efficiency; non-spherulitic structures showed poor extractability.

Chemical Doping

Chemical doping of the blends, using AsF_5 vapor, resulted in highly conductive materials. The previous chapter showed that blending PPV results in increased conductivity and more rapid doping. In this chapter the composition dependence of this effect will be presented.

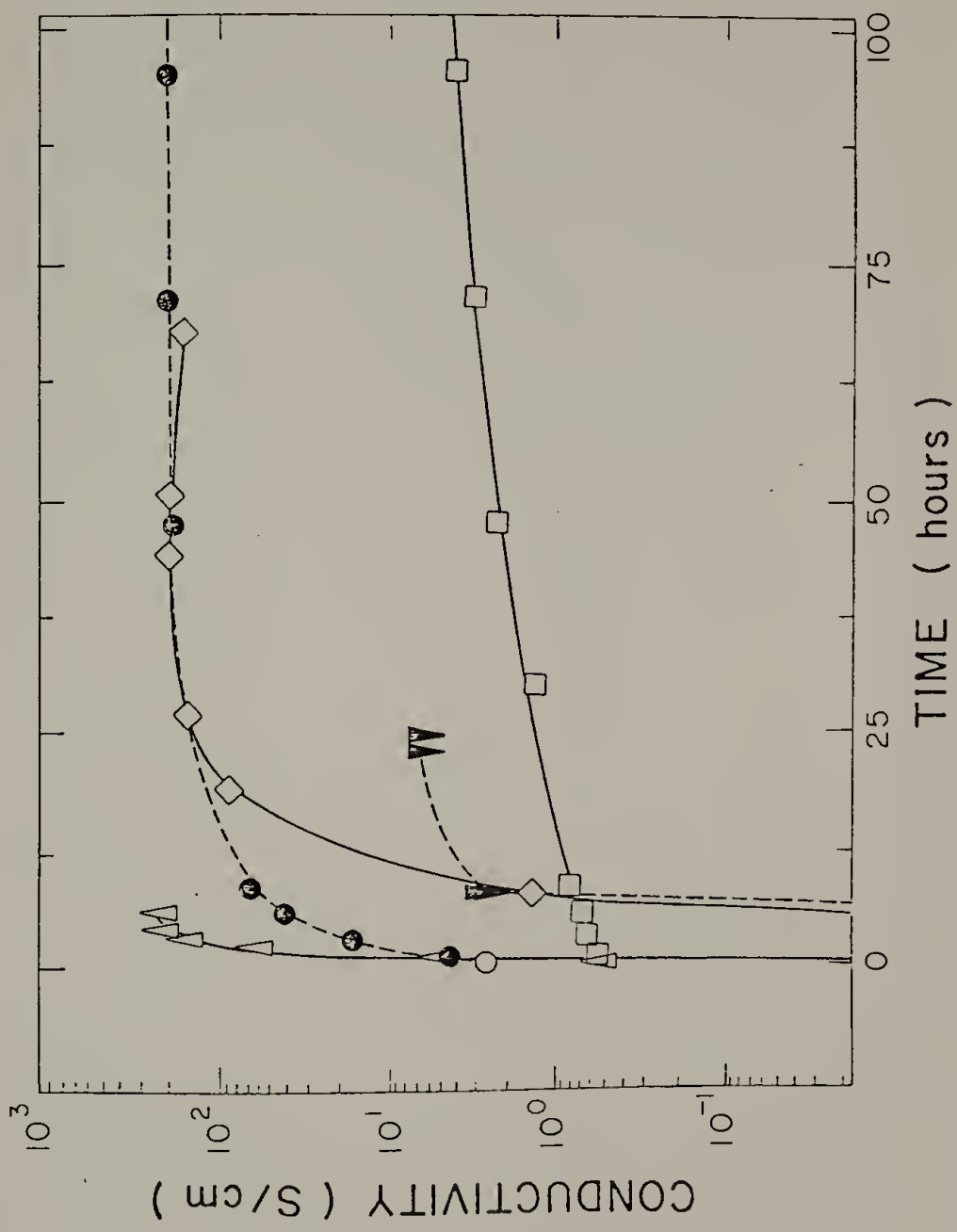
Figure 43 (page 152) shows the increase in conductivity as a function of time upon exposure to dopant vapor for samples of various composition. Pure PPV shows a very rapid initial increase in conductivity, associated with surface doping, followed by a very slow rate of further increase. Asymptotic values may take as long as four to five weeks to be attained under the conditions employed. This response is associated with the slow diffusion of dopant molecules through the PPV film. Poor dopant transport is commonly observed in conducting polymers possessing dense morphologies such as "Durham" polyacetylene¹⁶⁰ and is sufficient to completely prevent doping in highly ordered single-crystals of poly(diacetylenes).¹⁶¹ In the present case, blending PPV with PEO in

the manner described results in greatly enhanced doping rates. It may be noted for example in Figure 43 that a 40/60 wt% PPV/PEO blend, doped under the same conditions as pure PPV, attained a maximum conductivity within only two days of exposure and achieved an appreciably higher conductivity than the pure material. In fact, even blends containing modest amounts of PEO (90/10 wt% PPV/PEO) exhibited complete doping within two days and achieved a final conductivity greater than 200 S/cm. These PPV-rich formulations may prove to be the most useful because they retain the rapid doping and enhanced conductivity of blends without compromising the mechanical strength and unique processing characteristics of pure PPV.

PEO-rich formulations also doped to high conductivities. However, these materials exhibited a composition-dependant induction period before high conductivity was achieved. For compositions \leq 40 wt % PPV, this period lasted approximately six hours. We attribute this effect to a very PEO-rich surface, or electro-inactive skin, which coats the blend during the recrystallization of the PEO phase following the thermal conversion process. The direct observation of this phenomenon using hot stage microscopy was discussed earlier.

Figure 43. Electrical conductivity as a function of time of exposure of 65 torr AsF_5 (dopant) to a variety of PPV/PEO blends.

□ : pure PPV
● : 90/10 wt % PPV/PEO
◇ : 42/58 wt % PPV/PEO
▼ : 10/90 wt % PPV/PEO
Δ : 48/52 wt % PPV/PEO (cast at 90°C)



Blends which were prepared by casting at elevated temperatures exhibited the maximum doping rates. In Figure 43 a 48/52 wt% PPV/PEO cast from aqueous solution at 90°C is shown to have reached a maximum conductivity of 250 S/cm within five hours of doping. This represents a reduction by two orders of magnitude in doping time compared to pure PPV, demonstrating the important role that morphology can play in controlling dopant transport.

In Figures 44 (page 154) and 45 (page 155) a quantitative treatment of AsF₅ diffusion into PPV, PEO and a 50/50 wt% PPV/PEO blend is presented. Dopant uptake of sample films was monitored as a function of time using a quartz spring. Figure 44 shows the weight uptake of dopant, normalized to the film surface area, of unblended PPV doped with two vapor pressures of AsF₅. The data was analyzed according to a Fickian model of planar semi-infinite diffusion:

$$Q/A = \frac{2D^{\frac{1}{2}} t^{\frac{1}{2}} C_0}{\pi^{\frac{1}{2}}}$$

where Q/A is the normalized weight uptake (mg/cm²), D is the diffusion coefficient, and C₀ is the surface concentration of dopant. C₀ was obtained from the limiting concentration of dopant found after long doping times (1 AsF₅ per 4 PPV repeat units for the lower pressure and 1 AsF₅ per PPV repeat unit for the higher pressure).¹⁶² Values of D calculated for the higher and lower pressures were 3 X 10⁻¹³ cm²s⁻¹ and 4 X 10⁻¹³ cm²s⁻¹, respectively, which compare very well with diffusion coefficients obtained for the AsF₅ doping of Durham polyacetylene.^{160,163}

The rate of dopant uptake is much faster for PPV/PEO blends and for pure PEO, as shown in Figure 45. Doping kinetics are considerably

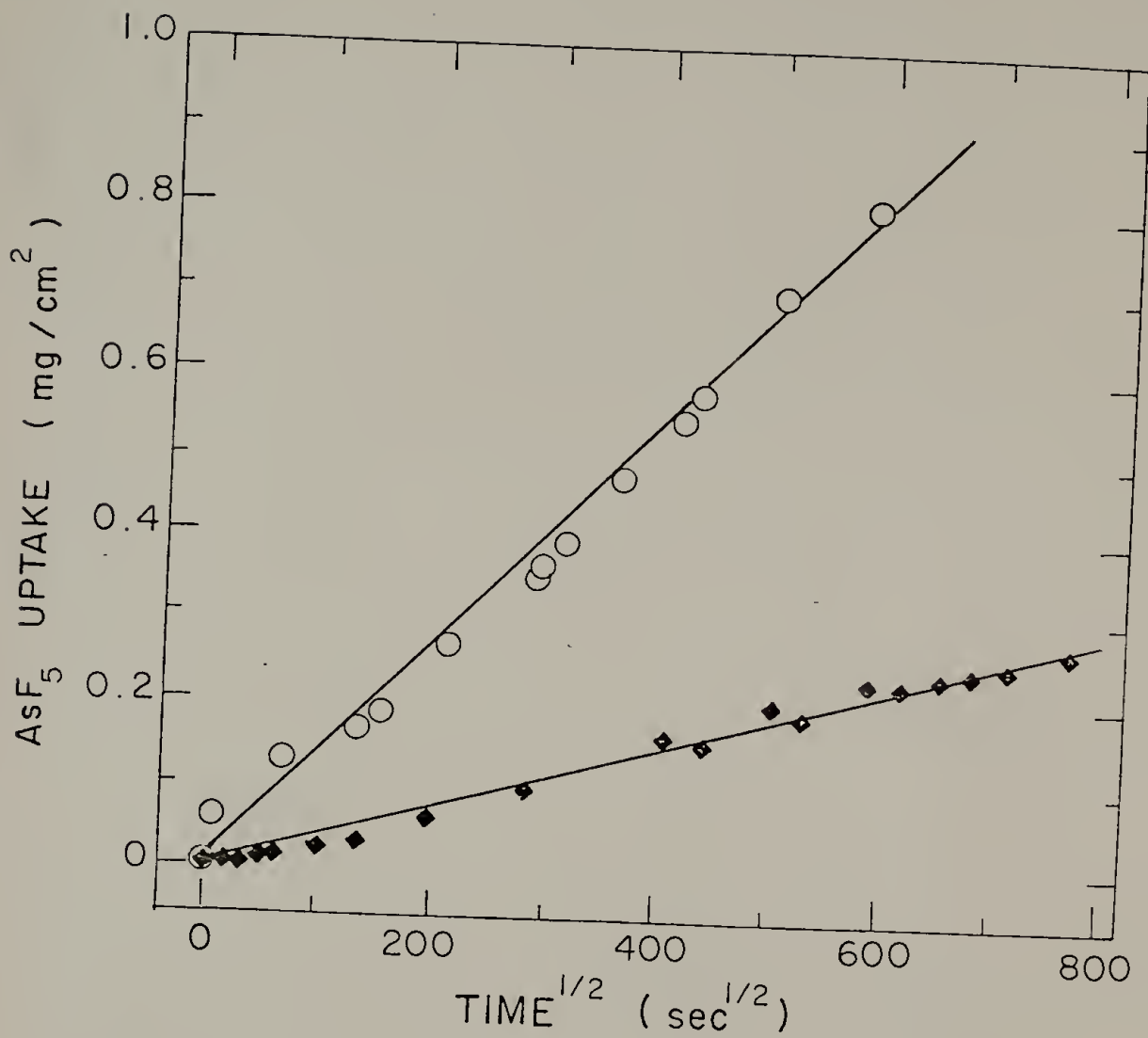


Figure 44. Weight uptake of dopant (AsF_5) normalized to sample surface area as a function of $(\text{time})^{1/2}$ upon exposing PPV to dopant vapor.

◆ : 65 torr; ○ : 300 torr.

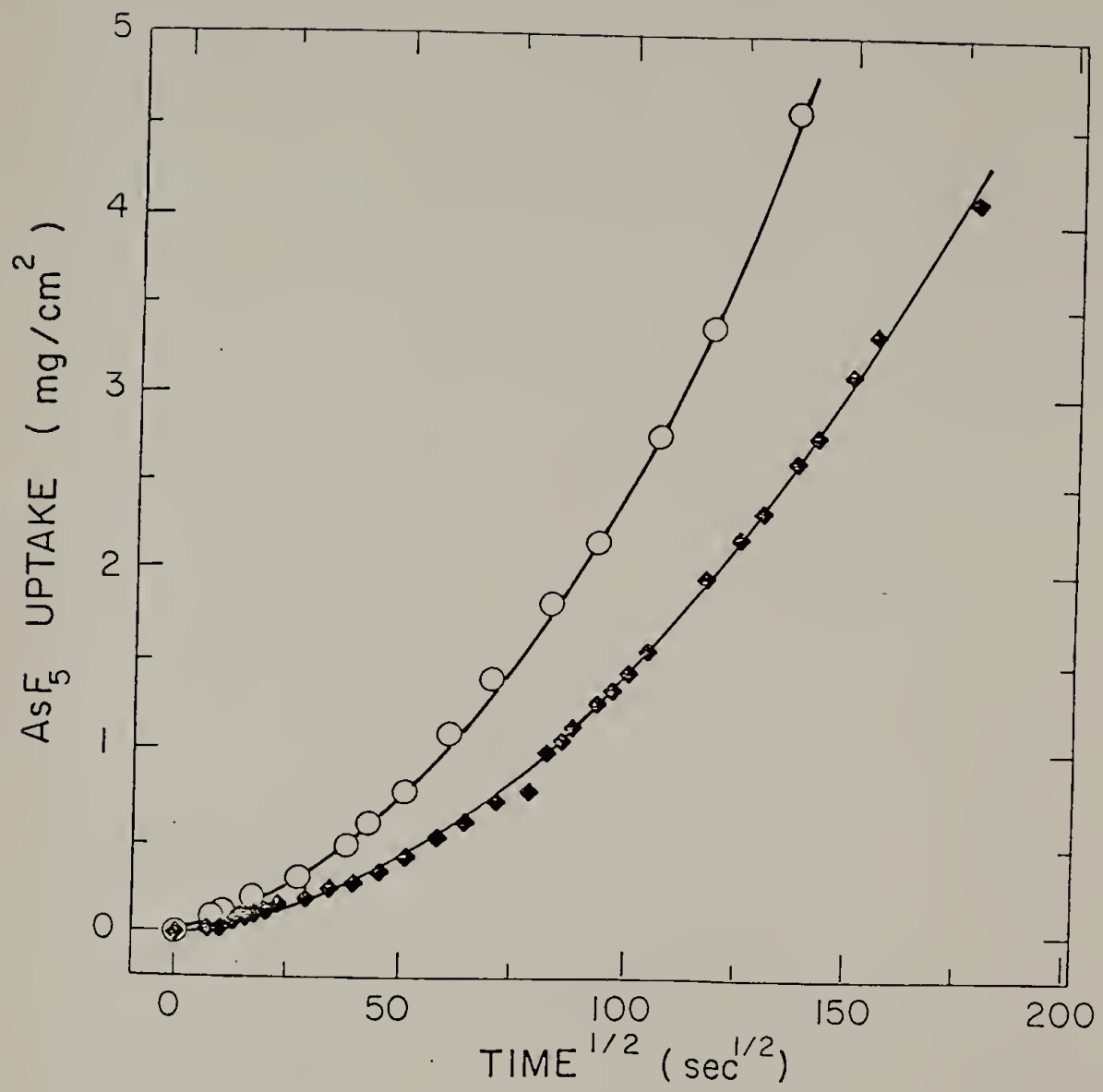


Figure 45. Weight uptake of dopant (AsF_5 ; 65 torr) as a function of $(\text{time})^{1/2}$ of exposure to dopant for \circ : pure PEO; \blacklozenge : 50/50 wt % PPV/PEO.

more complicated (and decidedly non-Fickian) for the PEO-containing systems, owing to the complex morphological factors and the fact that reaction between AsF_5 and PEO clearly destroys PEO crystallinity.

Of particular interest in the chemical doping study was the composition dependence of ultimate conductivity for this system. Shown in Figure 46 (page 157) are the final values of conductivity achieved as a function of the blend composition. Most notably, there is a wide range of compositions over which conductivity is rather insensitive to composition. Between 25 wt % and 90 wt % PPV content, the ultimate conductivity of the material falls between 100 and 200 S/cm, whereas PPV reached only 25 S/cm under identical conditions. Thus a highly connected yet very dopant accessible morphology is postulated over this range of composition.

We attribute the unexpectedly high conductivity of blends compared to the pure material to more complete doping of the PPV domains in the blends as a result of accelerated dopant diffusion. Thus blending results in greatly enhanced conductivity of the electroactive phase. A minimum conductivity for this phase can be estimated by normalizing the macroscopic conductivity of the sample by the volume fraction (we must substitute the weight fraction, w_{PPV}) of electroactive component. This assumption is equivalent to treating the two phases as parallel resistors and is admittedly inappropriate at low PPV loadings. However, in view of the highly connected morphologies discussed earlier, we will

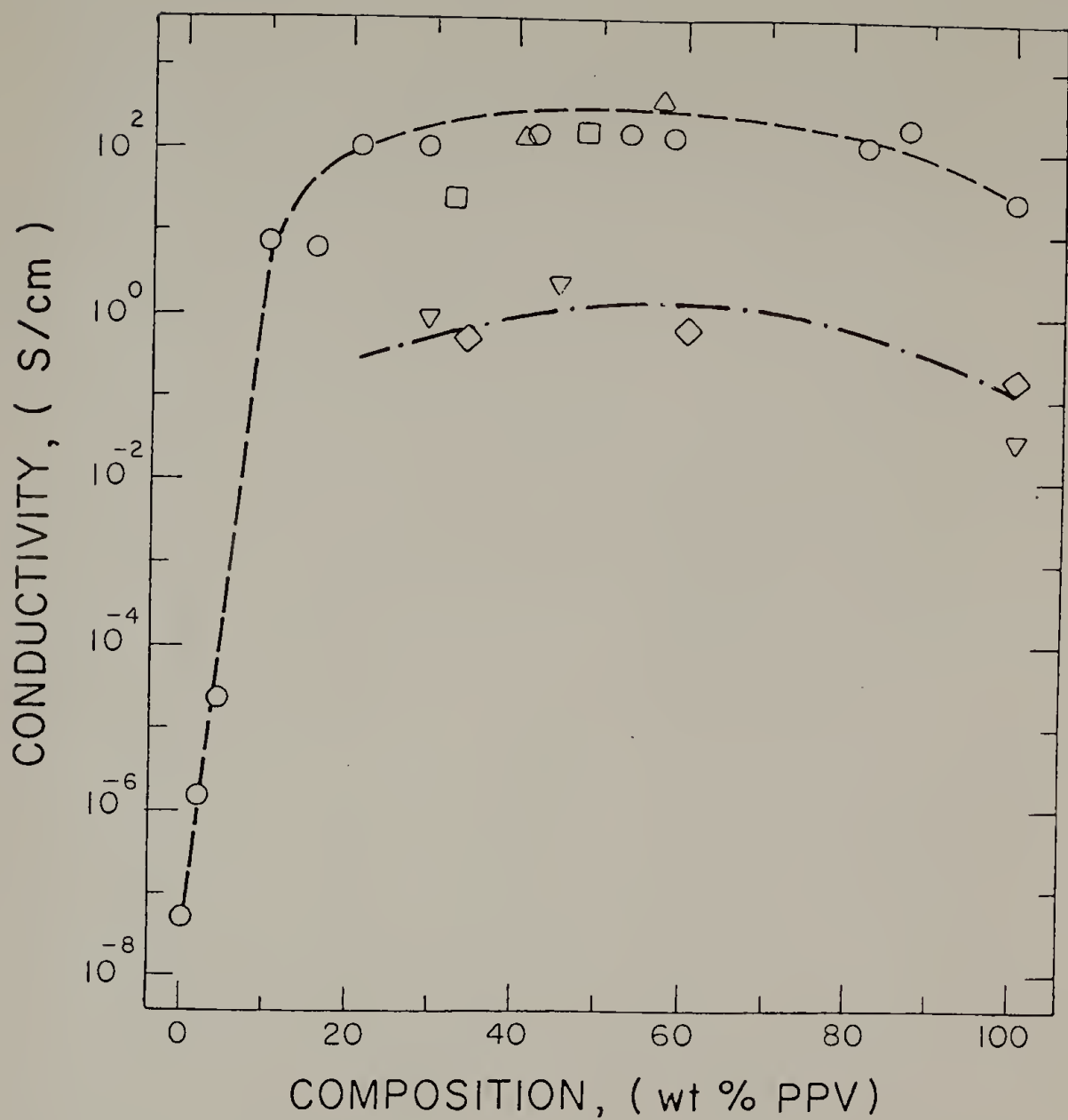


Figure 46. Final conductivity (after AsF_5 doping) as a function of composition for PPV/PEO blends prepared under various conditions.

- - cast from aqueous solution at R.T.;
- - cast from aqueous solution at 90°C;
- △ - PEO MW 4×10^6 ;
- ◇ - cast from DMF solution;
- ▽ - cast from acetonitrile solution

apply the formalism:

$$\sigma_{PPV} \geq \frac{\sigma_{Blend}}{w_{PPV}}$$

Thus for the 21/79 wt% PPV/PEO formulation which attained a conductivity of 109 S/cm, the minimum local conductivity of the PPV phase is 520 S/cm. This result strongly implies improved doping of PPV domains in the blends.

At very low loadings of PPV, the behavior is also of some interest. High conductivities are reached at very modest levels of PPV composition. Of course pure PEO does not become conductive even under prolonged exposure to dopant. However, upon adding 2 wt % and 4 wt % PPV, significant increases in conductivity were observed (see Figure 46). At 10 wt % PPV, conductivity rose abruptly reaching a value of 6 S/cm. Thus percolation of the conducting phase is observed between 4 and 10 wt % PPV. This observation is consistent with extraction and microscopy results which indicated the onset of a continuous PPV phase at or below 10 wt %. A percolation threshold below 16% PPV is consistent with the observed anisotropy of shape of PPV domains.¹⁶⁴

Blends containing high molecular weight PEO, also shown in Figure 46, attained conductivities which were comparable to their lower molecular weight counterparts. This was expected since the blend morphology did not change with higher molecular weight PEO. Also, extraction with chloroform (to remove PEO) did not seriously affect the attainable conductivity of a 50/50 wt% blend (see Table 13). Blends which were cast at elevated temperatures also attained high conductivities. The 50/50 wt %

blend of this type attained a conductivity of about 200 S/cm.

The behavior of PPV/PEO blends which were cast from DMF and acetonitrile warrants some discussion. The goal of these experiments was to determine the effect of the casting solvent on the properties of the blends, because many previous investigations of polymer blends have shown significant solvent dependence of morphology for solution cast materials.^{165,166} In the present case, in order to obtain an additional common solvent for the PPV precursor and PEO, an ion-exchange step had to be performed on the PPV precursor (PXD) to replace the chlorine anion in the polyelectrolyte with a tetrafluoroborate ion. The ion-exchanged precursor, $\text{PXD}^+\text{BF}_4^-$, exhibits excellent solubility in DMF and acetonitrile, which are also both good solvents for PEO. Thus these solvents were used to prepare additional PPV/PEO blends.

Surprisingly, pure PPV, prepared by casting the modified precursor from either DMF or acetonitrile solutions followed by thermal conversion and doping under standard conditions, resulted in materials with much lower conductivities than that of PPV prepared from the aqueous precursor. Doped PPV from the aqueous precursor, PXD^+Cl^- , rose to a conductivity of 25 S/cm in this study as stated earlier; however, PPV prepared from the organic precursor solution, $\text{PXD}^+\text{BF}_4^-$, only reached conductivities in the vicinity of 0.1 S/cm, a very substantial decrease. We attribute this difference to a cleaner and more complete elimination reaction for the chloride precursor relative to the tetrafluoroborate precursor, resulting in a more highly conjugated product for the former. Both products exhibit the characteristic IR absorbances of PPV, however,

the PPV arising from the chloride precursor exhibits the expected elemental analysis results (see Table 12) for pure PPV, with very little residual chlorine (<0.5 wt %). Yet PPV arising from the tetrafluoroborate precursor retained as much as 5 wt % residual fluorine after thermal conversion indicating incomplete conversion.

In spite of the lower conductivity found for the organic precursor system, blends with PEO were prepared. These blends showed the same synergistic behavior as those prepared from the aqueous system. That is, the PPV/PEO blends had conductivities which were about an order of magnitude larger than the corresponding unblended PPV, as shown in Figure 46. Thus PPV/PEO blends cast from DMF or acetonitrile solutions exhibited conductivities after AsF_5 doping in the vicinity of 1 S/cm. Blends cast from DMF and acetonitrile did not differ appreciably from each other. Both exhibited thermal behavior and spherulitic morphologies similar to those described for the aqueous systems. Thus although casting solvent and precursor counterion did affect the properties of the electroactive phase, they did not greatly affect the overall blending behavior with PEO.

The weight uptake of dopant (along with the ultimate conductivities) for each of the blends is listed in Table 13. As these data show, all the blends absorbed a considerable quantity of dopant. Typical samples absorbed greater than 200% of their original weight when doped to a maximum conductivity. By comparison, pure PPV absorbed only 11 wt % of dopant under the same conditions. Of course, it is not reasonable to attribute all of the weight increase in the blend samples to an

increased degree of doping of the PPV phase. AsF₅ is a strong oxidizing agent of rather low selectivity.¹⁶⁷ Thus it reacts with both the PPV phase forming a conducting complex and with the PEO phase resulting in a non-conducting adduct. From inspection of Table 13, it is evident that PEO rich blends tended to absorb more dopant than PPV rich compositions. In fact, we attribute the dopant's strong affinity for PEO to the rapid absorption by the blends giving rise to higher degrees of doping of the PPV domains and higher conductivities for these materials.

None of the blends in this study showed improvements in atmospheric stability compared to pure doped PPV. For typical doped samples of various compositions, conductivity decreased by over an order of magnitude within one hour of air exposure and by four orders of magnitude within one day of exposure. It is likely however that blending with hydrophobic polymers would lead to improved stability, as has been suggested by Wnek.⁹⁰

Table 13
Conductivity and dopant uptake of chemically
doped PPV/PEO blends

| Composition (wt/wt PPV/PEO) | Conductivity (S/cm) | Dopant Uptake (wt %) |
|--------------------------------|------------------------|-------------------------|
| 0/100 | 5.1×10^{-8} | 644 |
| 2/98 | 1.5×10^{-6} | 159 |
| 4/96 | 2.4×10^{-3} | 78 |
| 10/90 | 6.94 | -- |
| 16/84 | 5.69 | 288 |
| 21/79 | 109 | 106 |
| 29/71 | 112 | 149 |
| 42/58 | 166 | 265 |
| 53/47 | 148 | -- |
| 58/42 | 136 | 299 |
| 82/18 | 131 | 105 |
| 87/13 | 210 | 36 |
| 100/0 | 25.9 | 11 |
| 41/59 ^a | 165 | 242 |
| 57/43 ^a | 464 | 208 |
| 42/58 ^b | 103 | 262 |
| 32/68 ^c | 28 | 122 |
| 48/52 ^c | 162 | 188 |
| 48/52 ^c | 250 | -- |
| 34/66 ^d | 0.554 | 146 |
| 60/40 ^d | 0.699 | 293 |
| 100/0 ^d | 0.175 | 48 |
| 29/71 ^e | 0.810 | 153 |
| 45/55 ^e | 2.19 | 287 |
| 100/0 ^e | 0.0324 | 18 |

^a Blends were prepared with high molecular weight PEO (4×10^6).

^b Blend was extracted with chloroform before doping.

^c Blends were cast at 90°C under vaccuum.

^d Blends were prepared with ion-exchanged precursor and cast from DMF solutions.

^e Blends were prepared with ion-exchanged precursor and cast from acetonitrile solutions.

Electrochemical Doping

Electrochemical doping has proven to be a valuable method for the accurate and homogeneous doping of conducting polymers.¹⁶⁸ A requirement for electrochemical doping is the diffusion of "dopant" ions, supplied by the electrolyte, into the doped material to preserve charge neutrality. Such ionic transport processes generally prove to be the rate determining step in the electrochemical doping of conducting polymers. In the last chapter it was demonstrated that blending PPV with appropriate polymers leads to greatly enhanced electrochemical activity. In the present chapter the rate of doping as a function of the PPV/PEO blend composition will be presented in order to define the optimum composition range for the applications of PPV that require electrochemical activity, such as rechargeable battery electrodes.¹⁴⁸

PPV blends were studied over the composition range 100/0 to 20/80 wt% PPV/PEO (10/90 PPV/PEO were too fragile after doping). Two similar samples of each composition were then cut and sandwiched together in the doping cell. A doping potential of +4.1 vs. Li was applied for 410 minutes and charge was recorded as a function of time. At the end of the doping period samples were removed, peeled apart, and their four-probe conductivities measured. The purpose of using this sandwich configuration was to obtain an estimate of the homogeneity of the doping process. In Table 14, the ratio of the conductivity of the film closest to the electrode (σ_{inner}) to that of the film facing the electrolyte (σ_{outer}) is given, along with the final conductivity of the film that was most conducting. Doping appears to be relatively homogeneous with

the trend towards slightly higher conductivities for regions of the sample that are closer to the platinum electrode. It should be noted that the maximum conductivity value in Table 14, at a composition of 60 wt% PPV probably represents a compromise between faster doping due to higher PEO content and greater ultimate conductivity due to higher PPV content. In other words, the compositions containing greater than 60 % PPV have probably not reached their limiting value in the time allowed for doping.

Also listed in Table 14 is the current density for each sample after five minutes of charging. This provides a direct measure of doping rate. It is evident that at PEO contents above 30 wt %, PPV blends may be charged considerably faster. For example, as a result of changing composition from 70/30 wt % PPV/PEO to 30/70 wt % PPV/PEO, the charging current (doping rate) increases by a factor of twenty. In Figure 47 (page 167), the doping level, determined coulometrically, is plotted as a function of time at constant potential. The enhancement of doping rate with increasing PEO content is clearly evident. The effect of PEO content upon the attainable level of doping is also apparent. The blends richer in PEO have all reached the same doping level at the end of the doping period (0.6 charges per PPV repeat unit) whereas PPV rich materials are doped to lower levels on the time scale of the experiment. This abrupt change in electrochemical behavior is correlated to a morphological change (spherulite to continuous) at the same composition. Thus we ascribe the marked increase in dopant ion transport, as indicated by higher charging rates and higher doping levels, to the for-

mation of a continuous PEO phase at around 40 wt % PEO (consistent with morphological investigations) which is then extracted on exposure to electrolyte. Extraction and swelling of PEO by electrolyte does not lead to a collapse of the remaining interconnected PPV since upon doping films increased in volume by 5-20% over the whole composition range studied.

In light of the results obtained in this investigation, we can divide the morphological and electrical behavior of the PPV/PEO system into three distinct composition regimes. At extremely low PPV content (less than 10 wt %) a spherulitic morphology is formed which resembles pure PEO, the PPV constituent in this regime does not form a continuous phase and although it may be effectively doped, the macroscopic conductivity remains insulating or at best lightly semiconducting (up to 10^{-3} S/cm). The second regime extends from 10 wt % PPV to 60 wt % PPV and is characterized by a spherulitic morphology in which the PPV domains are excluded into interfibrillar regions forming a highly connected network. Materials in this range can be doped very quickly to high conductivity (>100 S/cm). The third regime consists of materials containing greater than 60 wt % PPV. Materials in this region are flexible and tough containing highly dispersed PEO domains in a PPV matrix. In this region the PEO constituent is still effective in accelerating chemical doping, however, it is less effective in accelerating electrochemical doping. Conductivities in this regime reach a maximum (>200 S/cm).

Figure 47. Doping level (measured coulometrically) as a function of time at constant potential (+4.1V vs Li) during electrochemical doping of PPV/PEO blends of various compositions.

▲ - 25/75 PPV/PEO
○ - 46/54 PPV/PEO
● - 59/41 PPV/PEO
△ - 73/27 PPV/PEO
● - 85/15 PPV/PEO
○ - 90/10 PPV/PEO

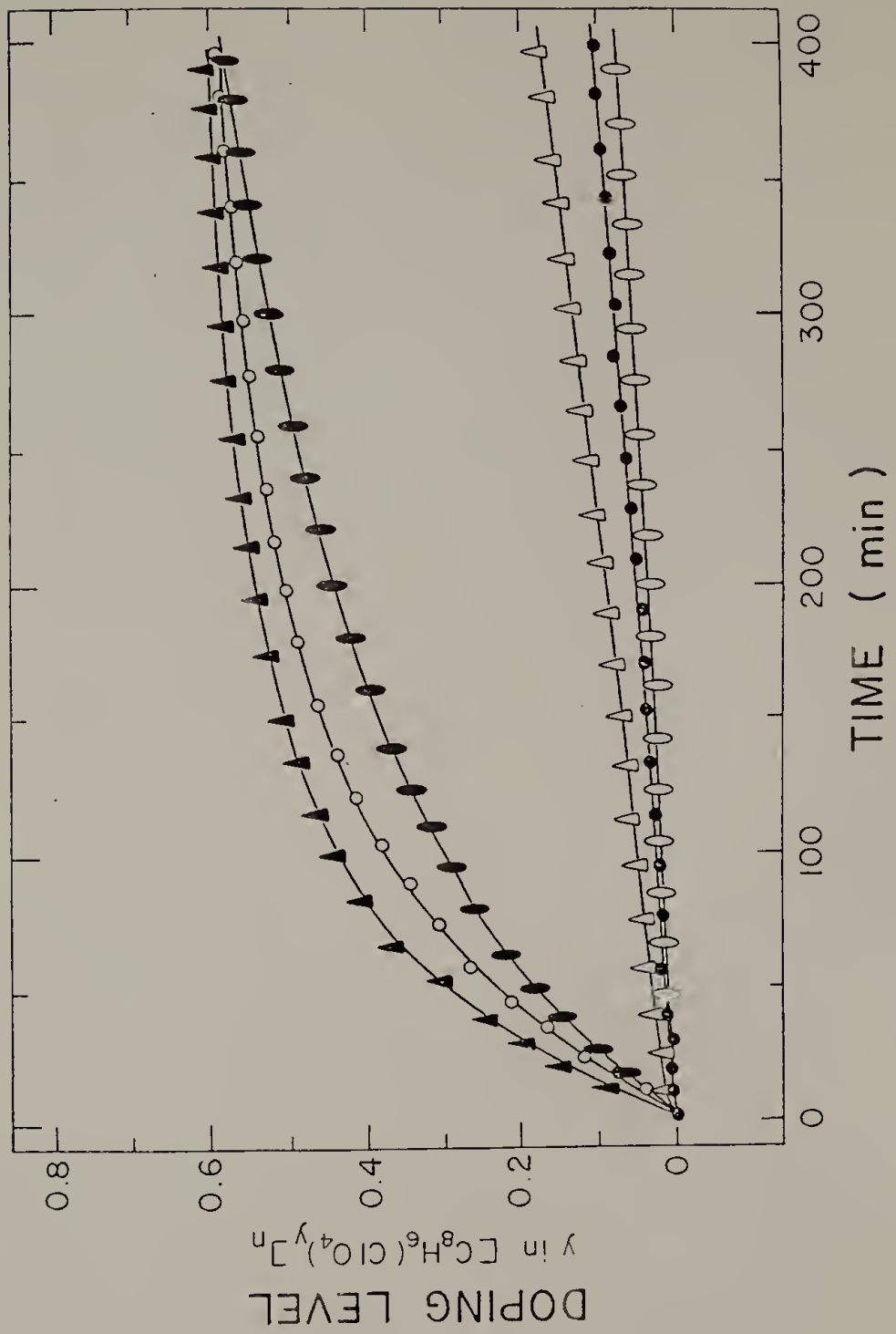


Table 14. Charging rate, conductivity, and conductivity ratio (doping homogeneity) upon electrochemical doping of PPV/PEO blends

| Blend Composition PPV/PEO wt% | Charging Rate after 5 min. (mA/g PPV) | Conductivity (S/cm) | Conductivity Ratio $\left[\frac{\sigma_{\text{inner}}}{\sigma_{\text{outer}}} \right]$ |
|-------------------------------------|---|------------------------|---|
| 92/8 | 7 | 0.2 | 0.5 |
| 85/15 | 6 | 6.7 | 0.5 |
| 73/27 | 16 | 3.0 | 1.4 |
| 67/33 | 95 | 33 | 1.3 |
| 59/41 | 80 | 55 | 1.2 |
| 48/52 | 150 | 34 | 1.3 |
| 46/54 | 145 | 20 | 1.1 |
| 30/70 | 315 | 6.1 | 1.3 |
| 25/75 | 315 | 5 | - |

CHAPTER IX

CONCLUSIONS

The unifying objective of this dissertation was to exploit advantages associated with the PPV precursor in order to expand the range of processing techniques and material properties available to conducting polymers. In this final chapter, the major results of the work will be summarized and put into perspective with respect to how they contribute to the field of conducting polymers and how they may point the way to further efforts in this area.

Processing

In this work it was shown that the PPV precursor can be prepared reproducibly on a large scale without compromising material purity. The most significant aspect of the scaled-up procedure was the ability to isolate the precursor polymer by precipitation into a non-solvent (isopropanol). Precipitation represented a significant time savings in comparison to the previously used procedure, membrane dialysis. Much more important, however, was the ability to isolate the precursor polymer in the pure, bulk state. This greatly facilitated storage of up to 500g of the material which would represent well over 100L of typical dialyzed solution. It also allowed the preparation of concentrated casting dopes required for the preparation of uniform, large area films.

One of the major advances in this work was the development of a continuous process for the preparation of uniaxially oriented PPV films.

This represents an increased level of sophistication in the processing of conducting polymer materials. It allowed the preparation of PPV film, oriented under controllable, reproducible, and well-defined conditions. The utility of the roller geometry used was three-fold: (1) it allowed the development of steady flow conditions, permitting continuous operation and, for the first time, the preparation of uniformly stretched samples of low draw ratio, (2) it involves a short residence time of film elements on the heated roll, thus minimizing the thermal history of the film in the presence of oxygen and reducing the extent of oxidative degradation accompanying stretching, (3) the roller geometry imposes a resistance to "necking down" during stretching, permitting the preparation of very wide films for the accurate measurement of transverse properties.

IR dichroism studies showed that the PPV films oriented by this process exhibited exceptionally high degrees of molecular orientation. At draw ratios greater than five, orientation functions of over 0.95 were measured. This efficiency was rationalized in terms of the combined effects of volume reduction accompanying stretching and a strain induced crystallization process. Oriented PPV was chemically doped with SbF₅ and AsF₅ vapors. SbF₅ doping resulted in electrical conductivities of up to 2500 S/cm in the machine direction. With AsF₅ doping, conductivities in the machine direction of up to 10,000 S/cm could be achieved. The anisotropy of electrical conductivity increased with draw ratio up to a value of about 80.

The mechanical properties of oriented PPV were also reported. The tensile modulus, measured in the machine direction, increased from about 2 GPa for isotropic film to nearly 40 GPa at high draw ratios. Tensile strength in the machine direction reached a maximum of over 500 MPa at a draw ratio of six. These results show that the mechanical properties of conducting polymers, which have been thought to be poor, can exceed those of many high performance engineering polymers if the conditions of processing are optimized. The anisotropy of mechanical properties closely parallels the anisotropy of electrical properties for PPV stretched to similar draw ratios.

Two processing techniques were introduced which were used to prepare biaxially oriented PPV film. The first was a two-stage sequential stretching operation which was used to impose a wide range of biaxial deformation histories to the material. This was shown to influence both the state of molecular orientation and electrical conductivity of the material. For example, the electrical anisotropy was varied between 0.05 and 80 using this technique. The second process was a bubble inflation technique which imposed an equibiaxial extensional deformation to the material. This induced a planar orientation and improved the electrical conductivity in the plane of the film. The goals of the biaxial orientation studies were to further expand the processing capabilities associated with the PPV precursor and to further demonstrate how the state of orientation influences the electrical properties of this system.

Blends

The precursor process was shown to be part of a useful and versatile method for the preparation of blends of a conducting and an insulating polymer. In this work blends were prepared between PPV and a series of commercially available water soluble polymers. Thermal analysis showed these blends to be phase separated mixtures. For certain of these blends a strong synergistic effect was observed for the rate of chemical and electrochemical doping and for the magnitude of final conductivity. For chemical doping the synergistic effect was found to depend upon the glass transition of the second constituent. For electrochemical doping, it depended upon the ability of the electrolyte to swell the second constituent. Accelerated doping in the blends was attributed to improved dopant transport through the insulating phase thereby improving dopant access to the electroactive domains. The effect of blending is particularly relevant to electrochemical studies because it introduces PPV to a range of applications requiring rapid, reversible electroactivity such as secondary battery electrodes and electronic display devices.

Of the blend systems studied, PPV/PEO was the most attractive for further investigation as a result of its good thermal stability, robust mechanical properties, rapid doping, high conductivity and variable morphology. Therefore, a detailed study of this system was undertaken. The morphology of PPV/PEO blends varied between spherulitic, grainy, and continuous depending upon composition and casting conditions. For spherulitic compositions, interfibrillar phase segregation of PPV domains within the PEO spherulites was observed.

Conductivity synergism in PPV/PEO blends was found to extend over a wide range of composition. Under equivalent doping conditions, the conductivity of blends exceeded that of pure PPV, for all compositions between 20 and 90 wt % PPV. Percolation of the electroactive phase was found to occur between 4 and 10 wt % PPV in the blends. For electrochemical applications, particularly battery electrodes, the optimum composition was between 50 and 60 wt % PPV, corresponding to the maximum content of PPV which supported a spherulitic morphology. At this composition the blend exhibited maximum energy density, high current density and maximum conductivity.

Future Directions

It is hoped that this dissertation has introduced useful techniques which may lead to further developments and improvements in conducting polymer processing methods. A straightforward and worthwhile extension of this work is the stretching of PPV blends, analogues, and copolymers using the continuous heated roll process. Indeed, the manual stretching of blends was successfully performed and found to improve conductivity in the stretching direction.¹⁶⁹ However, the stretching of substituted PPV copolymers would be expected to yield the most significant results. These materials have been shown to exhibit good atmospheric stability and low ionization potentials⁸⁶, characteristic of the substituted PPV homopolymers, and may be expected to most closely approach the processing characteristics (high orientability) of unsubstituted PPV.

The dry spinning of highly oriented PPV fibers would be a logical continuation of the present work. In this case spinning from concentrated methanolic solutions would be suggested to improve the solvent evaporation rate. It may be expected that fibers would exhibit optimum uniaxial drawing characteristics and thus produce the maximum attainable electrical conductivity and mechanical properties.

The preliminary results obtained for biaxial orientation justify further efforts in this area. There is substantial opportunity for improvements of the processing methods, for quantification of the states of molecular orientation, and for interpretation of the relationship between orientation and electrical properties.

As a result of the rapid rate of polymerization exhibited by the bis-sulfonium monomer, a reactive processing method has already shown limited success.¹⁷⁰ Reactive processing always introduces significant engineering difficulties. However, in this case the required effort is justified not only by the usual economic advantages but also by the opportunity to extend this technique to any of the PPV analogues (or copolymers) which often exhibit a tendency to gel rapidly on standing.

Certainly the possibilities associated with PPV blend preparation have not been exhausted. Based upon the principles derived from this work, blend formulations aimed at specific end-use applications could be prepared. With respect to battery electrode applications, blends containing PPV analogues with more desirable ionization potentials could be pursued in order to improve the Coulombic efficiency of the cells.¹⁷¹ With respect to electronic display applications multi-component blends

could be investigated where each constituent contributes a different electrochromic effect; thus allowing the fabrication of a multi-color display.

Further studies involving the chemical doping of conducting blends should include secondary components which are chemically inert towards the dopant. This is perhaps most easily achieved by using as the conducting component a substituted PPV which can be doped with the milder dopant, iodine.

An alternate novel technique for blend preparation is the ionic coprecipitation which results from combining aqueous solutions of the poly(sulfonium salt) precursor and any anionic polyelectrolyte (e.g. polyacrylic acid). These coprecipitates are expected to be molecularly mixed and upon thorough drying and powdering would be expected to exhibit some degree of melt processibility (e.g. compression molding).

In light of the present work, as well as continuing advances involving the Durham polyacetylene precursor and poly (3-substituted thiophenes), it is hoped that the unqualified statement that conducting polymers lack processibility will become an increasingly difficult position to defend.

REFERENCE SECTION

- 1) Hayes, W. *Contemp. Phys.* 1985, 26, 421.
- 2) Mainthia, S.B.; Kronick, P.L.; Labes, M.M. *J. Chem. Phys.* 1964, 41, 2206.
- 3) Miyasaka, K.; Watanabe, K.; Jojima, E.; Aida, H.; Sumita, M.; Ishikawa, K. *J. Mater. Sci.* 1982, 17, 1610.
- 4) Shriver, D.F.; Papke, B.L.; Ratner, M.A.; Dupon, R.; Wong, T.; Brodwin, M. *Sol. St. Ionics* 1981, 5, 83.
- 5) Pekker, S.; Jánossy, A. In Handbook of Conducting Polymers; Skotheim, T.A., Ed.; Marcel Dekker: New York: 1986, Chapter 2 p 45.
- 6) Shirakawa, H.; Louis, E.J.; MacDiarmid, A.G.; Chiang, C.K.; Heeger, A.J. *J. Chem. Soc., Chem. Commun.* 1977, 578.
- 7) Chien, J.C.W.; Wnek, G.E.; Karasz, F.E.; Hirsch, J.A. *Macromolecules* 1981, 14, 479.
- 8) Polydiacetylenes: Synthesis, Structure and Electronic Properties; Bloor, D.; Chance, R. Eds.; NATO ASI No. 102, Martinus Nijhoff: Dordrecht, The Netherlands, 1985.
- 9) Ivory, D.M.; Miller, G.G.; Sowa, J.M.; Shaklette, L.W.; Chance, R.R.; Baughman, R.H. *J. Chem. Phys.* 1979, 71, 1506.
- 10) Hörrhold, H.H.; Helbig, M. *Makromol. Chem., Macromol. Symp.* 1987, 12, 229.
- 11) Diaz, A.F.; Bargon, J. In Handbook of Conducting Polymers; Skotheim, T.A., Ed.; Marcel Dekker: New York, 1986; Chapter 3, p 81.
- 12) Tourillon, G.; Garnier, F. *J. Electroanal. Chem.* 1982, 135, 173.

- 13) Merlet, N.; Dian, G.; Barbey, G.; Outurquin, F.; Paulmier, C. Synth. Met. 1988, 24, 77.
- 14) MacDiarmid, A.G.; Chiang, J.C.; Richter, A.F.; Epstein, A.J. Synth. Met. 1987, 18, 285.
- 15) Swager, T.M.; Grubbs, R.H. J. Am. Chem. Soc. 1987, 109, 894.
- 16) Bargon, J.; Mohmand, S.; Waltman, R.J. IBM J. Res. Develop. 1983, 27, 330.
- 17) Jow, T.R.; Jen, K.Y.; Elsenbaumer, R.L.; Shacklette, L.W.; Angelopoulos, M.; Cava, M.P. Synth. Met. 1986, 14, 53.
- 18) McLeod, G.G.; Mahboubian-Jones, M.G.B.; Pethrick, R.A.; Watson, S.D.; Truong, N.D.; Galin, J.C.; Francois, J. Polymer 1986, 27, 455.
- 19) Nigrey, P.J.; MacInnes, D.; Nairns, D.P.; MacDiarmid, A.G.; J. Electrochem. Soc. 1981, 128, 1651.
- 20) Chiang, C.K. Polymer 1981, 22, 1454.
- 21) Shacklette, L.W.; Maxfield, M.; Gould, S.; Wolf, J.F.; Jow, T.R.; Baughman, R.H. Synth. Met. 1987, 18, 611.
- 22) Münstedt, H.; Köhler, G.; Möhwald, H.; Naegele, D.; Bitthin, R.; Ely, G.; Meissner, E. Synth. Met. 1987, 18, 259.
- 23) Inganäs, O.; Lundström, I. Synth. Met. 1987, 21, 13.
- 24) Genies, E.M.; Lapkowski, M.; Santier, C.; Vieil, E. Synth. Met. 1987, 18, 631.
- 25) Passiniemi, P.; Österholm, J.E. Synth. Met. 1987, 18, 637.
- 26) Duke, C.B. Synth. Met. 1987, 21, 5.
- 27) Garnier, F.; Horowitz, G. Synth. Met. 1987, 18, 693.

- 28) Tomozawa, H.; Braun, D.; Phillips, S.; Heeger, A.J.; Kroemer, H. *Synth. Met.* 1987, 22, 63.
- 29) Chien, J.C.W. *Polyacetylene: Chemistry, Physics, and Material Science*; Academic: Orlando, FL, 1984; Chapter 12, p 580.
- 30) Chen, S.N.; Heeger, A.J.; Kiss, Z.; MacDiarmid, A.G.; Gau, S.C.; Peebles, D.L. *Appl. Phys. Lett.* 1980, 36, 96.
- 31) Koezuka, H.; Tsumura, A.; Ando, T. *Synth. Met.* 1987, 18, 699.
- 32) Potember, R.S.; Hoffman, R.C.; Hu, H.S.; Cocchiaro, J.E.; Viands, C.A., Murphy, R.A.; Poehler, T.O. *Polymer* 1987, 28, 574.
- 33) Kobel, W.; Kiess, H.; Egli, M. *Synth. Met.* 1988, 22, 265.
- 34) Yoneyama, H.; Wakamoto, K.; Tamura, H. *J. Electrochem. Soc.* 1985, 132, 2414.
- 35) Ellis, J.R. In *Handbook of Conducting Polymers*; Skotheim, T.A., Ed.; Marcel Dekker: New York, 1986; Chapter 13, p 489.
- 36) Ulrich, D.R. *Polymer* 1987, 28, 533.
- 37) Clarke, T.C.; Street, G.B. *Synth. Met.* 1979, 1, 119.
- 38) Bredas, J.L.; Street, G.B. *Acc. Chem. Res.* 1985, 18, 309.
- 39) Whitney, D.H.; Wnek, G.E. *Macromolecules* 1988, 21, 266.
- 40) Osterholm, J.E.; Yasuda, H.K.; Levenson, L.L. *J. Appl. Polym. Sci.* 1982, 27, 931.
- 41) Druy, M.A.; Rubner, M.F.; Walsh, S.P. *Synth. Met.* 1986, 13, 207.
- 42) Deits, W.; Cukor, P.; Rubner, M.; Jopson, H. *Synth. Met.* 1982, 4, 199.

- 43) Chien, J.C.W.; Babu, G.N. J. Chem. Phys. 1985, 82, 441.
- 44) Galvin, M.E.; Wnek, G.E. Polym. Bull. 1985, 13, 109.
- 45) Aldissi, M. J. Chem. Soc., Chem. Commun. 1984, 1347.
- 46) Aldissi, M. Synth. Met. 1986, 13, 87.
- 47) Bates, F.S.; Baker, G.L. Macromolecules 1983, 16, 704.
- 48) Bolognesi, A.; Catellani, M.; Destri, S. Mol. Cryst. Liq. Cryst. 1985, 117, 29.
- 49) Elsenbaumer, R.L.; Jen, K.Y.; Oboodi, R. Synth. Met. 1986, 15, 169.
- 50) Elsenbaumer, R.L.; Jen, K.Y.; Miller, G.G.; Shacklette, L.W., Synth. Met. 1987, 18, 277.
- 51) Sato, M.; Tanaka, S.; Kaeriyama, K. Makromol. Chem. 1987, 188, 1763,
- 52) Sato, M.; Tanaka, S.; Kaeriyama, K. Synth. Met. 1987, 18, 229.
- 53) Patil, A.O.; Ikenoue, Y.; Wudl, F.; Heeger, A.J. J. Am. Chem. Soc. 1987, 109, 1858.
- 54) Marvel, C.S.; Sample, J.H.; Roy, M.F. J. Am. Chem. Soc. 1939, 61, 3241.
- 55) Perichaud, A.; Dhainaut, S.; Bernier, P.; Lefrant, S. Synth. Met. 1988, 24, 7.
- 56) Edwards, J.H.; Feast, W.J. Polymer 1981, 21, 595.
- 57) Harper, K.; James, P.G. Mol. Cryst. Liq. Cryst. 1985, 117, 55.
- 58) Edwards, J.H.; Feast, W.J.; Bott, D.C. Polymer 1984, 25, 395.

- 59) Leising, G. Polym. Bull. 1984, 11, 401.
- 60) Leising, G. Polym. Commun. 1984, 25, 201.
- 61) Leising, G.; Leitner, O.; Kahlert, H. Mol. Cryst. Liq. Cryst. 1985, 117, 67.
- 62) Bott, D.C.; Brown, C.S.; Winter, J.N.; Barker, J. Polymer 1987, 28, 601.
- 63) Lugli, G.; Pedretti, U.; Perego, G. Mol. Cryst. Liq. Cryst. 1985, 117, 43.
- 64) Townsend, P.D.; Pereira, C.M.; Bradley, D.D.C.; Horton, M.E.; Friend, R.H. J. Phys. C: Sol. St. Phys. 1985, 18, L283.
- 65) Chen, Y.C.; Akagi, K.; Shirakawa, H. Synth. Met. 1986, 14, 173.
- 66) Naarmann, H.; Theophilou, N. Synth. Met. 1987, 22, 1.
- 67) Gilliom, L.R.; Grubbs, R.H. J. Am. Chem. Soc. 1986, 108, 733.
- 68) Klavetter, F.L.; Grubbs, R.H. A.C.S. Polym. Prepr. 1987, 28 (2), 425.
- 69) Ballard, D.G.; Courtis, A.; Shirley, I.M.; Taylor, S.C. J. Chem. Soc., Chem. Commun. 1983, 954.
- 70) McDonald, R.N.; Campbell, T.W. J. Am. Chem. Soc. 1960, 82, 4669.
- 71) Hörrhold, H.H.; Opfermann, J. Makromol. Chem. 1970, 131, 105.
- 72) Kanbe, M.; Okawara, M. J. Polym. Sci.: A-2 1968, 6, 1058.
- 73) Wessling, R.A.; Zimmerman, R.G. U.S. Patent 3 401 152, 1968.
- 74) Wessling, R.A. J. Polym. Sci., Polym. Symp. Ed. 1985, 72, 55.

- 75) Lahti, P.M.; Modarelli, D.A.; Denton, F.R.; Lenz, R.W.; Karasz, F.E. J. Am. Chem. Soc., in press.
- 76) Wessling, R.A. U.S. Patent 3 706 677, 1972.
- 77) Gagnon, D.R.; Capistran, J.D.; Karasz, F.E.; Lenz, R.W. Polym. Bull. 1984, 12, 293.
- 78) Murase, I.; Ohnishi, T.; Noguchi, T.; Hirooka, M. Polym. Commun. 1984, 25, 327.
- 79) Gagnon, D.R.; Karasz, F.E.; Thomas, E.L.; Lenz, R.W. Synth. Met. 1987, 20, 85.
- 80) Bradley, D.D.C.; Friend, R.H.; Lindenberger, H.; Roth, S. Polymer 1986, 27, 1709.
- 81) Murase, I.; Ohnishi, T.; Noguchi, T.; Hirooka, M.; Murakami, S. Mol. Cryst. Liq. Cryst. 1985, 118, 333.
- 82) Antoun, S.; Gagnon, D.R.; Karasz, F.E.; Lenz, R.W. Polym. Bull. 1986, 15, 181.
- 83) Murase, I.; Ohnishi, T.; Noguchi, T.; Hirooka, M. Polym. Commun. 1985, 26, 362.
- 84) Antoun, S.; Gagnon, D.R.; Karasz, F.E.; Lenz, R.W. J. Polym. Sci., Polym. Lett. Ed. 1986, 24, 503.
- 85) Jen, K.Y.; Maxfield, M.; Shacklette, L.W.; Elsenbaumer, R.L. J. Chem. Soc., Chem. Commun. 1987, 309.
- 86) Han, C.C.; Lenz, R.W.; Karasz, F.E. Polym. Commun. 1987, 28, 261.
- 87) Galvin, M.E.; Wnek, G.E. Polym. Commun. 1982, 23, 795.
- 88) Wessling, B.; Volk, H. Synth. Met. 1986, 15, 183.

- 89) DePaoli, M.A.; Waltman, R.J.; Diaz, A.F.; Bargon, J. J. Chem. Soc., Chem. Commun. 1984, 1015.
- 90) Galvin, M.E.; Wnek, G.E. J. Polym. Sci., Polym. Chem. Ed. 1983, 21, 2727.
- 91) Rueda, D.R.; Cagiao, M.E.; Balta Calleja, F.J.; Palacios, J.M. Synth. Met. 1987, 22, 53.
- 92) Rubner, M.F.; Tripathy, S.K.; Georger, J.; Cholewa, P. Macromolecules 1983, 16, 870.
- 93) Lee, K.I.; Jopson, H. Polym. Bull. 1983, 10, 105.
- 94) Bjorklund, R.B.; Liedberg, B. J. Chem. Soc., Chem. Commun. 1986, 1293.
- 95) Niwa, O.; Tamamura, T. J. Chem. Soc. Chem. Commun. 1984, 817.
- 96) Bi, X.; Pei, Q. Synth. Met. 1987, 22, 145.
- 97) Bates, N.; Cross, M.; Lines, R.; Walton, D. J. Chem. Soc., Chem. Commun. 1985, 871.
- 98) Jasne, S.J.; Chiklis, C.K. Synth. Met. 1986, 15, 175.
- 99) Hotta, S.; Rughooputh, S.D.D.V.; Heeger, A.J. Synth. Met. 1987, 22, 79.
- 100) Gagnon, D.R.; Capistran, J.D.; Karasz, F.E.; Lenz, R.W.; Antoun, S. Polymer 1987, 28, 567.
- 101) Lenz, R.W.; Han, C.C.; Stenger-Smith, J.; Karasz, F.E. J. Polym. Sci., Polym. Chem. Ed., in press.
- 102) Zbinden, R., Infrared Spectroscopy of High Polymers; Academic: New York, 1964.

- 103) Structure and Properties of Oriented Polymers; Ward, I.M., Ed.; Applied Science: London, 1975.
- 104) American Society for Testing and Materials Annual Book of Standards, 1986, 8.01, 454.
- 105) Gagnon, D.R. Ph.D. Dissertation, University of Massachusetts, 1986.
- 106) Wnek, G.E. Ph.D. Dissertation, University of Massachusetts, 1980.
- 107) MacKnight, W.J.; Karasz, F.E.; Fried, J.R. In Polymer Blends, Vol. I; Paul, D.R.; Newman, S., Eds.; Academic: NY, 1978; Chapter 5.
- 108) Mandelkern, L. J. Appl. Phys. 1954, 25, 830.
- 109) Reynolds, J.R.; Schlenoff, J.B.; Chien, J.C.W. J. Electrochem. Soc. 1985, 132, 1131.
- 110) Machado, J.M.; Denton, F.R.; Schlenoff, J.B.; Karasz, F.E.; Lahti, P.M. J. Polym. Sci., Polym. Phys. Ed., in press.
- 111) Bradley, D.D.C. J. Phys. D: Appl. Phys. 1987, 20, 1389.
- 112) Sawyer, L.C.; Grubb, D.T. Polymer Microscopy; Chapman and Hall: London, 1987.
- 113) Schuur, G.; Van der Vegt, A.K. In Structure and Properties of Oriented Polymers; Ward, I.M., Ed., Applied Science: London, 1975; Chapter 12.
- 114) Montaudo, G.; Vitalini, D.; Lenz, R.W. Polymer 1987, 28, 837.
- 115) Rice, D.; Simpson, J.; Egger, N.; Karasz, F.E. to be published.
- 116) Glenz, W.; Peterlin, A. J. Polym. Sci.: A-2 1971, 9, 1191.

- 117) Marrinan, H.J. J. Polym. Sci. 1959, 39, 461.
- 118) Kratky, O. Kolloid-Z 1933, 64, 213.
- 119) Gaylord, R.J. J. Polym. Sci., Polym. Lett. Ed. 1975, 13, 337.
- 120) Granier, T.; Thomas, E.L.; Gagnon, D.R.; Karasz, F.E.; Lenz, R.W. J. Polym. Sci., Polym. Phys. Ed. 1986, 24, 2793.
- 121) Wedgewood, A.R.; Seferis, J.C. In Interrelations Between Processing, Structure, and Properties of Polymeric Materials; Seferis, J.C.; Theocaris, P.S., Eds.; Elsevier Science: The Netherlands, 1984.
- 122) Bohn, C.R.; Schaefgen, J.R.; Statton, W.O. J. Polym. Sci. 1961, 55, 531.
- 123) Takenaka, T.; Shimura, Y.; Gotoh, R. Kolloid-Z 1970, 237, 13.
- 124) Rietsch, F.; Jasse, B. Polym. Bull. 1984, 11, 287.
- 125) Cunningham, A.; Ward, I.M.; Willis, H.A.; Zichy, V. Polymer 1974, 15, 749.
- 126) Masse, M.A.; Martin, D.C.; Karasz, F.E.; Thomas, E.L. Proc. ACS Div. Pol. Mat. Sci. and Eng. 1987, 57, 441.
- 127) Masse, M.A.; Karasz, F.E. to be published.
- 128) Druy, M.A.; Tsang, C.H.; Brown, N.; Heeger, A.J.; MacDiarmid, A.G. J. Polym. Sci., Polym. Phys. Ed. 1980, 18, 429.
- 129) Shirakawa, H.; Ikeda, S. Synth. Met. 1979, 1, 175.
- 130) Diaz, A.F.; Hall, B. IBM J.Res.Dev. 1983, 27, 342.
- 131) Wynne, K.J.; Street, G.B. Macromolecules 1985, 18, 2361.

- 132) Karasz, F.E.; Chien, J.C.W.; Galkiewics, R.; Wnek, G.E. Nature 1979, 282, 286.
- 133) Baughman, R.G.; Gleiter, H.; Sendfeld, N. J. Polym. Sci., Pol. Phys. Ed. 1975, 13, 1871.
- 134) Duckett, R.A.; Ward, I.M.; Zihliff, A.M. J. Mater. Sci. 1972, 7, 480.
- 135) Bridle, C.; Buckley, A.; Scanlon, J. J. Mater. Sci. 1968, 3, 622.
- 136) Hadley, D.W.; Pinnock, P.R.; Ward, I.M. J. Mater. Sci. 1969, 4, 152.
- 137) Northolt, M.G.; Van Aartsen, J.J. J. Polym. Sci., Polym. Symp. Ed., 1977, 58, 283.
- 138) Wynne, K.J.; Zachariades, A.E.; Inabe, T.; Marks, T.J. Polym. Commun. 1985, 26, 162.
- 139) Zachariades, A.E. In Interrelations Between Processing, Structure, and Properties of Polymeric Materials; Seferis, J.C.; Theocaris, P.S., Eds.; Elsevier Science: The Netherlands, 1984; p 279.
- 140) Farrell, G.W.; Fellers, J.F. J. Polym. Eng. 1986, 6, 263.
- 141) White, J.L. J. Polym. Eng. 1985, 5, 275.
- 142) White, J.L. In Interrelations Between Processing, Structure, and Properties of Polymeric Materials; Seferis, J.C.; Theocaris, P.S., Eds.; Elsevier Science: The Netherlands, 1984; p 765.
- 143) Cakmak, M.; White, J.L.; Spruiell, J.E. J. Polym. Eng. 1986, 6, 291.
- 144) Granier, T.; Thomas, E.L.; Gagnon, D.R.; Karasz, F.E.; Lenz, R.W. J. Polym. Sci., Polym. Phys. Ed. 1986, 24, 2793.

- 145) Okajima, S.; Kurihara, K.; Homma, K. J. Appl. Polym. Sci. 1967, 11, 1703.
- 146) Elsenbaumer, R.L.; Shacklette, L.W. In Handbook of Conducting Polymers; Skotheim, T.A., Ed.; Marcel Dekker: NY, 1986; Chapter 7, p 213.
- 147) Obrzut, J.; Karasz, F.E. J. Chem. Phys. 1987, 87, 6178.
- 148) Kaneto, K.; Maxfield, M.; Nairns, D.P.; MacDiarmid, A.G.; Heeger, A.J. J. Chem. Soc., Farad. Trans.(1) 1982, 78, 3417.
- 149) Natov, M.; Peeva, L.; Djagarova, E.J. J. Polym. Sci., Polym. Symp. Ed. 1968, 16, 4197.
- 150) Greco, R.; Hopfenberg, H.B.; Martuscelli, E.; Ragosta, G.; Demma, G. Polym. Eng. Sci. 1978, 18, 654.
- 151) Stein, R.S.; Khambatta, F.B.; Warner, F.P.; Russell, T.; Escala, A.; Balizer, E. J. Polym. Sci. Polym. Symp. 1978, 63, 313.
- 152) Keith, H.D.; Padden, F.J. J. Appl. Phys. 1964, 35, 1270.
- 153) Martuscelli, E.; Silvestre, C.; Addonizio, M.; Amelino, L. Makromol. Chem. 1986, 187, 1557.
- 154) Khambatta, F.B.; Warner, F.; Russell, T.; Stein, R.S. J. Polym. Sci., Polym. Phys. Ed. 1976, 14, 1391.
- 155) Carter, A.J.; Davies, C.K.L.; Thomas, A.G. Polymer Blends; Martuscelli, E.; Polumbo, R.; Kryszewski, M., Eds.; Plenum: NY, 1980; p 101,
- 156) Martuscelli, E.; Demma, G.B. Polymer Blends; Martuscelli, E.; Polumbo, R.; Kryszewski, M., Eds.; Plenum: NY, 1980; p 101.
- 157) Ramos, M.A.; Collar, E.P. J. Polym. Eng. 1987, 7, 137.
- 158) Folkes, M.J.; Keller, A. Polymer 1971, 12, 222.

- 159) Gagnon, D.R.; Karasz, F.E. unpublished results.
- 160) Bott, D.C.; Brown, C.S.; Chai, C.K.; Walker, N.S.; Feast, W.J.; Foot, P.J.S.; Calvert, P.D.; Billingham, N.C.; Friend, R.H. *Synth. Met.* 1986, 14, 245.
- 161) Ebisawa, F.; Kurihara, T.; Tabei, H. *Synth. Met.* 1987, 18, 431.
- 162) Masse, M.A., Karasz, F.E., to be published.
- 163) Foot, P.J.S.; Mohammed, F.; Calvert, P.D.; Billingham, N.C. *J. Phys. D: Appl. Phys.* 1987, 20, 1354.
- 164) Balberg, I.; Binenbaum, N. *Phys. Rev. B* 1983, 28, 3799.
- 165) Bank, M.; Leffingwell, J.; Thies, C. *Macromolecules* 1971, 4, 43.
- 166) Saldanha, J.M.; Kyu, T. *Macromolecules* 1987, 20, 2840.
- 167) Cotton, F.A.; Wilkinson, G. Advanced Inorganic Chemistry: A Comprehensive Text, 2nd ed.; Wiley: NY, 1962; p 381.
- 168) Nigrey, P.J.; MacDiarmid, A.G.; Heeger, A.J. *J. Chem. Soc., Chem. Commun.* 1979, 594.
- 169) Machado, J.M.; Karasz, F.E.; Lenz, R.W. *Polymer*, in press.
- 170) Machado, J.M.; Masse, M.A.; Karasz, F.E., unpublished results.
- 171) Schlenoff, J.B.; Karasz, F.E., to be published.

BIBLIOGRAPHY

Aldissi, M. J. Chem. Soc., Chem. Commun. 1984, 1347.

Aldissi, M. Synth. Met. 1986, 13, 87.

American Society for Testing and Materials Annual Book of Standards,
1986, 8.01, 454.

Antoun, S.; Gagnon, D.R.; Karasz, F.E.; Lenz, R.W. Polym. Bull. 1986, 15, 181.

Antoun, S.; Gagnon, D.R.; Karasz, F.E.; Lenz, R.W. J. Polym. Sci., Polym. Lett. Ed. 1986, 24, 503.

Balberg, I.; Binenbaum, N. Phys. Rev. B 1983, 28, 3799.

Ballard, D.G.; Courtis, A.; Shirley, I.M.; Taylor, S.C. J. Chem. Soc., Chem. Commun. 1983, 954.

Bank, M.; Leffingwell, J.; Thies, C. Macromolecules 1971, 4, 43.

Bargon, J.; Mohmand, S.; Waltman, R.J. IBM J. Res. Develop. 1983, 27, 330.

Bates, F.S.; Baker, G.L. Macromolecules 1983, 16, 704.

Bates, N.; Cross, M.; Lines, R.; Walton, D. J. Chem. Soc., Chem. Commun. 1985, 871.

Baughman, R.G.; Gleiter, H.; Sendfeld, N. J. Polym. Sci., Pol. Phys. Ed. 1975, 13, 1871.

Bi, X.; Pei, Q. Synth. Met. 1987, 22, 145.

Bjorklund, R.B.; Liedberg, B. J. Chem. Soc., Chem. Commun. 1986, 1293.

Polydiacetylenes: Synthesis, Structure and Electronic Properties;
Bloor, D.; Chance, R. Eds.; NATO ASI No. 102, Martinus
Nijhoff: Dordrecht, The Netherlands, 1985.

Bohn, C.R.; Schaeffgen, J.R.; Statton, W.O. *J. Polym. Sci.* 1961,
55, 531.

Bolognesi, A.; Catellani, M.; Destri, S. *Mol. Cryst. Liq. Cryst.*
1985, 117, 29.

Bott, D.C.; Brown, C.S.; Winter, J.N.; Barker, J. *Polymer* 1987,
28, 601.

Bott, D.C.; Brown, C.S.; Chai, C.K.; Walker, N.S.; Feast, W.J.;
Foot, P.J.S.; Calvert, P.D.; Billingham, N.C.; Friend, R.H.
Synth. Met. 1986, 14, 245.

Bradley, D.D.C.; Friend, R.H.; Lindenberger, H.; Roth, S.
Polymer 1986, 27, 1709.

Bradley, D.D.C. *J. Phys. D: Appl. Phys.* 1987, 20, 1389.

Bredas, J.L.; Street, G.B. *Acc. Chem. Res.* 1985, 18, 309.

Bridle, C.; Buckley, A.; Scanlon, J. *J. Mater. Sci.* 1968, 3, 622.

Cakmak, M.; White, J.L.; Spruiell, J.E. *J. Polym. Eng.* 1986, 6,
291.

Carter, A.J.; Davies, C.K.L.; Thomas, A.G. Polymer Blends;
Martuscelli, E.; Polumbo, R.; Kryszewski, M., Eds.; Plenum: NY,
1980; p 101,

Chen, S.N.; Heeger, A.J.; Kiss, Z.; MacDiarmid, A.G.; Gau, S.C.;
Peebles, D.L. *Appl. Phys. Lett.* 1980, 36, 96.

Chen, Y.C.; Akagi, K.; Shirakawa, H. *Synth. Met.* 1986, 14, 173.

Chiang, C.K. *Polymer* 1981, 22, 1454.

Chien, J.C.W.; Wnek, G.E.; Karasz, F.E.; Hirsch, J.A.
Macromolecules 1981, 14, 479.

Chien, J.C.W.
Polyacetylene: Chemistry, Physics, and Material Science;
Academic: Orlando, FL, 1984; Chapter 12, p 580.

Chien, J.C.W.; Babu, G.N. J. Chem. Phys. 1985, 82, 441.

Clarke, T.C.; Street, G.B. Synth. Met. 1979, 1, 119.

Cotton, F.A.; Wilkinson, G. Advanced Inorganic Chemistry: A Comprehensive Text, 2nd ed.; Wiley: NY, 1962; p 381.

Cunningham, A.; Ward, I.M.; Willis, H.A.; Zichy, V. Polymer 1974, 15, 749.

Deits, W.; Cukor, P.; Rubner, M.; Jopson, H. Synth. Met. 1982, 4, 199.

DePaoli, M.A.; Waltman, R.J.; Diaz, A.F.; Bargon, J. J. Chem. Soc., Chem. Commun. 1984, 1015.

Diaz, A.F.; Bargon, J. In Handbook of Conducting Polymers; Skotheim, T.A., Ed.; Marcel Dekker: New York, 1986; Chapter 3, p 81.

Diaz, A.F.; Hall, B. IBM J.Res.Dev. 1983, 27, 342.

Druy, M.A.; Rubner, M.F.; Walsh, S.P. Synth. Met. 1986, 13, 207.

Druy, M.A.; Tsang, C.H.; Brown, N.; Heeger, A.J.; MacDiarmid, A.G. J. Polym. Sci., Polym. Phys. Ed. 1980, 18, 429.

Duckett, R.A.; Ward, I.M.; Zihliff, A.M. J. Mater. Sci. 1972, 7, 480.

Duke, C.B. Synth. Met. 1987, 21, 5.

Ebisawa, F.; Kurihara, T.; Tabei, H. *Synth. Met.* 1987, 18, 431.

Edwards, J.H.; Feast, W.J. *Polymer* 1981, 21, 595.

Edwards, J.H.; Feast, W.J.; Bott, D.C. *Polymer* 1984, 25, 395.

Ellis, J.R. In Handbook of Conducting Polymers; Skotheim, T.A., Ed.; Marcel Dekker: New York, 1986; Chapter 13, p 489.

Elsenbaumer, R.L.; Jen, K.Y.; Oboodi, R. *Synth. Met.* 1986, 15, 169.

Elsenbaumer, R.L.; Jen, K.Y.; Miller, G.G.; Shacklette, L.W., *Synth. Met.* 1987, 18, 277.

Elsenbaumer, R.L.; Shacklette, L.W. In Handbook of Conducting Polymers; Skotheim, T.A., Ed.; Marcel Dekker: NY, 1986; Chapter 7, p 213.

Farell, G.W.; Fellers, J.F. *J. Polym. Eng.* 1986, 6, 263.

Folkes, M.J.; Keller, A. *Polymer* 1971, 12, 222.

Foot, P.J.S.; Mohammed, F.; Calvert, P.D.; Billingham, N.C. *J. Phys. D: Appl. Phys.* 1987, 20, 1354.

Gagnon, D.R. Ph.D. Dissertation, University of Massachusetts, 1986.

Gagnon, D.R.; Capistran, J.D.; Karasz, F.E.; Lenz, R.W. *Polym. Bull.* 1984, 12, 293.

Gagnon, D.R.; Karasz, F.E.; Thomas, E.L.; Lenz, R.W. *Synth. Met.* 1987, 20, 85.

Gagnon, D.R.; Capistran, J.D.; Karasz, F.E.; Lenz, R.W.; Antoun, S. *Polymer* 1987, 28, 567.

Galvin, M.E.; Wnek, G.E. *Polym. Bull.* 1985, 13, 109.

Galvin, M.E.; Wnek, G.E. Polym. Commun. 1982, 23, 795.

Galvin, M.E.; Wnek, G.E. J. Polym. Sci., Polym. Chem. Ed. 1983, 21, 2727.

Garnier, F.; Horowitz, G. Synth. Met. 1987, 18, 693.

Gaylord, R.J. J. Polym. Sci., Polym. Lett. Ed. 1975, 13, 337.

Genies, E.M.; Lapkowski, M.; Santier, C.; Vieil, E. Synth. Met. 1987, 18, 631.

Gilliom, L.R.; Grubbs, R.H. J. Am. Chem. Soc. 1986, 108, 733.

Glenz, W.; Peterlin, A. J. Polym. Sci.: A-2 1971, 9, 1191.

Granier, T.; Thomas, E.L.; Gagnon, D.R.; Karasz, F.E.; Lenz, R.W. J. Polym. Sci., Polym. Phys. Ed. 1986, 24, 2793.

Granier, T.; Thomas, E.L.; Gagnon, D.R.; Karasz, F.E.; Lenz, R.W. J. Polym. Sci., Polym. Phys. Ed. 1986, 24, 2793.

Greco, R.; Hopfenberg, H.B.; Martuscelli, E.; Ragosta, G.; Demma, G. Polym. Eng. Sci. 1978, 18, 654.

Hadley, D.W.; Pinnock, P.R.; Ward, I.M. J. Mater. Sci. 1969, 4, 152.

Han, C.C.; Lenz, R.W.; Karasz, F.E. Polym. Commun. 1987, 28, 261.

Harper, K.; James, P.G. Mol. Cryst. Liq. Cryst. 1985, 117, 55.

Hayes, W. Contemp. Phys. 1985, 26, 421.

Hotta, S.; Rughooputh, S.D.D.V.; Heeger, A.J. Synth. Met. 1987, 22, 79.

Hörhold, H.H.; Helbig, M. Makromol. Chem., Macromol. Symp. 1987, 12, 229.

Hörhold, H.H.; Opfermann, J. Makromol. Chem. 1970, 131, 105.

Inganäs, O.; Lundström, I. Synth. Met. 1987, 21, 13.

Ivory, D.M.; Miller, G.G.; Sowa, J.M.; Shaklette, L.W.; Chance, R.R.; Baughman, R.H. J. Chem. Phys. 1979, 71, 1506.

Jasne, S.J.; Chiklis, C.K. Synth. Met. 1986, 15, 175.

Jen, K.Y.; Maxfield, M.; Shacklette, L.W.; Elsenbaumer, R.L. J. Chem. Soc., Chem. Commun. 1987, 309.

Jow, T.R.; Jen, K.Y.; Elsenbaumer, R.L.; Shacklette, L.W.; Angelopoulos, M.; Cava, M.P. Synth. Met. 1986, 14, 53.

Kanbe, M.; Okawara, M. J. Polym. Sci.: A-2 1968, 6, 1058.

Kaneto, K.; Maxfield, M.; Nairns, D.P.; MacDiarmid, A.G.; Heeger, A.J. J. Chem. Soc., Farad. Trans.(1) 1982, 78, 3417.

Karasz, F.E.; Chien, J.C.W.; Galkiewics, R.; Wnek, G.E. Nature 1979, 282, 286.

Keith, H.D.; Padden, F.J. J. Appl. Phys. 1964, 35, 1270.

Khambatta, F.B.; Warner, F.; Russell, T.; Stein, R.S. J. Polym. Sci., Polym. Phys. Ed. 1976, 14, 1391.

Klavetter, F.L.; Grubbs, R.H. A.C.S. Polym. Prepr. 1987, 28 (2), 425.

Kobel, W.; Kiess, H.; Egli, M. Synth. Met. 1988, 22, 265.

Koezuka, H.; Tsumura, A.; Ando, T. Synth. Met. 1987, 18, 699.

Kratky, O. Kolloid-Z 1933, 64, 213.

Lahti, P.M.; Modarelli, D.A.; Denton, F.R.; Lenz, R.W.; Karasz, F.E. J. Am. Chem. Soc., in press.

Lee, K.I.; Jopson, H. Polym. Bull. 1983, 10, 105.

Leising, G. Polym. Bull. 1984, 11, 401.

Leising, G. Polym. Commun. 1984, 25, 201.

Leising, G.; Leitner, O.; Kahlert, H. Mol. Cryst. Liq. Cryst. 1985, 117, 67.

Lenz, R.W.; Han, C.C.; Stenger-Smith, J.; Karasz, F.E. J. Polym. Sci., Polym. Chem. Ed., in press.

Lugli, G.; Pedretti, U.; Perego, G. Mol. Cryst. Liq. Cryst. 1985, 117, 43.

MacDiarmid, A.G.; Chiang, J.C.; Richter, A.F.; Epstein, A.J. Synth. Met. 1987, 18, 285.

Machado, J.M.; Denton, F.R.; Schlenoff, J.B.; Karasz, F.E.; Lahti, P.M. J. Polym. Sci., Polym. Phys. Ed., in press.

Machado, J.M.; Karasz, F.E.; Lenz, R.W. Polymer, in press.

MacKnight, W.J.; Karasz, F.E.; Fried, J.R. In Polymer Blends, Vol. I; Paul, D.R.; Newman, S., Eds.; Academic: NY, 1978; Chapter 5.

Mainthia, S.B.; Kronick, P.L.; Labes, M.M. J. Chem. Phys. 1964, 41, 2206.

Mandelkern, L. J. Appl. Phys. 1954, 25, 830.

Marrinan, H.J. J. Polym. Sci. 1959, 39, 461.

Martuscelli, E.; Silvestre, C.; Addonizio, M.; Amelino, L.
Makromol. Chem. 1986, 187, 1557.

Martuscelli, E.; Demma, G.B. Polymer Blends; Martuscelli, E.;
Polumbo, R.; Kryszewski, M., Eds.; Plenum: NY, 1980; p 101.

Marvel, C.S.; Sample, J.H.; Roy, M.F. J. Am. Chem. Soc. 1939,
61, 3241.

Masse, M.A.; Martin, D.C.; Karasz, F.E.; Thomas, E.L. Proc. ACS
Div. Pol. Mat. Sci. and Eng. 1987, 57, 441.

McDonald, R.N.; Campbell, T.W. J. Am. Chem. Soc. 1960, 82, 4669.

McLeod, G.G.; Mahboubian-Jones, M.G.B.; Pethrick, R.A.; Watson, S.D.;
Truong, N.D.; Galin, J.C.; Francois, J. Polymer 1986, 27, 455.

Merlet, N.; Dian, G.; Barbey, G.; Outurquin, F.; Paulmier, C.
Synth. Met. 1988, 24, 77.

Miyasaka, K.; Watanabe, K.; Jojima, E.; Aida, H.; Sumita, M.;
Ishikawa, K. J. Mater. Sci. 1982, 17, 1610.

Montaudo, G.; Vitalini, D.; Lenz, R.W. Polymer 1987, 28, 837.

Murase, I.; Ohnishi, T.; Noguchi, T.; Hirooka, M. Polym. Commun.
1984, 25, 327.

Murase, I.; Ohnishi, T.; Noguchi, T.; Hirooka, M.; Murakami, S.
Mol. Cryst. Liq. Cryst. 1985, 118, 333.

Murase, I.; Ohnishi, T.; Noguchi, T.; Hirooka, M. Polym.
Commun. 1985, 26, 362.

Münstedt, H.; Köhler, G.; Möhwald, H.; Naegele, D.; Bitthin, R.;
Ely, G.; Meissner, E. Synth. Met. 1987, 18, 259.

Naarmann, H.; Theophilou, N. Synth. Met. 1987, 22, 1.

Natov, M.; Peeva, L.; Djagarova, E.J. J. Polym. Sci., Polym. Symp. Ed. 1968, 16, 4197.

Nigrey, P.J.; MacInnes, D.; Nairns, D.P.; MacDiarmid, A.G.; J. Electrochem. Soc. 1981, 128, 1651.

Nigrey, P.J.; MacDiarmid, A.G.; Heeger, A.J. J. Chem. Soc., Chem. Commun. 1979, 594.

Niwa, O.; Tamamura, T. J. Chem. Soc. Chem. Commun. 1984, 817.

Northolt, M.G.; Van Aartsen, J.J. J. Polym. Sci., Polym. Symp. Ed., 1977, 58, 283.

Obrzut, J.; Karasz, F.E. J. Chem. Phys. 1987, 87, 6178.

Okajima, S.; Kurihara, K.; Homma, K. J. Appl. Polym. Sci. 1967, 11, 1703.

Osterholm, J.E.; Yasuda, H.K.; Levenson, L.L. J. Appl. Polym. Sci. 1982, 27, 931.

Passiniemi, P.; Österholm, J.E. Synth. Met. 1987, 18, 637.

Patil, A.O.; Ikenoue, Y.; Wudl, F.; Heeger, A.J. J. Am. Chem. Soc. 1987, 109, 1858.

Pekker, S.; Jánossy, A. In Handbook of Conducting Polymers; Skotheim, T.A., Ed.; Marcel-Dekker: New York, 1986; Chapter 2 p 45.

Perichaud, A.; Dhainaut,S.; Bernier, P.; Lefrant,S. Synth. Met. 1988, 24, 7.

Potember, R.S.; Hoffman, R.C.; Hu, H.S.; Cocchiaro, J.E.; Viands, C.A., Murphy, R.A.; Poehler, T.O. Polymer 1987, 28, 574.

Ramos, M.A.; Collar, E.P. J. Polym. Eng. 1987, 7, 137.

Reynolds, J.R.; Schlenoff, J.B.; Chien, J.C.W. *J. Electrochem. Soc.* 1985, 132, 1131.

Rietsch, F.; Jasse, B. *Polym. Bull.* 1984, 11, 287.

Rubner, M.F.; Tripathy, S.K.; Georger, J.; Cholewa, P. *Macromolecules* 1983, 16, 870.

Rueda, D.R.; Cagiao, M.E.; Balta Calleja, F.J.; Palacios, J.M. *Synth. Met.* 1987, 22, 53.

Saldanha, J.M.; Kyu, T. *Macromolecules* 1987, 20, 2840.

Sato, M.; Tanaka, S.; Kaeriyama, K. *Makromol. Chem.* 1987, 188, 1763,

Sato, M.; Tanaka, S.; Kaeriyama, K. *Synth. Met.* 1987, 18, 229.

Sawyer, L.C.; Grubb, D.T. Polymer Microscopy; Chapman and Hall: London, 1987.

Schuur, G.; Van der Vegt, A.K. In Structure and Properties of Oriented Polymers; Ward, I.M., Ed., Applied Science: London, 1975; Chapter 12.

Shacklette, L.W.; Maxfield, M.; Gould, S.; Wolf, J.F.; Jow, T.R.; Baughman, R.H. *Synth. Met.* 1987, 18, 611.

Shirakawa, H.; Louis, E.J.; MacDiarmid, A.G.; Chiang, C.K.; Heeger, A.J. *J. Chem. Soc., Chem. Commun.* 1977, 578.

Shirakawa, H.; Ikeda, S. *Synth. Met.* 1979, 1, 175.

Shriver, D.F.; Papke, B.L.; Ratner, M.A.; Dupon, R.; Wong, T.; Brodwin, M. *Sol. St. Ionics* 1981, 5, 83.

Stein, R.S.; Khambatta, F.B.; Warner, F.P.; Russell, T.; Escala, A.; Balizer, E. *J. Polym. Sci. Polym. Symp.* 1978, 63, 313.

Swager, T.M.; Grubbs, R.H. J. Am. Chem. Soc. 1987, 109, 894.

Takenaka, T.; Shimura, Y.; Gotoh, R. Kolloid-Z 1970, 237, 13.

Tomozawa, H.; Braun, D.; Phillips, S.; Heeger, A.J.; Kroemer, H. Synth. Met. 1987, 22, 63.

Tourillon, G.; Garnier, F. J. Electroanal. Chem. 1982, 135, 173.

Townsend, P.D.; Pereira, C.M.; Bradley, D.D.C.; Horton, M.E.; Friend, R.H. J. Phys. C: Sol. St. Phys. 1985, 18, L283.

Ulrich, D.R. Polymer 1987, 28, 533.

Structure and Properties of Oriented Polymers; Ward, I.M., Ed.; Applied Science: London, 1975.

Wedgegood, A.R.; Seferis, J.C. In Interrelations Between Processing, Structure, and Properties of Polymeric Materials; Seferis, J.C.; Theocaris, P.S., Eds.; Elsevier Science: The Netherlands, 1984.

Wessling, B.; Volk, H. Synth. Met. 1986, 15, 183.

Wessling, R.A. J. Polym. Sci., Polym. Symp. Ed. 1985, 72, 55.

Wessling, R.A. U.S. Patent 3 706 677, 1972.

Wessling, R.A.; Zimmerman, R.G. U.S. Patent 3 401 152, 1968.

White, J.L. J. Polym. Eng. 1985, 5, 275.

White, J.L. In Interrelations Between Processing, Structure, and Properties of Polymeric Materials; Seferis, J.C.; Theocaris, P.S., Eds.; Elsevier Science: The Netherlands, 1984; p 765.

Whitney, D.H.; Wnek, G.E. Macromolecules 1988, 21, 266.

Wnek, G.E. Ph.D. Dissertation, University of Massachusetts, 1980.

Wynne, K.J.; Street, G.B. Macromolecules 1985, 18, 2361.

Wynne, K.J.; Zachariades, A.E.; Inabe, T.; Marks, T.J. Polym. Commun. 1985, 26, 162.

Yoneyama, H.; Wakamoto, K.; Tamura, H. J. Electrochem. Soc. 1985, 132, 2414.

Zachariades, A.E. In Interrelations Between Processing, Structure, and Properties of Polymeric Materials; Seferis, J.C.; Theocaris, P.S., Eds.; Elsevier Science: The Netherlands, 1984.

Zbinden, R., Infrared Spectroscopy of High Polymers; Academic: New York, 1964.

PHYSICAL SCIENCES
LIBRARY

MAY 4 2 1989

